DOI:10.14753/SE.2020.2417

Stress-induced changes in the metabolism, gut microbiome and behavior

PhD thesis

Dániel Kuti

Neurosciences ("János Szentágothai") Doctoral School

Semmelweis University

Supervisor:	Krisztina Kovács, D.Sc
Official reviewers:	Barna Vásárhelyi, MD, D.Sc József Halász, MD, Ph.D
Head of the Final Examination Committee:	Árpád Dobolyi, D.Sc
Members of the Final Examination Committee:	Attila Patócs, MD, D.Sc Máté Tóth, Ph.D

Budapest
2020

DOI:10.14753/SE.2020.2417

Table of Contents

Abbreviations 5
1. Introduction 8
1.1. Stress in general 8
1.2. Hypothalamo-pituitary-adrenocortical (HPA) axis 9
1.3. Central regulation of food intake and energy metabolism 10
1.4. Effect of stress on the metabolic system 14
1.5. Effect of stress on gastrointestinal tract (GI) 16
1.6. Gut brain axis 16
1.7. Targeting the microbiome 19
2. Aim 21
3. Materials and methods 22
3.1. Animals 22
3.2. Stereotaxic surgery 22
3.3. Stress procedures 22
3.3.1. Acute and repeated stress 22
3.3.2. Chronic variable stress (CVS) 23
3.3.3. Two-hits stress protocol 25
3.4. General procedure in rifaximin experiment 26
3.5. Metabolic measurements 27
3.6. Behavior tests 28
3.6.1. Sucrose consumption test 28
3.6.2. Open field test 28
3.6.3. Novel environment test 28
3.6.4. Elevated plus maze 29
3.7. Gut permeability test in vivo 29
3.8. Hormone, endotoxin, glucose and triglyceride measurement from plasma 29
3.9. Gene expression analysis 30
3.10. Microbiome analysis 31
3.11. Bacterial load in mesenteric lymph node 32
3.12. Histological methods 33
3.12.1. Perfusion and tissue processing 33
3.12.2. Haematoxylin & eosin staining, imaging and quantification 33
3.12.3. Immunostaining, imaging and quantification 33
3.13. Epidemiological data collection 34
3.14. Statistics 35

4. Results 36
4.1. Basal metabolic and locomotor activity 36
4.2. Acute restraint stress 38
4.3. Effects of acute psychological stress on locomotor behaviour and metabolic variables....39
4.3.1. Locomotor activity 39
4.3.2. Cumulative food intake 41
4.3.3. Energy expenditure (EE) 43
4.3.4. Respiratory exchange ratio (RER) 44
4.3.5. Body composition....45
4.4. Chemogenetic activation of CRH^{PVN} neurons....45
4.5. Effect of CRH^{PVN} activation on locomotor behavior and metabolism....46
4.5.1. Locomotor activity 46
4.5.2. Cumulative food intake 47
4.5.3. Energy expenditure (EE) 48
4.5.4. Respiratory exchange ratio (RER) 49
4.5.5. Body composition....50
4.6. Control experiments 51
4.7. Effects of chronic stress 52
4.8. Effect of chronic variable stress on metabolism 54
4.8.1. Locomotor activity 54
4.8.2. Cumulative food intake 56
4.8.3. Energy expenditure....57
4.8.4. Respiratory exchange ratio (RER) 58
4.8.5. Body composition....59
4.9. Effect of chronic stress on gut microbiome and its restoration after rifaximin treatment....60
4.10. Effect of rifaximin treatment on chronic stress-induced changes in organ weights, hormones and metabolic markers 61
4.11. Effect of rifaximin on chronic stress-induced changes on behavior 63
4.11.1. Ethogram 63
4.11.2. Open field, EPM, sucrose consumption test....65
4.12. Effect of MS+CVS and rifaximin treatment on the gut and gut-related immunity 67
4.12.1. Colon mucosa, tight junction protein expression and gut permeability 67
4.12.2. Gut permeability, macrophage infiltration, local- and systemic bacterial load.69
4.13. Hypothesis: correlation between Parkinson's disease prevalence, consumption of certain antibiotics and gut microbial dysbiosis 71

DOI:10.14753/SE.2020.2417

5. Discussion 73
5.1. The effect of acute stress and effect of the activation of CRH^{PVN} on metabolic system 73
5.2. Metabolic changes after chronic stress and during recovery 76
5.3. Chronic stress effect on colon microbiome and gut 79
5.4. Antibiotic effect on gut microbiome 81
6. Conclusion 84
7. Summary 85
8. Összefoglalás 86
9. References 87
10. Publication of the author 106
11. Acknowledgement 108

DOI:10.14753/SE.2020.2417

Abbreviations

5-HT – Serotonin

AAV – Adeno-associated virus

ACC – Anterior cingulate cortex

ACTH – Adrenocorticotropic hormone

AGRP – Agouti-related peptide

ahCRF – α-helical CRF9–41

AMP – Antimicrobial peptide

ARC – Arcuate nucleus

AVP – Arginine vasopressin

BAT – Brown adipose tissue

BNST – Bed nucleus of stria terminals

CART – Cocaine- and amphetamine-regulated transcript

CB1 – Cannabinoid-1 receptor

CCK – Cholecystokinin

CNO – Clozapine-N-oxide

CORT – corticosterone

CRH-Ires-Cre – Corticotropin releasing hormone-Internal ribosomal entry side-Cre

CVS – Chronic variable stress

DMH – Dorsomedial nucleus of the hypothalamus

DNA – deoxyribonucleic acid

DREADD – Designer receptor exclusively activated by designer drug

ECDC – European Centre for Disease Prevention and Control

EDTA – Ethylenediaminetetraacetic acid

EE – Energy expenditure

ENS – Enteric nervous system

EPM – Elevated plus maze

ESAC – European Surveillance of Antibiotic Consumption network

eWAT – Epididymal white adipose tissue

FITC – Fluorescein isothiocyanate

FMT – Fecal microbiota transplant

GABA – γ-aminobutyric acid

GAPDH – Glyceraldehyde 3-phosphate dehydrogenase

GHSR1 – Ghrelin receptor

GIT – Gastrointestinal tract

GLP-1 – Glucagon-Like Peptide 1

GR – Glucocorticoid receptor

H&E – Hematoxylin & eosin

HPA axis – Hypothalamic-pituitary-adrenal axis

IBD – Inflammatory bowel disease

IBS – Irritable bowel syndrome

icv – Intracerebroventricular

IDO – Indoleamine 2,3 dioxygenase

LAL – Limulus amebocyte lysate (assay)

LepR – Leptin receptor

LHA – Lateral hypothalamic area

LPS – Lipopolysaccharide

MCH – Melanin-concentrating hormone

MD – Minimal disease

MLN – Mesenteric lymph node

MR – Mineralocorticoid receptor

MRI – Magnetic resonance imaging

mRNA – messenger ribonucleic acid

MS – Maternal separation

MSH – Melanocyte-stimulating hormone

NA – Noradrenaline

NAc – Nucleus accumbens

NCBI – National Center for Biotechnology Information

NPY – Neuropeptide Y

NTS – Nucleus of the solitary tract

OF – Open field

PBS – Phosphate buffered saline

PCR – Polymerase chain reaction.

PD – Parkinson’s disease

PFC – Prefrontal cortex

PMv – Premammillary nucleus of the hypothalamus

POA – Preoptic area

POMC – Proopiomelanocortin

PVH – Paraventricular nucleus of hypothalamus

PVN – Paraventricular nucleus

PYY – Pancreatic Peptide YY_{3-36}

Reg3b – Regenerating islet-derived protein 3-beta

RER – Respiratory exchange ratio

Retnlb – Resistin-like beta

RIA – Radioimmunoassay

SCFA – Short chain fatty acids

SCh – Suprachiasmatic nucleus

SEM – Standard error of mean

sWAT – Subcutan white adipose tissue

TG – Triglyceride

TH – Tyrosine hydroxylase

TJP1-3 – Tight junction protein 1-3

TLR – Toll- like receptor

VMH – Ventromedial nucleus of the hypothalamus

vSbc – Venral subiculum

VTA – Ventral tegmental area

Y1,2 and 5 receptors –Y1,2 and 5 receptors of Neuropeptide Y

αSyn – α-synuclein

DOI:10.14753/SE.2020.2417

1. Introduction

1.1. Stress in general

Each living organism continuously struggle to maintain an internal homeostasis, as it was first defined by Walter Cannon [1]. Homeostasis is an equilibrium condition for many different physiological variables: body temperature, ionic composition and osmolality, pH, and blood glucose level etc. For survival in a continuously changing external and internal environment, these variables should be kept in well-defined range [2]. In 1936, Hans Selye published a paper in Nature entitled "A syndrome produced by diverse nocuous agents" and introduced the stress concept. He wrote: "*…if the organism is severely damaged by acute non-specific nocuous agents, a typical syndrome appears, the symptoms of which are independent of the nature of the damaging agent, and represent rather a response to damage as such*" [3]. He noticed that the same pathological triad (adrenal gland enlargement, thymus involution, gastrointestinal ulceration) evolves in response to many different stressors (bacterial infection, toxins, physical stimuli) [3]. A few years later, Selye defined the General Adaptation Syndrome, GAS as an *"integrated syndrome of closely inter-related adaptive reactions to non-specific stress itself"* [4]. GAS develops in three successive stages: 1. alarm reaction, 2. active resistance, 3. exhaustion (Fig. 1.) [5].

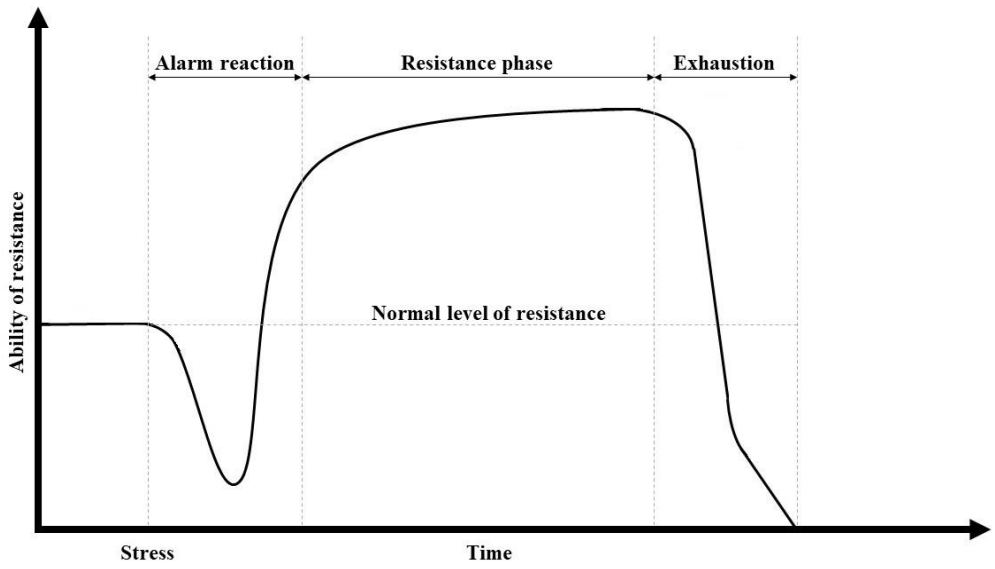

Figure 1. ***General adaptation system.***

Sterling and Eyer were the first, who introduced the expression allostasis, which basically the maintenance of homeostasis through changes. The expended energy for allostasis is the allostatic load [6].

In response to various external and internal stressors catecholamines release from adrenal medulla, induced by the activation of sympathetic nervous system (SNS), and the hypothalamo-pituitary-adrenocortical (HPA) axis became rapidly activated. [7]. In response to the activation of both sympathetic nervous system and HPA, bodily resources are mobilized for fight or flight, including centrally mediated cardiovascular adaptations with increased heart rate and blood pressure and redistribution of blood supply between muscles and skin. During acute stress, respiration is also increased to support increased metabolic demands with oxygen. Increased vigilance, alertness and arousal are also specific features of stress. [8]. From the pathophysiological point of view, it is important to distinguish between acute and chronic stress. Acute stress is a short term challenge, while during chronic stress the body is exposed to stressors for a prolonged time or frequently exposed to various different stressors, chronically [9].

1.2. Hypothalamo-pituitary-adrenocortical (HPA) axis

Different environmental stimuli trigger stress response and activate the neuroendocrine stress axis as a reflex regulation. In first step, corticotropin-releasing hormone (CRH) and vasopressin (AVP) are released from the parvocellular neurons of the hypothalamic paraventricular nucleus (PVN). These hormones are secreted to the hypophyseal portal circulation and trigger adrenocorticotropic hormone (ACTH) release from the adrenocorticotropic cells of anterior pituitary gland. Then, ACTH reaches the adrenal cortex via the blood circulation and stimulates cortisol (in human) and corticosterone (in rodents) release from the zona fasciculata. Corticosteroids act through mineralocorticoid (MR) and glucocorticoid (GR) nuclear receptors [10]. The basal occupancy of MR is around nine fold higher than GR; because affinity of MR is higher (Kd = 0.1–0.5 nM) for corticosterone than that of GR (Kd = 2–5 nM). For this reason, occupancy of GR is increased seven-fold higher during stress, while MRs are alre ady fully occupied even at no stress conditions [11]. Therefore, stress effects occur rather through GR than MR. MR is involved in the appraisal process and the early-phase of stress [10]. Inhibitory feedback by glucocorticoids plays a major role in stress response. This suppression occurs at several node of the axis, at pituitary, at hypothalamus or

extrahypothalamic sites (hippocampus, cortex) and inhibit expression of effector molecules [12].

The neural regulation of HPA axis is originated from different brain regions, which depends on the nature and intensity of stressor. The information of physical and metabolic stressors (hypovolemia, hypoglycaemia) are transported through ascending neurons from the brainstem and spinal cord and these neurons have direct projection to the PVN. These projections originated from the nucleus of the solitary tract (NTS) and C1 and C3 catecholaminergic neurons. Brainstem pathways also interact with other structures such as dorsal raphe and dorsomedial hypothalamic nucleus (DMH) [10].

By contrast, psychogenic stressors require more complex polysynapthic pathways, which include limibic brain regions such as prefrontal cortex (PFC), hippocampus, amygdala and bed nucleus of stria terminals (BNST). PFC projects both inhibitory and stimulatory information to PVN. These inputs are mediated through interconnections with other structures such as hippocampus, ventral subiculum (vSbc) and amygdala. The hippocampus is mainly suppress the activation of HPA axis. The projection of hippocampus reach indirectly the PVN. The projection occurs via vSbc and PFC. These regions innervate the periventricular region that projects glutamatergic and GABAergic neurons to the CRH neurons. There are neuronal innervations as well as from basolateral and medial amygdala to the PVN that potentiate the HPA axis. The central nucleus of amygdala express also CRH and has essential role in the stress induce behavioural responses (especially fear). The BNST is an integrative centre between limbic brain regions and PVN. The projections of BNST innervates the periventricular GABA- and glutamatergic neurons and suppress the inhibiting signals of GABAergic interneurons [10].

1.3. Central regulation of food intake and energy metabolism

In the beginning of this chapter, I would like to clarify few metabolism related concepts for the better understand ability. Orexigen is any substance, which stimulates appetite; by contrast, anorexigen inhibits appetite. Catabolism is the set of metabolic pathways that breaks down molecules into smaller units and anabolism constructs molecules from smaller units.

To govern neuroendocrine autonomic and behvaioral stress responses, hypothalamus is also a key node of metabolic regulation [13]. Arcuate nucleus (ARC), paraventricular

nucleus of the hypothalamus (PVH), ventromedial nucleus (VMH) and lateral hypothalamic area (LHA) were described as a key feeding regulatory centers in the hypothalamus [14]. Circulating metabolic-related hormones mediate information to these centers about the energy status from periphery. These hormones bind to specific receptors and can alter the physiology of the receptor containing neurons. Leptin, insulin and ghrelin all target multiple brain neurons involved in energy intake [15-17].

Leptin is secreted by adipocytes and secreted in proportions of adipose depots. The hormone has a key role in the regulation of glucose and lipid metabolism, by suppressing food intake by decreasing meal size rather than meal number [18-20]. In particular, leptin receptor (LepR) expressed in the retrochiasmatic area, arcuate- (ARC), dorsomedial- (DMH), ventral premammillary- (PMv) and ventromedial (VMH) nuclei of the hypothalamus. Elias et al. examined neuronal activation after leptin administration [21]. Leptin-induced c-Fos expression was detected in Lepr-expressing neurons in the hypothalamus and hindbrain [21]. In addition, other studies demonstrated that fos expression was very low in PVH, unlike in ARC and DMH, because of the secondary activation of leptin-dependent pathways [22, 23].In addition, leptin also aim hindbrain and the midbrain ventral tegmental area (VTA) to affect the reward system. Following studies showed that dopamine is an important neurotransmitter in this influence because of the dopaminergic inputs to the nucleus accumbens (NAc) from VTA [24-26]. LepR expressed also in the medial part of the nucleus of the solitary tract (NTS) and expression of leptin activation marker (pSTAT3) was demonstrated in this brain region after leptin injection [27].

Insulin is able to reduce blood glucose concentrations by facilitating glucose uptake into muscle, liver and adipose tissue through insulin dependent glucose transporter protein GLUT4. The hormone is secreted by the β cells of Langerhans islets of pancreas [28]. Insulin enters the brain from blood circulation [29] and reduces food intake there by suppressing neuropeptide Y (NPY) and increases the activation of melanocyte stimulating hormone (α-MSH) neurons in ARC [30]. Insulin also able to alter reward and motivation processes through insulin receptors (IRs) in the limbic system [31, 32]. In addition, insulin reduces the meal size by promoting the effect of cholecystokinin (CCK) [33]. It is also secreted at the proportion of adipose tissue [34]. Insulin receptors (IR) are expressed in different locations of the brain: olfactory bulb, cerebellum, parts of the cortex, hippocampus, choroid plexus, VTA and ARC [35]. However, arcuate nucleus of

hypothalamus is in the focus of investigation of insulin's action in the aspect of metabolic function [36].

Ghrelin is a gastrointestinal (GI) hormone, which induces food intake. It is secreted by the stomach and proximal small intestine [37]. The ghrelin receptor (GHSR1) belongs to the G-protein coupled receptor family and affects adenylate cyclase activity and intracellular Ca^{2+} channels. GHSR1 expressed in most of the brain regions where IR or LepR are found [17]. Ghrelin also influences glucose homeostasis and reward [37].

Pancreatic Peptide YY_{3-36} (PYY) and Glucagon-Like Peptide 1 (GLP-1) are secreted by L cells in the distal part of small intestine. Both hormone inhibit food intake but on different ways. PYY binds Y2 receptor in the ARC and regulates energy homeostasis. In contrast, GLP-1 enhances the secretion of insulin but has direct effect on vagal afferents [38-40].

Cholecystokinin (CCK) is synthesized by I cells in the proximal part of intestine. The hormone regulates metabolism via vagal nerve and hindbrain. It has a powerful effect to decrease meal size [41].

Arcuate nucleus ARC harbors two separate neuron population that exert opposite influence on food intake (Fig. 2.). Neuropeptide Y (NPY) and Agouti-related peptide (AgRP) colocalized neurons mediate anabolic effects. These neurons located in the medial portion of ARC and the cells are GABAergic [42]. Intracerebroventricular administration of NPY or direct injection into hypothalamus stimulates food intake and reduce energy metabolism. Consequently, continuous central dosage of NPY leads to obesity [43, 44], however, NPY–KO mice display normal food intake and normal leptin and insulin levels [45]. It is likely that other orexigenic neuropeptides, such as AgRP, orexin or melanin-concentrating hormone (MCH), may compensate the lack of NPY. Orexin and MCH are expressed in the lateral hypothalamic area and adjust food intake to the arousal state [46, 47]. NPY expressing neurons are key mediators of the orexigenic effect of ghrelin while they are inhibited by leptin and insulin. In addition, NPY/ AgRP neurons project a tonic GABAergic inhibition to the anorexigenic proopiomelanocortin (POMC)/ cocaine- and amphetamine-regulated transcript (CART) neurons [48].

The other major metabolic-related neuron population in the ARC is anorexigenic. These cells are located in the lateral part of the nucleus and express POMC (alpha-melanocyte-stimulating hormone (MSH) and CART. Neurons in this region are equipped with leptin and insulin receptors and mediate their anorexigenic effect by increasing energy expenditure. [49]. In mice, CART is colocalized with POMC, however, CART is

coexpressed rather in orexigenic NPY/AgRP neurons than POMC neurons in human [50]. Besides that, CART is translated with MCH in the lateral hypothalamus in several species [51].

The anorexigenic effect of POMC neurons in ARC projects to PVN, ventromedial nucleus and lateral hypothalamus and reduce food intake with increased energy expenditure (EE) [52]. Similarly, NPY/AgRP neurons of ARC project to the same hypothalamic regions (PVN, VMH, LH) as POMC neurons, however orexigenic neurons of arcuate nucleus send axons also to the dorsomedial nuclei of hypothalamus. In these nuclei (PVN, VMH, LH, DMH), NPY neurons affect on the contrary of POMC food intake and EE via Y1,2 and 5 receptors; while, AgRP alters energy homeostasis as an antagonist of melanocortin 4 receptor (MC4R), thus inhibit the effect of α-MSH [50, 53]. The projected information of arcuate nucleus influences the parvo- and parvicellular neurons of PVN, where different hormones are expressed, such as corticotrophin-releasing hormone (CRH), thyrotrophin-releasing hormone (TRH) and oxytocin, thus regulates different neuroendocrine pathways [54].

Huge number of VMH are glucose-responsive neurons, which mediate the anorexigenic effect of leptin [55]. These neurons are also intervened by POMC neurons of ARC and mediate the effect of leptin-induced anorexia partly to the PVN via brain-derived neurotrophic factor (BDNF) [56].

DOI:10.14753/SE.2020.2417

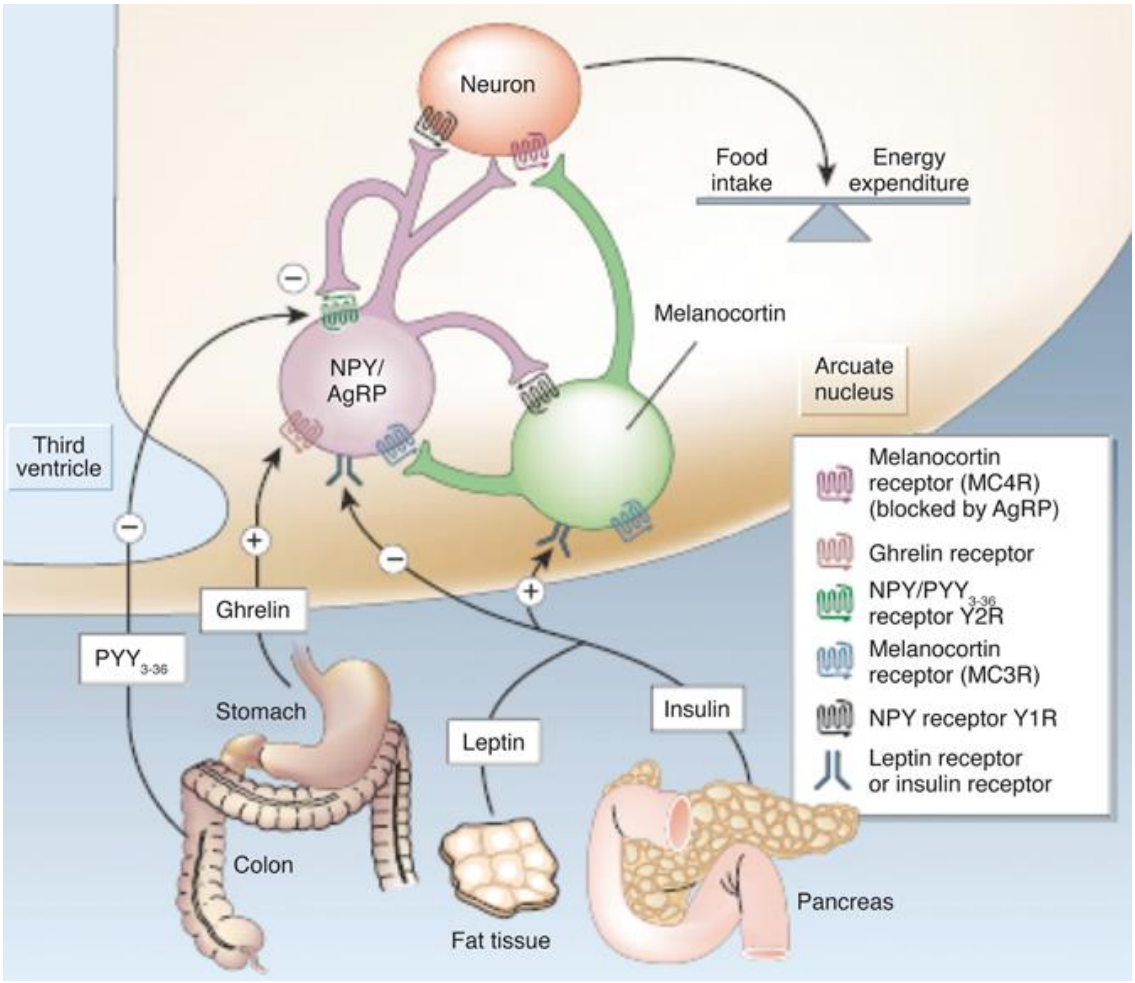

Figure 2. ***Schematic representation of metabolic regulation in arcuate nuclei of the hypothalamus [57].***

The dorsomedial nucleus is received inputs from other hypothalamic areas which are involved in food intake regulation. Furthermore, DMH interconnected with the circadian centre, suprachiasmatic nuclei (SCh) and includes neurons, which express circadian genes, sensitive to the daily schedule [58]. DMH intervenes preoptic area (POA), PVN and LH. Therefore, different studies propose that DMH plays an essential role in the circadian effect of thermoregulation, endocrine function, arousal and food intake [59], however, some studies disagree this hypothesis [58].

1.4. Effect of stress on the metabolic system

Stress is accompanied with increased energy expenditure and metabolic rate to promote coping. Food intake and appetite is inhibited during acute stress, which accompanied with high-energy expenditure. Both major classes of stress mediator

hormones, - the glucocorticoids and catecholamines (adrenaline and noradrenaline) - have profound metabolic effects. Epinephrine is synthetized in the adrenal medulla of adrenal gland by the chromaffin cells. These cells have sympathetic innervation and release upon sympathetic stimuli. Epinephrine is rapid mediator of stress response and acts on nearly all body tissues. Stress is accompanied with a rapid elevation of blood glucose, which is regulated by adrenaline. At cellular level, adrenaline phosphorylates enzymes of glycogenolysis in the liver and muscle, which results glycogen conversion to glucose. Furthermore, adrenaline has an indirect effect on blood glucose level by triggering glucagon release and inhibiting insulin secretion. In the adipose tissues, adrenaline activates lipolysis [60].

Glucocorticoids are steroid hormones, which released from the zona fasciculata of adrenal cortex to the stress-induced activation of HPA axis. Glucocorticoids increase blood glucose level by increasing the synthesis of gluconeogenesis enzymes. The hormone mobilizes also the substrates for gluconeogenesis from other tissues via mobilization of amino acids from extrahepatic tissues and stimulates lipolysis in adipose tissues. In addition, these steroid hormones decrease energy uptake in muscle and adipose tissues to inhibit energy storage [61]. The effects of glucocorticoids are relatively slow, compared to other metabolic hormones like insulin, leptin or catecholamines, because these changes mediated through gene expression rather than direct control of enzymes regulation [62]. In addition, significant level of GRs are localized in different brain regions that influencing metabolic system, such as ARC, VMH and PVH [61].

The permanent presence of stressors seriously affect the resistance of the body, therefore the energy homeostasis may collapse during prolonged chronic stress. Catabolic changes may dominate in response to high level of glucocorticoids. Furthermore, due to the chronically elevated blood glucose level results in increased insulin secretion, which leads to insulin resistance and type2 diabetes on the long run [63]. Besides that, hormone sensitive lipase is continuously activated during chronic stress, which elevates glycerine and fatty acid levels in the blood and these changes accompanied with other metabolic related maladaptive processes like hypertriglyceridemia, non-alcoholic fatty liver disease (NAFLD) or atherosclerosis [64].

The sympathetic nervous system and glucocorticoid hormones act together to alter central metabolic pathways. Sympathetic activation results in suppression of food intake by inhibiting orexigenic NPY action [65]. In addition, α-MSH neurons of ARC potentiate CRH release in PVN. Leptin receptors, which are expressed in PVN, induce CRH

expression and results in activation of sympathetic preganglionic neurons projecting the brain stem and spinal cord. Leptin also inhibits NPY neurons in ARC, and activates the ventro- and dorsomedial hypothalamic projection of PVN [66].

1.5. Effect of stress on gastrointestinal tract (GI)

It is well known, that symptoms of different GI disorders worsen in prolonged stress and negative emotions. Activation of HPA axis and sympathoadrenal system alter various physiological functions of GI such as gastric secretion, gut motility, visceral sensitivity, mucosal blood flow, barrier function and triggers different gastrointestinal relevant symptoms like dyspepsia, diarrhoea or abdominal pain. Chronic activation of the stress system can lead to severe GI disorders such as irritable bowel syndrome (IBS) or inflammatory bowel disease (IBD). Enteric nervous system (ENS) plays an essential role in the regulation of gut functions. It has a great impact on motility and secretion of GI neuropeptides and hormones. Strong evidences confirm that, prolonged stress as well as early life stress are able to alter central pain circuitry, influence motility and permeability through GI [67, 68].

In the last decade, emerging studies demonstrated important interaction between the gut microbiome and host. Stress induces a notable shift in the composition of microbiota, with the growth of pathogenic bacteria and this alteration further aggravate the symptoms of GI disorders. For example, norepinephrine enhances the virulence of *E. coli* or *C. jejuni* [67, 68]. Infants with altered microbiota composition showed higher level of infant GI symptoms and allergic reactions.

The gut microbiome able to modify the interaction between HPA axis and immune system. Stress increases gut permeability and results in “leaky gut” which underpins chronic low-grade inflammation, due to the elevated plasma level of bacterial lipopolysaccharide (LPS) [69]. CRF, which is also produced within the gut, plays an essential role in the stress-induced gut permeability dysfunction, modulation of inflammation in gut, and contributes to visceral hypersensitivity via CRF receptors. Of note, early life stress causes elevated plasma corticosterone level and results in increased gut permeability and bacterial translocation to spleen and liver [69].

1.6. Gut brain axis

The microbiome is a complex and dynamic mixture of microorganisms, which includes different bacteria, fungi, archaea and viruses [70]. These microbial communities

present in different parts of the human body such as the oro-naso-pharyngeal cavity, skin, vagina, gastrointestinal tract etc. These communities interact with host and influence health and disease [71]. The largest proportion of the microbiome is found in the gastrointestinal tract: from the stomach to the colon, bacterial biomass ranges from $10^{2–3}$ to 10^{11}–10^{12} cells/ml, among those approximately 95% being anaerobic [70]. The human gut microbiome consists of seven major phyla: *Bacteroidetes*, *Actinobacteria*, *Cyanobacteria*, *Fusobacteria*, *Proteobacteria*, and *Verrucomicrobia* [72]. The microbiome is exposed to different factors, which constantly change the composition of it. These factors include many variables such as birth, breast feeding, diet, stress, aging, drugs (antibiotics) etc. [73-75].

Gut microbiome widely interacts with the host's metabolic system (Fig.3.). The dietary ingredients can be metabolized differentially and it highly depend on the composition of microbiome. For instance, different bacteria can produce bile acid, short chain fatty acids (SCFA), choline etc. [69, 76]. SCFAs suppress histone deacetylases and able to modify intracellular signalling through their specific receptors that found throughout the body. For instance, propionic acid mediates advantageous effect on the regulation of body weight and glucose metabolism by influencing FFAR3 receptor containing nerve fibres in hepatic portal vein [77]. Recent studies indicate that microbiome is able to influence enteroendocrine cells in gut. E. coli produced proteins are able to induce secretion of GLP-1 and PYY hormones from enteroendocrine cells that affect food intake [78]. For these reason, microbiome can contribute to the development of different metabolic system-related disorders such as, obesity or diabetes [79, 80].

DOI:10.14753/SE.2020.2417

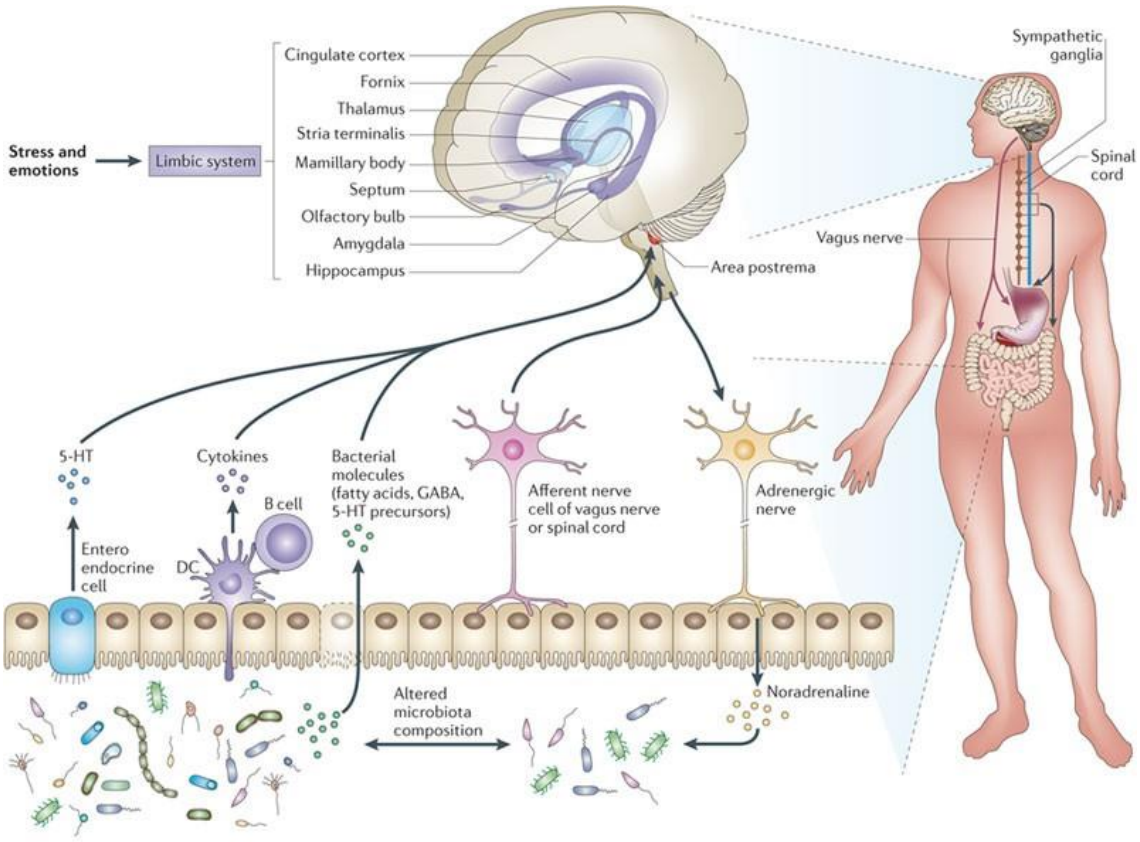

<u>Figure 3.</u> Schematic representation of different pathways of gut brain axis [81].

It is also well documented that a shift in gut microbiome can be associated with gastrointestinal disorders such as inflammatory bowel disease (IBD) and irritable bowel syndrome (IBS). A recent study identified key bacterial species that may be involved in the development of these gastrointestinal diseases and altering the gut microbiota has been proposed as a strategy for the treatment [82].

Growing body of evidence indicates dysbiosis of gut microbiota could contribute or, exaggerate several neuropsychiatric disorders such as anxiety, depression, Alzheimer disease, Parkinson disease, multiple sclerosis, autism etc. [75]. There are many different pathways, through which, microbiome can influence the normal function of brain. Recently, a number of microbial metabolites (referred to as neuro-active metabolites) produced through tryptophan metabolism have been suggested to influence the gut brain-axis. Interestingly, germ free mice have elevated level of circulating tryptophan beside lower level of 5-HT compared to conventionally colonized mice. Another study indicated that probiotic administration of *Lactobacillus* decreased the colonic tryptophan degradation by inhibiting indoleamine 2,3 dioxygenase (IDO – rate limiting enzyme of kynurenine pathways) [83]. Besides that, many microbes can metabolize

neurometabolites such as GABA, noradrenaline, serotonin, dopamine, acetylcholine, tryptophan that could directly affect brain functions [76]. In addition, gram-negative bacteria induce pro-inflammatory cytokines by their cell wall component, LPS; which stimulates toll- like receptor (TLR) coupled immunological pathways. Inflammatory mediators can also access to the brain. For instance, *Campylobacter jejuni* infection triggers neuronal activity in the vagal sensory ganglia and in the NTS. The vagus nerve has also an important role in the mediation of gut-brain communication. There are strong evidences, which demonstrate that microbiome is capable to alter the activity of vagal projection. Administration of *Lactobacillus reuteri* supported wound healing in mice by enhanced oxytocin secretion in hypothalamus, which was eliminated by vagotomy. Another experiment showed that administration of *Lactobacillus rhamnosus* induced anxiolytic and antidepressant-like behaviour, however, this effect was attenuated in vagotomized mice [69, 76].

1.7. Targeting the microbiome

As microbiome is a permanently changing community and the effects of microbiome on the host depend on which bacteria colonized the host's gut. Although the composition of the gut microbiome is relatively constant, it can be targeted by different factors, which provide the basis of microbiota- based therapies. [75]. There are specific dietary supplements through which the microbiome can be targeted. These are the probiotics, prebiotics and synbiotics.

Probiotics are living microorganisms, which provide beneficial effects to the host. Probiotics should survive the low pH in the stomach, biliary salts and should be able to colonise the gut [69]. The most popular probiotics belong to *Lactobacilli* and *Bifidobaceria*, however, yeasts, such as *Saccharomyces boulardii* are also used in probiotic preparations.

Prebiotics are also a manuipulating factor, which are non-digestible fibres. These fibres are selectively metabolized in the intestinal tract and as a result, promote the proliferation of beneficial bacteria. For example, a *Bifidobacterium* derived prebiotic (B-GOS) induced bifidogenic effect in microbiome of young volunteers [69].

Parabiotics are non-living, inactivated probiotics, but imitate the beneficial effect of the living microorganism. In the contrary of probiotics, parabiotics have some advantages in safety aspect. For example, the risk of infection, risk of microbial translocation and the

possibility of inflammatory responses are lower that may occur in individuals with weak immune system [84].

Postbiotics are water-soluble metabolites, which are metabolized by gut colonising bacteria. Postbiotics includes wide range of metabolites such as enzymes, proteins, peptides, saccharides, organic acid, SCFA etc. It is demonstrated, postbiotics can mimics the effects of probiotics without the risky inherent [84].

Antibiotics is an antimicrobial molecule, which inhibit the growth of bacteria. In case of bacterial infections, antibiotics are the primary agents of pharmacological defence. They target pathogenic bacteria, however, administration of antibiotics have also harmful effect on commensal bacteria in the gut and result reduced amount of microbiome and microbial diversity [69].

Faecal microbiota transplant (FMT) is a recently used administration. As it implies, FMT is a transplantation of faecal bacteria from healthy donor to a recipient. FMT was applied first in clinical trial against *Clostridioides difficile* infection and the treatment was highly effective against the infection. In addition, FMT is widely used application against different GI related disorders [85, 86].

DOI:10.14753/SE.2020.2417

2. Aim

My first aim was to investigate the effect of stress on the metabolic system. Therefore, I raised the following specific questions:

- How an acute restraint stress affects metabolic variables and locomotor behavior?
- What is the role of the hypothalamic paraventricular nucleus in the regulation of metabolic- and behavioral changes?
- What are the differences between metabolic changes seen in response to acute and chronic stress?

How the metabolic system recovers after repeated stress?

My second main aim was to test the hypothesis, whether rifaximin – non-absorbable antibiotic - restores chronic stress-induced gastrointestinal and inflammatory symptoms and changes in microbiome along with stress-induced changes in anxiety-like behaviour.

Third, we challenged the hypothesis if there is a relation between the systemic antibiotic consumption and the prevalence of Parkinson’s disease.

3. Materials and methods

3.1. Animals

All experiments were performed on male mice with C57BL/6J genetic background. CRH-Ires-Cre transgenic mouse line was used in the virus-injected experiments. Animals were born and housed at the minimal disease (MD) level of Medical Gene Technology Unit at the Institute of Experimental Medicine. Mice were housed in 12 h light/dark cycle (lights on from 6 a.m. to 6 p.m.) at 21–22 °C with humidity. Animals received standard pelleted rodent chow (VRF1, Special Diets Services (SDS), Witham, Essex, UK) containing 19,1 g% protein, 55,3 g% carbohydrate and 4,8 g% fat. Chow and water were provided ad libitum. Experiments were complied with the ARRIVE guidelines and performed in accordance with the guidelines of European Communities Council Directive (86/609 EEC), EU Directive (2010/63/EU) and the Hungarian Act of Animal Care and Experimentation (1998; XXVIII, Sect. 243/1998). All procedures and experiments were approved by the Animal Care and Use Committee of the Institute of Experimental Medicine (permit number: PEI/001/29-4/2013).

3.2. Stereotaxic surgery

CRH-IRES-Cre transgenic mice were anesthetized with a cocktail of 100 mg/kg ketamine and 10 mg/kg xylazine (1 ml/100 g bw, i.p.). Bilateral stereotaxic injection of a virus vector construct (pAAV8/hSyn-DIO-hM3D(Gq)-mCherry, Addgene; 4-7,9 x 10^{12}/ml, UNC GTC Vectore Core) was performed into both side of paraventricular nucleus (PVN) (30 nl/side). PVN was approached by a glass cannula at the following coordinates from Bregma: AP:-0,7mm; lat: -0,035mm DV: -0,5mm. After surgery, mice recovered for 3 weeks before the beginning of metabolic measurements. Control animals have been injected with pAAV-hSyn-DIO-mCherry.

3.3. Stress procedures

3.3.1. Acute and repeated stress

Mice were exposed to restraint acute stress for 1h (n=8). For the procedure, 50ml Falcon tubes were used with small holes on side and one at the end for breathing and ventilating. Tubes were filled with paper towel from the opening of tube and closed with own cap to avoid turning around. With this procedure, mice were immobilized without

being harmful and provided a stressful event. During the 1h, tubes were stabilized from outside. Experimental design and timeline diagram is shown on figure 4.

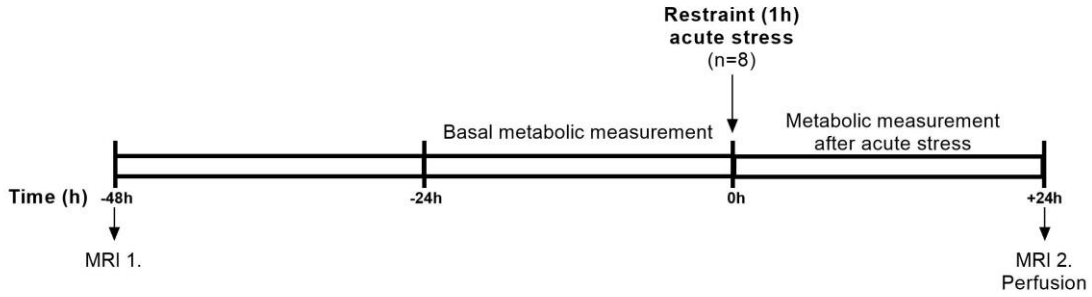

Figure 4. ***Overview of the acute stress experiment.***

3.3.2. Chronic variable stress (CVS)

During CVS, experimental animals were stressed for 4 weeks, two times daily, by different psychogenic stressors:

- *Water avoidance stress (WAS)* – The test apparatus was a plastic tank (40 cm length × 40 cm width × 30 cm height) with a fixed glass cylinder (d=8 cm) in the center of the floor. The tank was filled with fresh water to 1 cm below the top of block. The stressed mice were placed on the block for 1 h.
- *Disturbed circadian rhythm* - Mice were exposed to changed or extended light or dark phase.
- *Social defeat* – Experimental mice (intruder) were placed one by one into the home cage of dominant CD1 male mice (aggressor) and they were left there for 8 minutes.
- *Footshock* - Mice were shocked in every 20 sec by 0,5 mA electric shock for 12 minutes.
- *Forced swim* - Mice were forced to swim for 6 min in 18 cm high and 14 cm diameter glass cylinders filled with clean tap water.
- *Slanted cage* – The home cage of experimental mice was tilted to a 45° angle
- *Soaked bed* – The bedding was mixed with water in the home cage
- *Shaking* – The cages of the mice were placed on a shaker for 1 hour. The shaking speed was randomly changed during one hour.

- *Crowding* – The moving area of the mice was reduced and the experimental mice were crowded. In case of rifaximin experiment, vehicle and rifaximin treated mice were separately crowded.
- *Rat feces odour* – Feces of male rats was collected and it was placed into a Falcon tube with small holes and the tube was placed into the home cage of the stressed mice.

Daily schedule of the stressors is found in table 1. After CVS procedure, a cohort of experimental animals (n=4/group) were transferred to cages of Phenomaster system for metabolic measurements. Open field test was done with another cohort of mice (n=5-6/group), then they were sacrificed, blood was collected on EDTA and plasma was stored at -20°C until assays. Adrenal glands were dissected and measured after autopsy. Experimental design and timeline diagram is shown on figure 5.

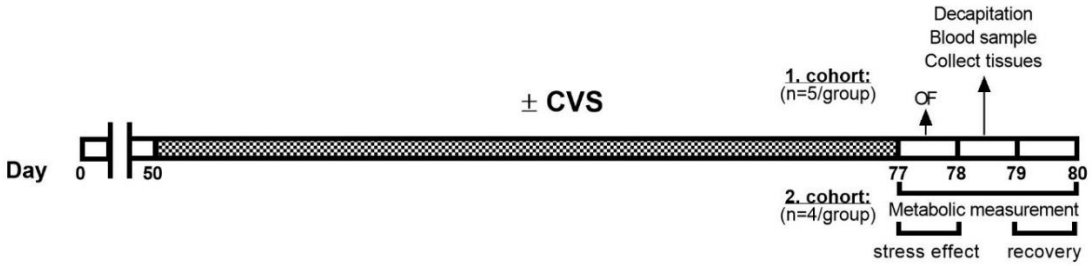

Figure 5. ***Overview of the chronic variable stress experiment.***

Chronic variable stress (2x daily); OF: Open field test.

Table 1. ***Daily schedule of the chronic variable stress.***

CVS protocol		
day	***a.m.***	***p.m.***
1.day	water avoidance	overnight light
2.day	social defeat	footshock
3.day	forced swimming	soaked bedding + slanted cages
4.day	crowding + shaking	crowding + dark for 18h
5.day	restraint	isolation
6.day	social defeat	forced swimming
7.day	crowding + shaking	soaked bedding + slanted cages
8.day	forced swimming	footshock
9.day	water avoidance	overnight light
10.day	social defeat	footshock
11.day	isolation + rat feces odour	isolation + rat feces odour + dark for 18h
12.day	crowding + shaking	crowding + soaked bedding + slanted cages
13.day	forced swimming	forced swimming
14.day	social defeat	restraint
15.day	rat feces odour + dark for 18h	crowding + shaking + overnight light
16.day	isolation + rat feces odour	footshock
17.day	forced swimming	crowding + soaked bedding
18.day	social defeat (6-10 min)	isolation + rat feces odour + dark for 18h
19.day	water avoidance	footshock
20.day	dark for 18h	crowding+shaking
21.day	crowding + soaked bedding + slanted cages	isolation + rat feces odour
22.day	footshock	forced swimming
23.day	water avoidance	overnight light
24.day	crowding + shaking	isolation + rat feces odour + dark for 18h
25.day	social defeat	slanted cages + soaked bedding
26.day	footshock	restraint + shaking

3.3.3. Two-hits stress protocol

This protocol is a frequently used procedure to induce anxiety or depression-like symptoms in experimental animals [87]. It started at postnatal day 1, when pups were separated from their mother (maternal separation MS) for 3 hours daily for 12 days (early life stress - first hit). During the three hours, mothers were placed into separate individual cages and offspring were transferred into a small box, which was placed on a heating pad

(30-33°C). Mothers and pups were in two separate rooms. Control litters were not separated and left undisturbed except the change of bedding once a week. Pups were weaned at the 21th day after born and they were housed 2-3/cages. At the age of 50 days, mice were exposed to chronic variable stress paradigm (CVS - second hit). The protocol followed the same CVS schedule, which is written in table 1.

3.4. General procedure in rifaximin experiment

During chronic variable stress, half of the animals received 300 mg/kg bw/day rifaximin, a non-absorbable antibiotic (Sigma). Animals from different litters were randomly assigned to rifaximin/vehicle groups. Rifaximin was dissolved in 5% hypromellose solution in drinking water. The other half of mice (controls) received 5% hypromellose to drink. Fluid intake and body weight of the animals was monitored and rifaximin concentration in the drinking water was adjusted. This experiment was performed on two different set of experimental mice. At the end of the experiment behaviour tests were performed on both sets (see below). After last test, one set of mice (n=5-7/groups) was decapitated (30 min after EPM) and trunk blood was collected on EDTA and plasma stored at -20°C. This blood sample was the measure of stress-induced CORT, as it was collected at the time of maximal adrenocortical CORT release provoked by EPM exposure. Adrenal glands and thymus were collected, cleaned and weighed for each mouse. Organ weights were normalized to final body weight and expressed as mg/g bw. Colon, liver, mesenteric lymph node and colon content were harvested and stored at -70°C until assay. The upper intestinal tract has a very low population of bacteria because of different factors like gastric acidity, propulsive motility and pancreatic enzymes. By contrast, the colon has a very stagnant motility with retropulsive contractions keeping the contents in the proximal colon and thus, the largest and “most constant” bacterial ecosystem located in the colon [88]. For this reason, colon tissue and content was used for further analysis. Experimental design and timeline diagram is shown on figure 6. The second set of mice (n=22) were exposed to gut permeability test after the last behavioural test (see below).

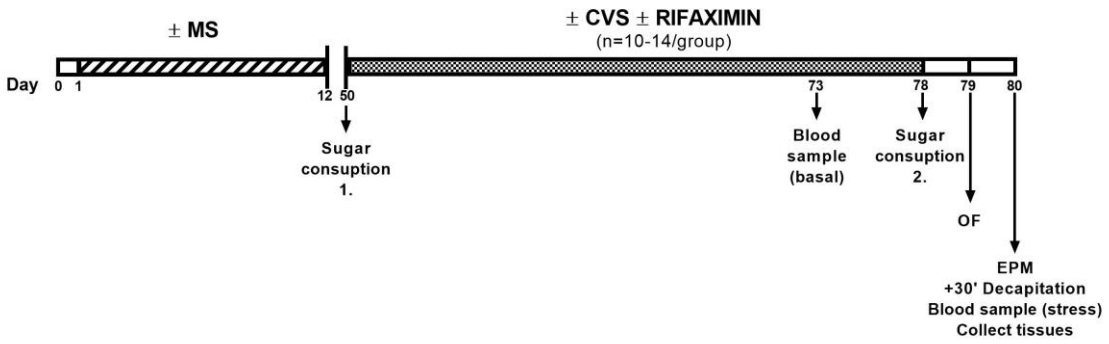

***Figure 6.** Overview of the rifaximin experiment.*

MS: Maternal separation (3h daily); CVS: Chronic variable stress (2x daily); OF: Open field test; EPM: Elevated plus maze test.

3.5. Metabolic measurements

Experimental mice were singly housed for 1 week before training. Then, the mice were housed in training boxes for 3 days for acclimatization to learn the use of feeders and drinking bottles. On the first day of acclimatization, body composition was measured by magnetic resonance imaging (MRI) scan (EchoMRI). One day long control measurement was performed in metabolic boxes (TSE Phenomaster) in normal circumstances after training (baseline). Then, mice were exposed to 1 h restraint acute stress. In case of virus-injected mice, control measurements were done after a saline injection, while the experimental mice were injected by clozapine-N-oxide (CNO). CNO was dissolved in 0,9 % saline solution (1 mg/ml) and was injected i.p. (dose:1mg/kg body weight). Control virus injected mice were treated by saline or CNO. After inducing stress response, and CNO/saline injections, the metabolic measurement was continued for further 24 hours. Experimental design and timeline diagram is shown on figure 7.

Chronically stressed mice were placed into metabolic cages and their metabolic changes were measured after the last stress of the CVS protocol for three days. Data of the first day were regarded as stress effect on metabolism and data of the third day were considered as recovery. Food- and O_2 consumption, CO_2 production and X-Y-Z locomotor activity data were automatically collected during the metabolic measurements. Energy expenditure (EE (kcal/h)) was calculated using a rearrangement of the abbreviated Weir equation as supplied by TSE Labmaster System: EE= (3.941 (VO2) + 1.106 (VCO2)) × 1.44. The respiratory exchange ratio (RER) was calculated also with the

following formula: VCO2/VO2. The body composition was determined again at the end of metabolic measurements.

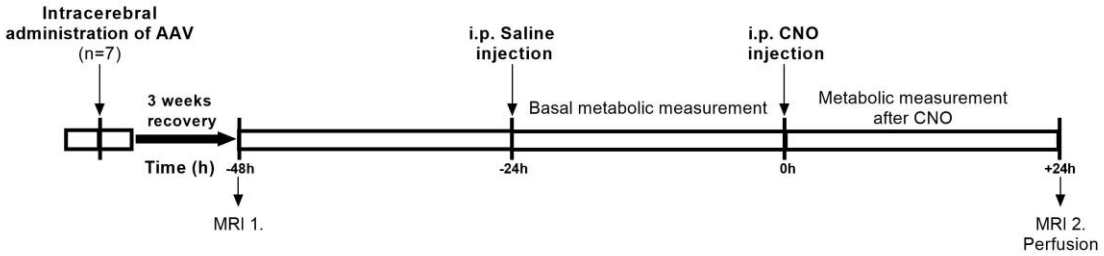

***Figure 7.** Experimental overview of the CNO induced metabolic measurement.*

3.6. Behavior tests

3.6.1. Sucrose consumption test

Sucrose consumption test was performed before the CVS part of two hits protocol and one day after chronic stress. Mice had free choice for 24h between two bottles: one with 1% sucrose solution and the other filled with tap water. The position of the two bottles was switched after 12h. Sucrose and tap water intakes were assessed by weighing bottles. The sucrose consumption was expressed as a percentage of total liquid intake. As we did not habituate the animals to sucrose, this test measures neophobia rather than sucrose preference [89].

3.6.2. Open field test

In open field test, mice were placed in the center of a 40x40x30cm, white, non-transparent plastic box and their exploration was video-recorded from above for 10 min and then analyzed by Noldus EthoVision XT 10 program. The open field was divided into 16 squares by a 4x4 grid in the software. The four inner squares of the grid were considered as central area.

3.6.3. Novel environment test

The first five minutes of the mouse behavior in the open field arena was analyzed by Solomon Coder software. Four different behavior elements were differentiated in this analysis: walk, survey, rearing and grooming. The analysis was carried out by two individuals blinded to subject treatment group. Walking was noted when the mouse changed its location or turned as long as the front paws moved. Surveying was noted

when all paws were on the floor and head directed upwards. Rearing was noted when two hind legs were on the floor and head directed upwards.

3.6.4. Elevated plus maze

The elevated plus maze (arm length-30 cm, arm width-7 cm, wall height-30 cm platform height-80 cm) apparatus was made of dark-grey painted Plexiglas. Open arms were surrounded by 0,3 mm high ledges. Mice were placed into the central area of the platform facing to one of the open arms and were allowed to explore the apparatus for 5 min. Mice were considered to enter a compartment when all four legs crossed the lines separating the compartments. Videos were analyzed by Noldus Observer software. Percentage of time spent in closed arms was used as a measure anxiety-like behavior.

3.7. Gut permeability test in vivo

To assess gut permeability, four experimental groups were formed: control, vehicle treated; control, rifaximin treated; chronically stressed, vehicle treated and chronically stressed, rifaximin treated mice. The dose of rifaximin was 300 mg/kg, vehicle was 5% hypromellose) After overnight of fasting, all animals received FITC-labelled 4kDa Dextran (Sigma-Aldrich) via oral gavage (dose: 44 mg/kg; 100 mg/ml). 2 hours later, 250-300 µl blood was collected from heart, centrifuged and serum was collected. Serum samples were diluted with an equal volume of PBS and FITC concentration was measured from 100 µl of diluted serum at excitation 485nm and emission 535nm wavelength using Cytation 5 Cell Imaging Multimode reader (Biotek Instruments). A standard curve was obtained by serial dilution of FITC-dextran solution in PBS (range: 0-16000 ng/ml). Equal volume of non-hemolytic serum from non- gavaged mice was added to the serial dilution before measurement.

3.8. Hormone, endotoxin, glucose and triglyceride measurement from plasma

Plasma corticosterone was measured from 10µl plasma by direct RIA as described Zelena et al. [90].

To determine plasma endotoxin levels, commercially available limulus amebocyte lysate (LAL) assay was used in accordance of the manufacturer's instructions (Pierce LAL Chromogenic Endotoxin Quantitation Kit, Thermo Scientific).

Plasma glucose level was determined by Glucose Colorimetric Detection Kit from plasma according to the manufacturer's protocol (Glucose Colorimetric Detection Kit, Invitrogen).

Plasma triglyceride (TG) level was measured by multiparameter diagnostic device for triglycerides (MultiCare-in; Biochemical Systems International Srl).

3.9. Gene expression analysis

Frozen colon tissue samples were homogenized by Bertin Technology Minilys homogenizer in 300 µl TRI reagent. Then, total mRNA was isolated from the homogenate using a Total mRNA Mini Kit (Geneaid) according the manufacturer's instruction. To eliminate genomic DNA contamination, DNase I (Fermentas) treatment was used. Sample quality control and the quantitative analysis were carried out by NanoDrop (Thermo Scientific). cDNA synthesis was performed with High Capacity cDNA Reverse Transcription Kit (Applied Biosystems). Real-Time PCR was carried out in ABI StepOnePlus instrument (Applied Biosystems) with Fast EvaGreen quantitative PCR master mix (Biotium) and gene-specific primers. Primers (Microsynth) were designed in our laboratory using Primer-BLAST software of the National Center for Biotechnology Information (NCBI). Forward and reverse primers used to quantify different mRNAs are listed in Table 2. Gene expression was analyzed by the $2^{-\Delta\Delta CT}$ method using the ABI StepOne Software v2.3 (Applied Biosystems). The amplicons were tested by melt curve analysis on ABI StepOnePlus instrument (Applied Biosystems). Relative changes in gene expression were normalized against GAPDH mRNA expression. Reference gene was selected based on the NormFinder software [91].

Table 2. ***Forward and reverse primers for the selected genes***

Genes	Forward primer	Reverse primer
GAPDH	*TGACGTGCCGC TGGAGAAA*	*AGTGTAGCCCAAGATGCCCTTCAG*
TJP1	*CGGCCGCTAAGAGCACAG*	*TGGAGGTTTCCCCACTCTGA*
TJP2	*GCAGAGACAACCCCCACTTT*	*CTTGACCACGATGGCTGCTA*
TJP3	*ACAGCATGCGGACCTACAAG*	*AGCCCTCGTCATCAGAGG AT*
Occludin	*CCGGCCGCCAAGGTTC*	*CATGCATCTCTCCGCCAT*
MUC2	*GCTGACGAGTGGTTGGTGAATG*	*GATGAGGTGGCAGACAGGAGAC*
Reg3b	*ACCCTCCGCACGCATTAGTT*	*TTTGGCAGGCCAGTTCTGCAT*
Retnlb	*TCAGTCGTCAAGAGCCTAAGAC*	*AGTCTGCCAGAAGACGTGAC*

3.10. Microbiome analysis

Total DNA was extracted from 200 mg colon content using QIAamp DNA Stool Mini Kit (Qiagen) according to the manufacturer's protocol. Total genomic DNA concentration and quality control was checked by using NanoDrop (Thermo Fisher). Targeting the bacterial 16S ribosomal RNA gene, dominant taxon of the gut microbiome were analyzed by real time quantitative PCR with Fast EvaGreen quantitative PCR master mix (Biotium) and taxon specific primers (Table 3.) on ABI StepOnePlus instrument (Applied Biosystems). In case of *Proteobacteria*, primer specificity for the phylum could not be confirmed, therefore, different subdivisions of the phylum were determined (*Alpha-*, *Beta-*, *Epsilon-* and *Gamma-Proteobacteria*). The position of the specific primers in 16S rRNA gene and primer references are found in Table 3. The primer specificity was tested by Melt Curve Analysis. DNA samples were diluted to the same concentration 5ng/µl. Quantification was done by using standard curves made from known concentrations of the respective amplicon for each set of primers. Gene expression was analyzed using ABI StepOne v2.3 program (Applied Biosystems). The results are expressed in copy number (CN) and it was calculated with the following formula: $CN = A*6x10^{23}/(L*660)*1x10^{9}$ ng/g; where A is the amount of the amplicon in ng, L is the length of the amplicon.

Table 3. **Forward and reverse primers of the targeted microorganism, the PCR amplicon position in the 16S rRNA gene and the references of primers.**

Target organism	Amplicon position in the 16S rRNA gene	Sequence	Ref.
Actinobacteria	Act920F3 Act1200R	f: TACGGCCGCAAGGCTA r: TCRTCCCCACCTTCCTCCG	[92]
Bacteroidetes	Bact934F Bact1060R	f: GGARCATGTGGTTTAATTCGATGAT r: AGCTGACGACAACCATGCAG	[93]
Clostridium sp.	Clos58-f Clos780-r	f: AAAGGAAGATTAATACCGCATAA r: ATCTTGCGACCGTACTCCCC	[94]
Cyanobacteria	Cya-F783 Cya-R1100	f: GGCAGCAGTGGGGAATTTTC r: GTMTTACCGCGGCTGCTGG	[95]
Firmicutes	928F-Firm 1040FirmR	f: TGAAACTYAAAGGAATTGACG r: ACCATGCACCACCTGTC	[92]
α-proteobacteria	A682F 908aR	f: CIAGTGTAGAGGTGAAATT r: CCCCGTCAATTCCTTTGAGTT	[96]
β-proteobacteria	Beta680F 1392R	f: CRCGTGTAGCAGTGA r: ACGGGCGGTGTGTACA	[97]
γ-proteobacteria	1080γF γ1202R	f: TCGTCAGCTCGTGTYGTG r: CGTAAGGGCCATGATG	[92]
Verrucomicrobia	VER_37F VER_673R	f: TGGCGGCGTGGWTAAGA r: TGCTACACCGWGAATTC	[98]
Total bacteria	331F 797R	f: TCCTACGGGAGGCAGCAGT r: GACTACCAGGGTATCTAATCCTGTT	[99]

3.11. Bacterial load in mesenteric lymph node

Mesenteric lymph nodes (MLN) were aseptically collected and stored at -70°C. Total DNA was isolated from MLN by Tissue Genomic DNA Mini Kit (Geneaid) according to the manufacturer. DNA concentration and quality control was checked by using NanoDrop (Thermo Scientific). Samples were diluted to the same DNA concentration. Then total DNA was amplified targeting bacterial 16S rRNA gene by using a universal bacterial primer (Table 3.). Amplification was processed by RT-PCR as described in 2.6.

3.12. Histological methods

3.12.1. Perfusion and tissue processing

24h after metabolic measurement, restraint stress was repeated on CRH-Ires-Cre x tdTomato transgenic mice. In rAAV8/hsyn-DIO-hM3D(Gq)-mCherry injected mice, a second treatment with CNO was performed. Two hours after the beginning of stress or CNO injection, (at the maximum of cFos expression) mice were anesthetized and perfused with ice cold fixative (4% paraformaldehyde in 0.1 M phosphate buffer pH 7.2) for histology. Chronically stressed mice, which were kept in metabolic cages, were perfused 72h after metabolic measurements. The fixed brain tissue was dissected, post-fixed in the same fixative supplemented with 10% sucrose and incubated overnight in KPBS with sucrose. Then, coronal sections (20 μm) were cut on freezing microtome and stored in cryoprotectant at −20 °C until use.

In case of rifaximin experiment, cleaned colon samples was placed immediately after decapitation into 10% buffered paraformaldehyde (pH=7.4) for 24 h. Fixed tissues were embedded in paraffin and sectioned 5 μm thick sections in two parallel series.

3.12.2. Haematoxylin & eosin staining, imaging and quantification

One series of the two parallel colon sections was deparaffinized and stained with haematoxylin & eosin (H&E) according to a standard protocol. Images of stained colon sections were captured under 20x magnification with Spot RT color digital camera on Nikon Eclipse 6000 microscope. Mucosa thickness was measured by using ImageJ software, in a blinded manner. From each mouse, five sections were randomly selected, from each section, 10 measurements were done and averaged.

3.12.3. Immunostaining, imaging and quantification

To check the place of virus injections and to verify the effect of acute stress, free-floating coronal brain sections were washed three times in KPBS. To avoid nonspecific binding, sections were incubated in 2% normal donkey serum (Jackson ImmunoResearch Laboratories) in PBS/0,3% Triton X100 at room temperature for 1h. Then, sections were incubated in rabbit anti-c-Fos antibody made in rabbit primer (sc-52 Santa Cruz Biotechnology, Santa Cruz, CA, 1:10000) at 4°C for 72h. After 3 times washing, sections were incubated in anti-rabbit Alexa Fluor 488 secondary antibodies produced in donkey (Life technologies 1:1000) for 1hour at room temperature. After incubation, sections were

washed again in KPBS and were cover-slipped with DAPI Fluoromount-G (SouthernBiotech). Digital images of hypothalamic paraventricular nucleus (PVN) were captured using Nikon C2+ confocal microscope.

F4/80 (murine macrophage marker) immunostaining was performed on colon samples by an immunohistochemical protocol for paraffin embedded sections. Slides were deparaffinized and rehydrated. Antigen retrieval pre-treatment was performed with proteinase K (Sigma; 10 mg/ml; diluted 1:25 in digestion puffer: 1M Tris and 0,5M EDTA). In this immunostaining, endogenous peroxidase was blocked by 0,3% H_2O_2. Next, slides were incubated in 2,5% normal rabbit serum then incubated in anti-mouse F4/80 antibody made in rat (BMA Biomedicals, T-2008; 1:50) overnight at 4°C in humidified boxes. After washing, slides were incubated in biotinylated secondary antibody (Vector Laboratories, 1:250) for 1 h. Then, immunoreactivity was visualized with Alexa FluorTM 488 Tyramide SuperBoostTM Kit, according to the manufacturer's instructions (Invitrogen by Thermo Fisher Scientific). Slides were cover slipped with DAPI Fluoromount-G (SouthernBiotech) and scanned with Pannoramic MIDI II Slide Scanner. Images were analyzed with Caseviewer 2.3. software by two different investigators, who were blinded to treatment. For quantitative analysis of the area% occupied by F4/80 immunoreactivity, ten images from each mouse were randomly selected and re-opened in Image J software. All images were set at a common threshold level and F4/80 positive areas were selected. Background subtraction procedure was performed equally in each image. The entire immunoreactive area fraction was then automatically measured by the program, with the same threshold. Area % was measured separately for submucosa and lamina propria.

3.13. Epidemiological data collection

Antibiotic consumption data, collected between 1997-2009 by the ESAC project (European Surveillance of Antibiotic Consumption network) and data from the ECDC (European Centre for Disease Prevention and Control) database (2010-2017) were used. Within the penicillin group, consumption data of narrow spectrum penicillins (J01CE) plus penicillinase resistant penicillins (J01CF) and the extended spectrum penicillins (J01CA) plus β lactamase inhibitor combination penicillins (J01CR) were separately compared to PD prevalence change data. Changes in PD prevalence between 1990-2016

were obtained from [100]. Correlation was calculated between antimicrobial consumption data and changes in PD prevalence.

3.14. Statistics

All data are shown as means ± SEM. Unpaired or paired two tailed Student's t-test were used when significant differences was determined between two groups. Statistical analysis was performed by two-way ANOVA (GraphPad Prism 7) followed by Sidak's multiple comparison test when the mean differences was calculated between groups that have been split on two independent factors. In case of sugar preference, data was analyzed by repeated-measures ANOVA followed by Sidak's post hoc test. Time was the repeated measure in paired two tailed Student's t-test and repeated-measures ANOVA. Correlation analysis was performed in our medical hypothesis between antimicrobial consumption and changes in PD prevalence. In all cases, differences were considered statistically significant at $p<0.05$.

DOI:10.14753/SE.2020.2417

4. Results

4.1. Basal metabolic and locomotor activity

Control, basal metabolic measurements were done on intact C57BL/6J mice for 72h. As seen on Fig. 8, locomotor activity and all metabolic parameters show circadian rhythmicity. Their locomotor activity, food intake, energy expenditure (EE) and respiratory exchange ratio (RER) are higher in the dark phase compared to the light phase (locomotor activity: $F(1,3) = 15.47$; $p = 0.0293$; food intake: $F(1.3) = 17,68$; $p = 0.0245$; EE: $F(1,3) = 39,94$; $p = 0.008$; RER: $F(1,3) = 24.4$; $p = 0.0159$). Two distinct peaks occur in all parameters during the active phase: the first at the beginning of dark phase and the second is before the inactive state.

DOI:10.14753/SE.2020.2417

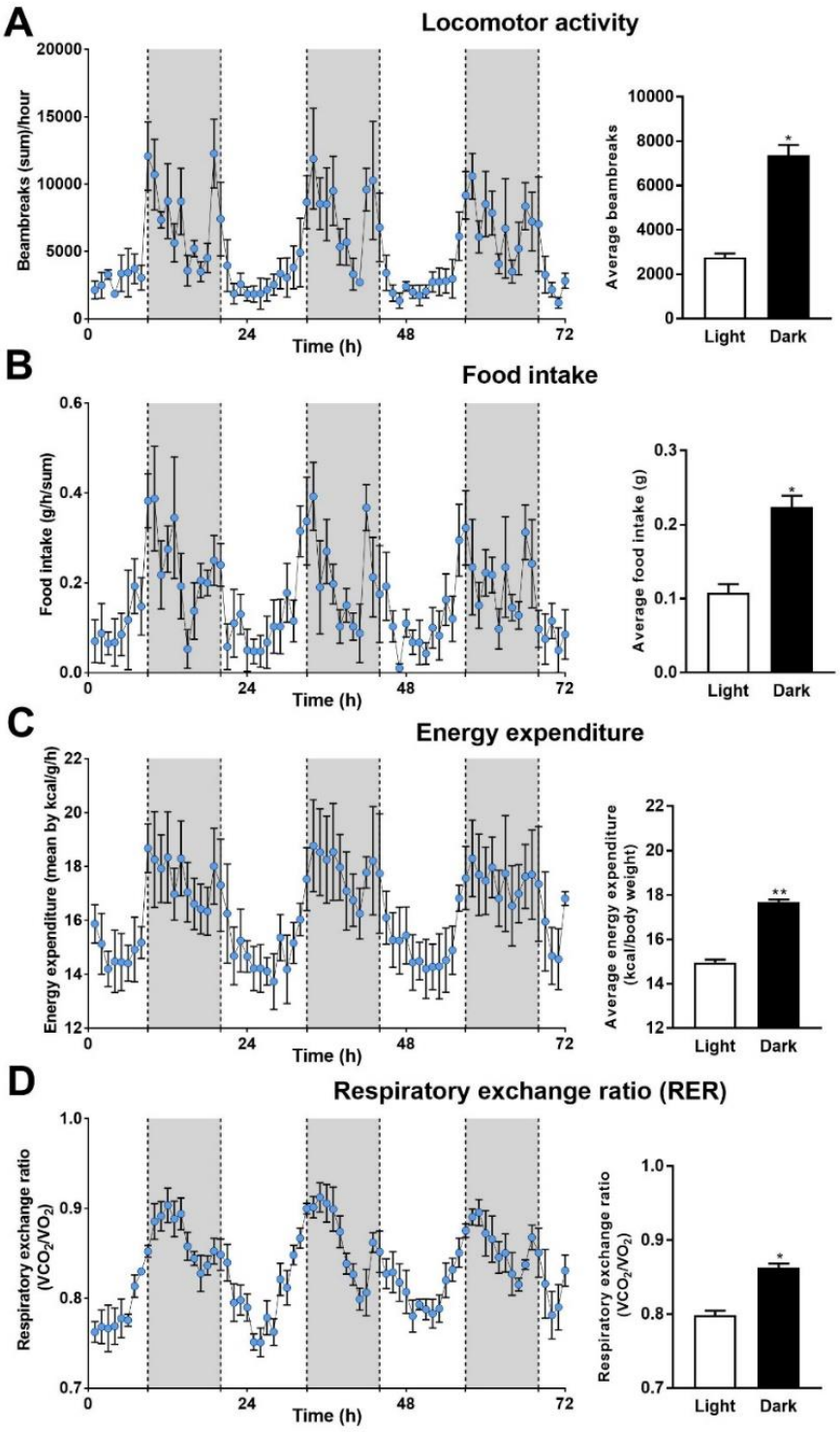

Figure 8. ***Basal metabolic measurement.***

*Baseline recordings of locomotor activity, food intake, energy expenditure (EE), respiratory exchange ratio (RER) and average of these activities in the light and dark phases. Data were analyzed by repeated two-way ANOVA (n =4). Time being the repeated measure. Mean ± SEM values, **p < 0.01 vs. control group [101].*

4.2. Acute restraint stress

Neuronal activity in the hypothalamus of CRH IRES Cre/TdTomato mice, as assessed by c-Fos immunostaining revealed selective activation of CRH neurons in response to 1h restraint stress. 60,5% of the CRH neurons were c-Fos positive in PVN of stressed mice. By contrast, CRH (Tomato) and c-Fos colocalization was not observed in the PVN of control, non-stressed mice (Fig. 9A). ACTH and corticosterone plasma levels were significantly increased in stressed mice compared to the controls [ACTH: t = 9.052; DF = 4; p = 0.0028; corticosterone: t = 4.461; DF = 4; p =0.0112] (Fig. 9B-C).

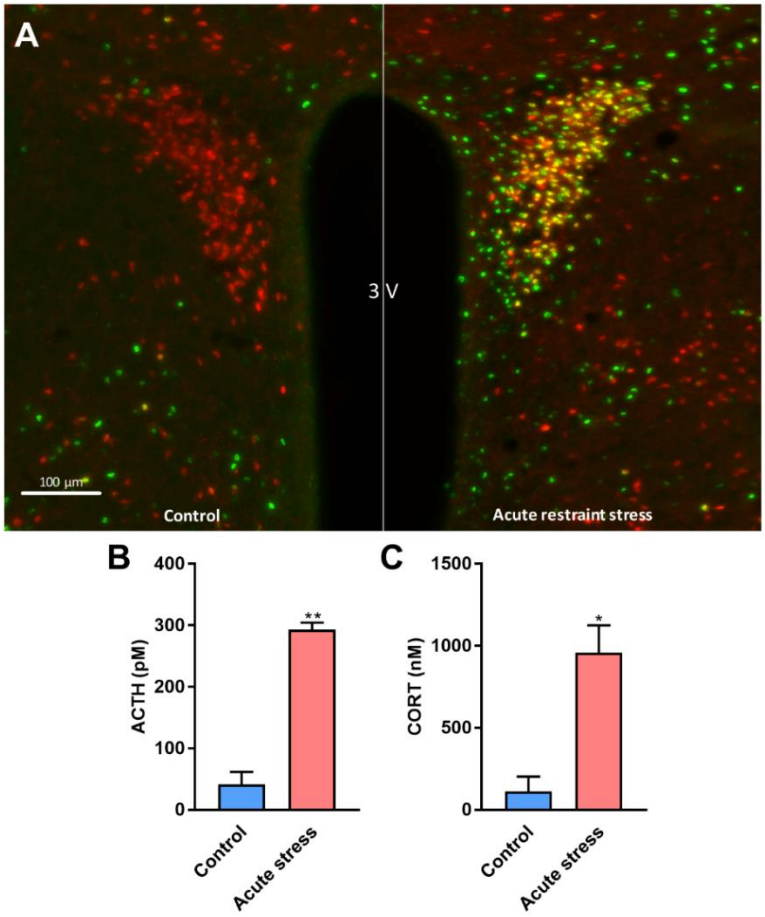

***Figure 9.* Effectiveness of acute stress.**

*Representative images of the hypothalamic paraventricular nucleus (PVN) from control and restrained mice. Red- tdTomato fluorescent protein expression in CRH neurons of CRH-IRES-Cre mice Green- c-Fos immunolabelled cell nuclei. Yellow- Stress-activated CRH neurons. 3V- third ventricle. Scale bar is 100µm (A) [not published] Plasma ACTH level (B) and plasma corticosterone level (C) in control vs. acutely restrained male mice. [101]. Data were analysed by unpaired t-test (n =3). Mean ± SEM values, *p<0.05, **p<0.01 vs. control group.*

DOI:10.14753/SE.2020.2417

4.3. Effects of acute psychological stress on locomotor behaviour and metabolic variables

4.3.1. Locomotor activity

Stressed mice displayed increased locomotor activity in the first hours after acute stress [measurement points during the first hour: 1. point: t = 0.3764; DF = 168; p = >0.9999; 2. point: t = 1.025; DF = 168; p = 0.9999; 3. point: t = 1.582; DF = 168; p = 0.9535; 4. point: t = 3.464; DF = 168; p = 0.0168; 5. point: t =3.656; DF = 168; p = 0.0085], it reminded elevated in the following three hours (Fig. 10B), however, average of the first four hours were not significantly changed [F(1,7) = 2.446; p = 0.1618] (Fig. 10C). The average locomotor activity was not changed when in the entire light phase was analyzed [F(1,7) = 1.427; p = 0.2712] (Fig. 10D). Nevertheless, locomotor activity of stressed animals was significantly decreased in dark phase compared to the basal measurements [F(1,7) = 6.823; p = 0.0348] (Fig. 10E).

DOI:10.14753/SE.2020.2417

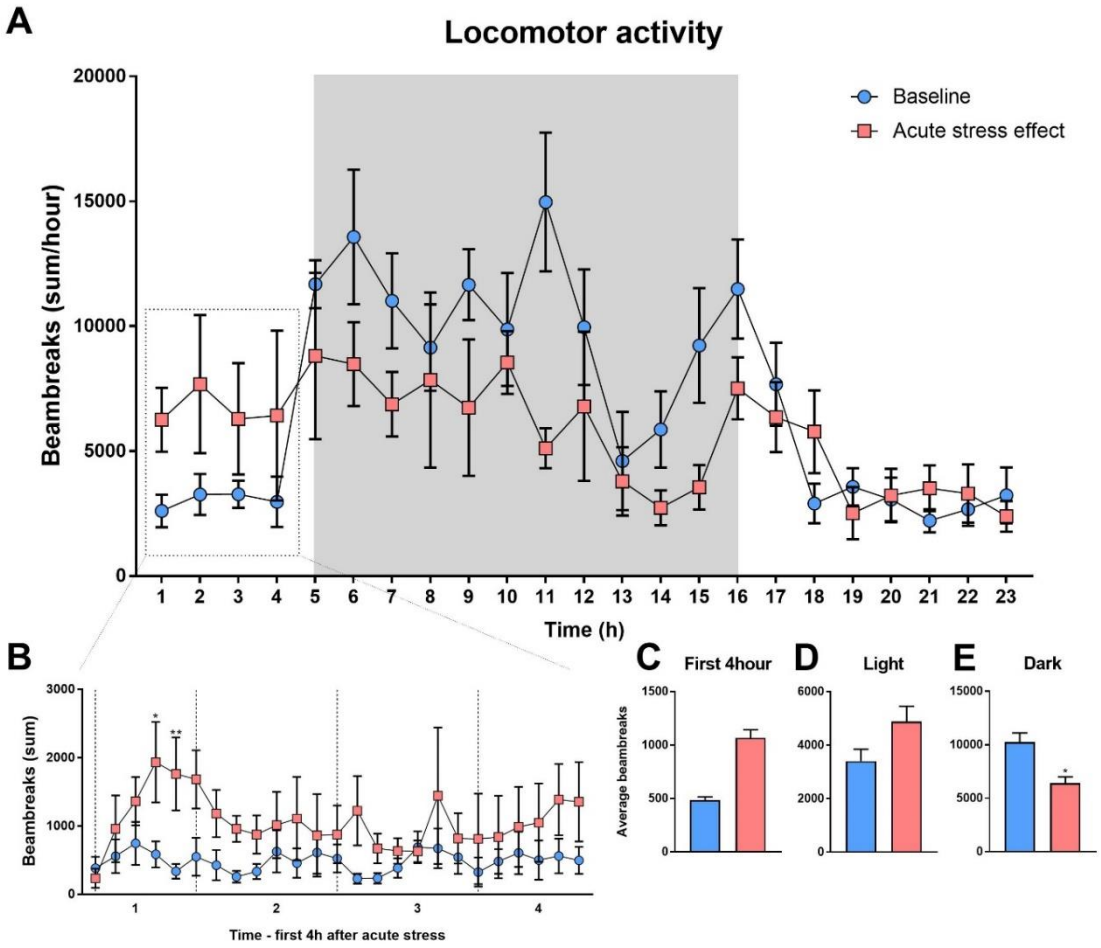

Figure 10. ***Acute stress effect on locomotor activity.***

*Daily timeline of locomotor activity after acute restraint stress compared to basal measurements (A). The first four (4) hour timeline of locomotor activity after acute stress compared to the basal measurements (B). Average locomotor activity in the first four hour (C), in the light phase (D) and in the dark phase (E) after acute stress. Data were analyzed by repeated measures two-way ANOVA. In case of the first four hours ANOVA was followed by Sidak's multiple comparison test (n =8). Time and treatment being the repeated measures. Mean ± SEM values, *p<0.05, **p<0.01 vs. control group [not published].*

DOI:10.14753/SE.2020.2417

4.3.2. Cumulative food intake

Stressed mice consumed more food in the first four hours after acute stress. After the third hour, significant difference was noticed between basal measurement and the measurements after acute stress [measurement points during the fourth hour: 1. point: $t = 3.16$; $DF = 168$; $p = 0.0457$; 2. point: $t = 3.917$; $DF = 168$; $p = 0.0033$; 3. point: $t = 4.34$; $DF = 168$; $p = 0.0006$; 4. point: $t = 3.316$; $DF = 168$; $p = 0.0276$; 5. point: $t = 3.539$; $DF = 168$; $p = 0.0129$; 6. point: $t = 3.872$; $DF = 168$; $p = 0.0038$] (Fig. 11B). However, this difference was equalized later and the cumulative food intake was not changed neither in the entire light phase [$t = 0.9107$; $DF = 7$; $p = 0.3927$] (Fig. 11D) nor in the entire dark phase [$t = 1.426$; $DF = 7$; $p = 0.1969$] (Fig. 11E).

DOI:10.14753/SE.2020.2417

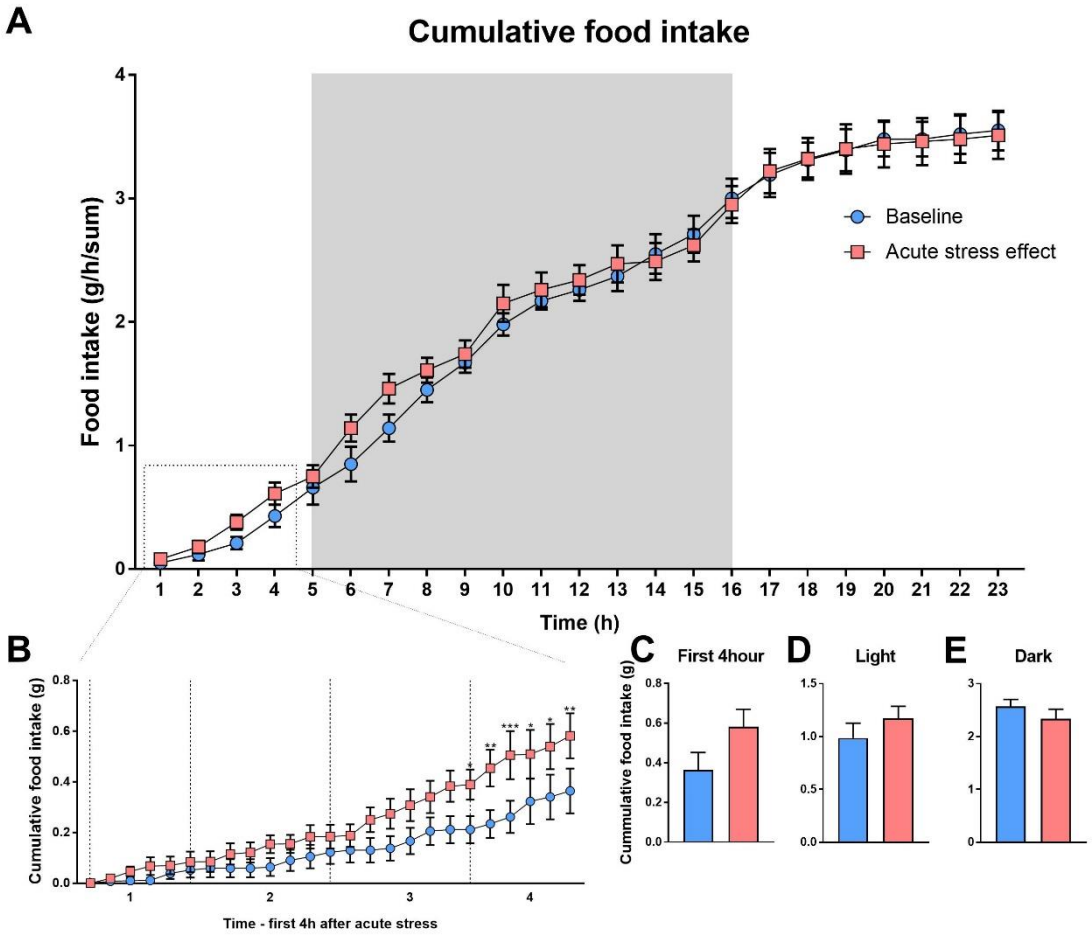

Figure 11. ***Effect of acute stress on food intake.***

*Daily timeline of cumulative food intake after acute restraint stress compared to the basal measurements (A). The first four hour timeline of cumulative food intake after acute stress compared to the basal measurements (B). Average cumulative food intake in the first four hour (C), in the light phase (D) and in the dark phase (E) after acute stress. Difference of cumulative food intake was tested by paired t-test. Time being the repeated measures. During the first four hours, significance of the continuous changes was analyzed by repeated measures two-way ANOVA followed by Sidak's multiple comparison test (n=8). Time and treatment being the repeated measures. Mean ± SEM values, *p<0.05, **p<0.01, ***p<0.001 vs. control group [not published].*

4.3.3. Energy expenditure (EE)

Energy expenditure (EE) was higher during the first four hours after acute stress [F(1,7) = 15.25; p = 0.0059] (Fig. 12B-C) and it was also significantly elevated in the entire light phase compared to the basal measurement [F(1,7) = 15; p = 0.0061] (Fig. 12D). However, there was no difference in the dark phase [F(1,7) = 0.000609; p = 0.981] (Fig. 12E).

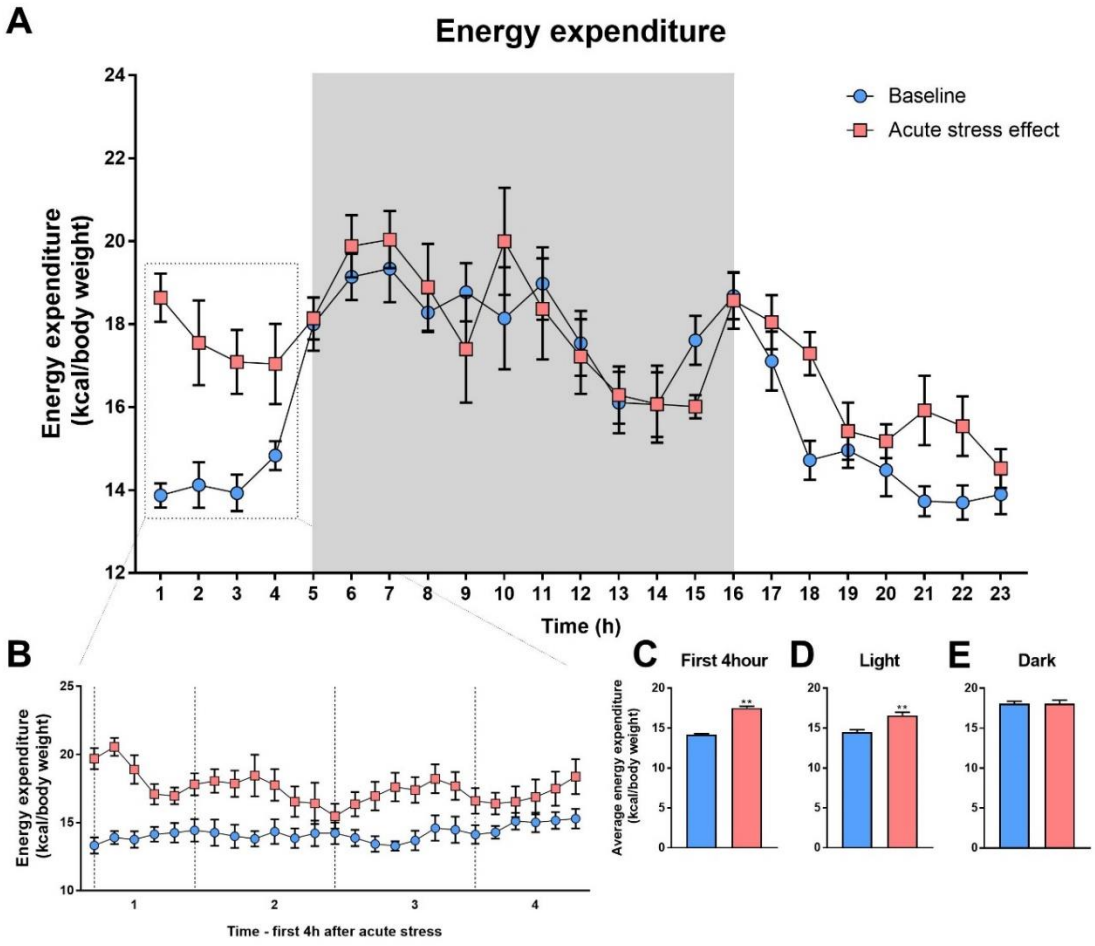

Figure 12. ***Effect of acute stress on energy expenditure.***

*Daily timeline of energy expenditure after acute restraint stress compared to the basal measurements (A). The first four hour timeline of energy expenditure after acute stress compared to the basal measurements (B). Average energy expenditure in the first four hour (C), in the light phase (D) and in the dark phase (E) after acute stress. Data were analyzed by repeated measures two-way ANOVA (n =8). Time and treatment being the repeated measures. Mean ± SEM values, **p<0.01 vs. control group [not published].*

4.3.4. Respiratory exchange ratio (RER)

RER is the ratio of carbon dioxide production (V_{Co2}) and oxygen (V_{O2}) used. The value indicates the predominant fuel source. The value usually changes between 0.7 and 1. RER of 1 indicates that carbohydrates was metabolized as the predominant fuel and RER of 0.7 indicates fat utilization. As seen on Figure 9, there were not significant differences in the utilization of energy sources in the first four hours (Fig. 13B-C) after acute stress neither in the light phase (Fig. 13D) nor in the dark phase (Fig. 13E).

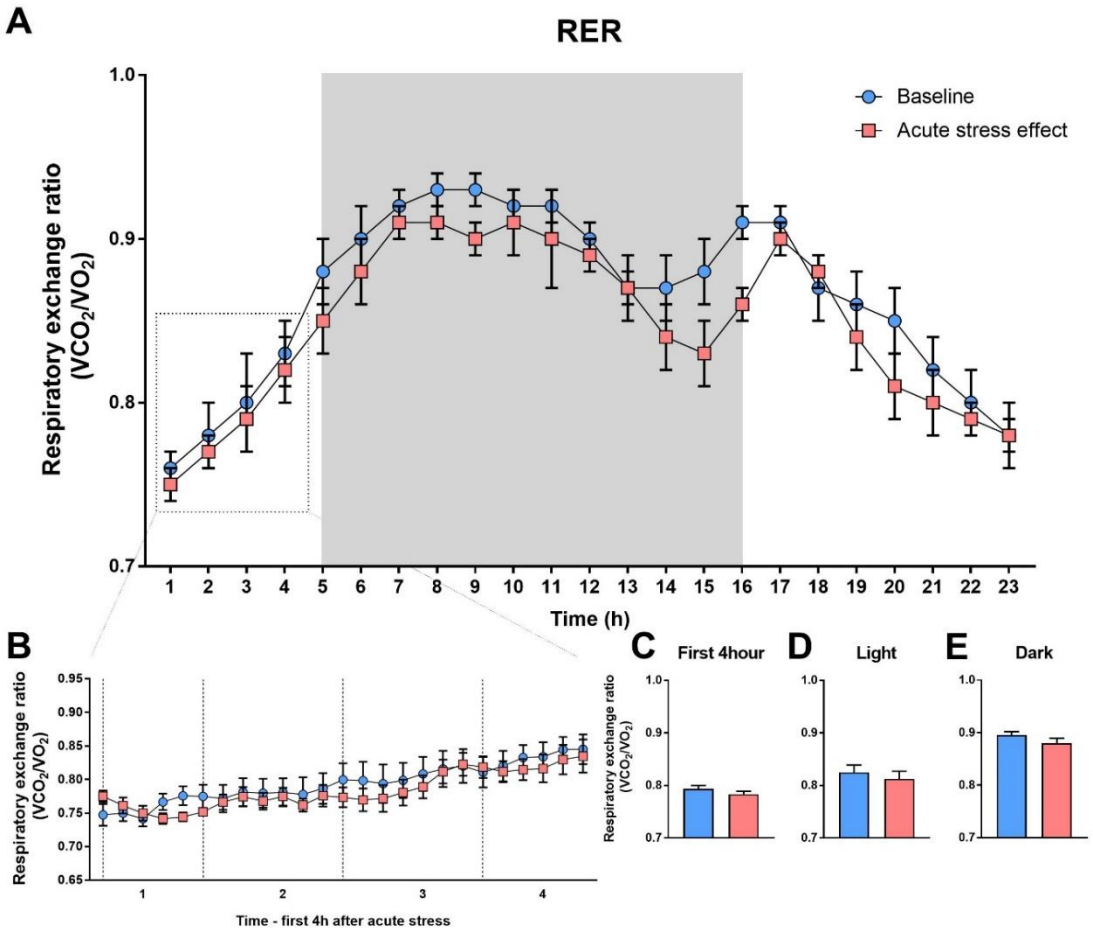

<u>Figure 13.</u> Effect acute stress on respiratory exchange ratio (RER).

Daily timeline of RER after acute restraint stress compared to the basal measurements (A). The first four hour timeline of RER after acute stress compared to the basal measurements (B). Average RER in the first four hour (C), in the light phase (D) and in the dark phase (E) after acute stress. Data were analyzed by repeated measures two-way ANOVA. In case of the first four hours ANOVA was followed by Sidak's multiple comparison test (n =8). Time and treatment being the repeated measures. Mean ± SEM values [not published].

4.3.5. Body composition

Body composition was measured before the beginning of 1h restraint stress and it was measured again 24h later by MRI. As seen on Figure 8., body weight and fat mass were decreased 24 hours later of acute stress [body weight: t = 2.437; DF = 7; p = 0.045; fat mass: t = 4.467 DF = 7; p = 0.0029] (Fig 14A-B). In lean mass, there was no effect of acute stress [t = 1.887; DF = 7; p = 0.1011] (Fig. 14C).

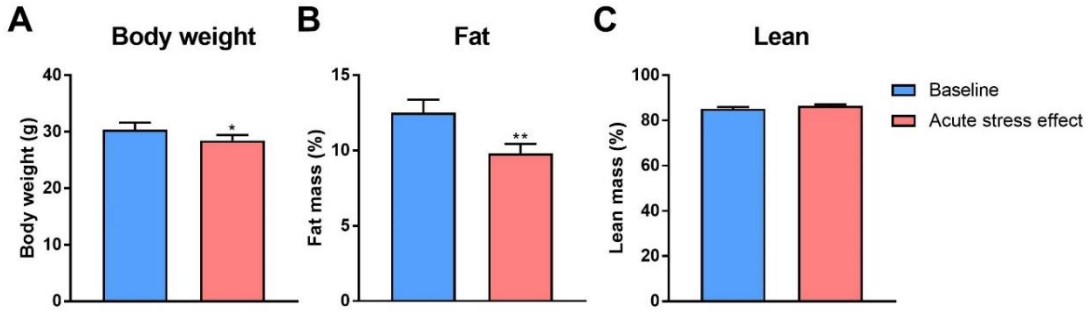

Figure 14. ***Effect of acute stress on body composition.***

*Body weight (A), fat mass (B) and lean mass (C) before and 24hours after acute restraint stress. Fat and lean mass represented as the percentage of body weight. Data were analyzed by paired t-test (n =8). Mean ± SEM values, *p<0.05, **p<0.01 vs. control group [not published]*.

4.4. Chemogenetic activation of CRH^{PVN} neurons

To reveal the contribution of stress-related CRH expressing neurons in challenge-induced locomotor and metabolic changes we chemogenetically manipulated these neurons in the paraventricular nucleus. To confirm that paraventricular CRH neurons (CRH^{PVN}) become activated after triggering Gq-DREADD receptors, CRH-IRES-Cre mice, -previously injected by Cre-dependent pAAV-hSyn-DIO-hM3D(Gq)-mCherry vector into the hypothalamic PVN region- received CNO injection (i.p.). Control animals were injected with pAAV-hSyn-DIO-mCherry vector and also challenged with CNO. In both cases, c-Fos expression was used an indirect marker of neuronal activity. As showed on Fig. 15., c-Fos induction was seen only in DREADD expressing mice. It has been noted that c-Fos expression after activation of CRH^{PVN} neurons goes beyond the nucleus and seen in non CRH neurons the peri-paraventricular region, possibly due to secondary neuronal activation originating in CRH^{PVN} cells.

DOI:10.14753/SE.2020.2417

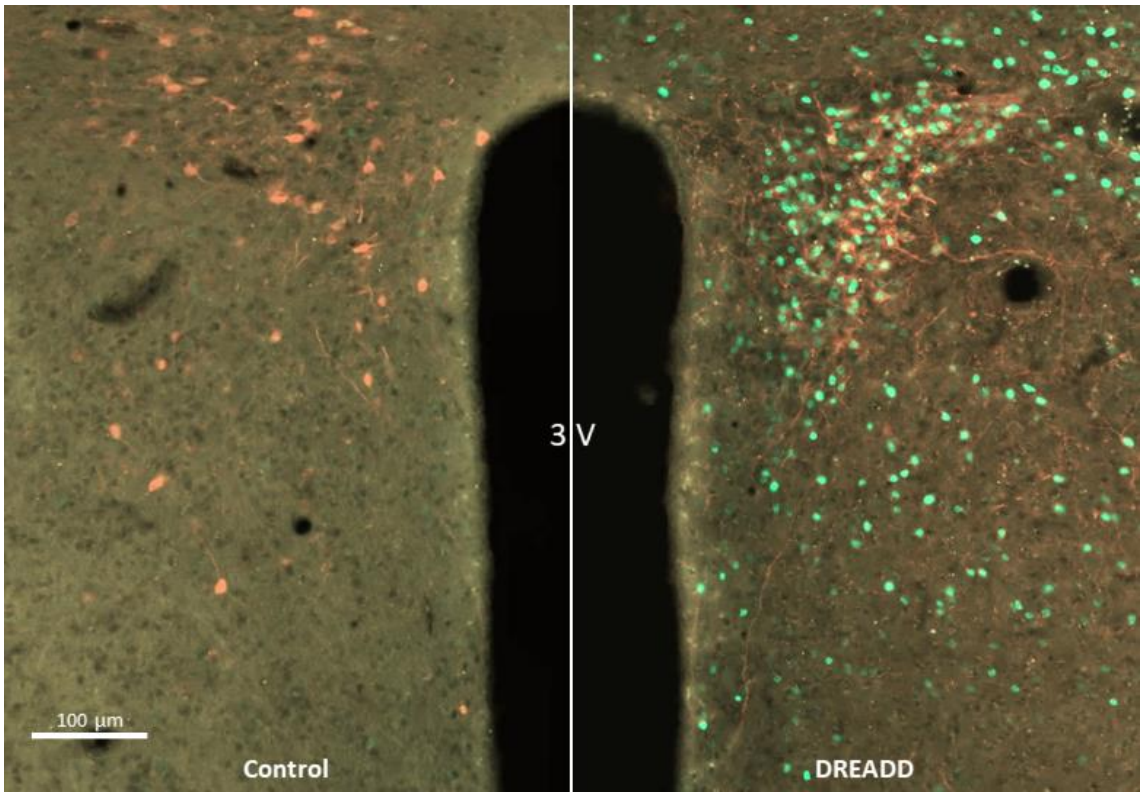

Figure 15. ***Activation of CRH neurons in PVN by DREADD.***

Representative images of the paraventricular hypothalamic area of control and DREADD virus injected mice. Red- mCherry fluorescent protein in CRH neurons; Green- c-Fos immunoreactive neurons. 3V-third ventricle. Scale bar is 100µm [not published].

4.5. Effect of CRH^{PVN} activation on locomotor behavior and metabolism

4.5.1. Locomotor activity

Locomotor activity did not change significantly after activation of CRH^{PVN} neurons within the first four hours after i.p. CNO treatment [$F(1,6) = 1.422$; $p = 0.2781$] (Fig. 16B-C), although there was a tendency for increased locomotion, when compared to saline injected mice. Similarly, there was no change in the average of locomotion neither in the light [$F(1,6) = 0.2377$; $p = 0.6432$] (Fig. 16D) nor in the dark phase [$F(1,6) = 0.7$; $p = 0.4348$] (Fig. 16E).

DOI:10.14753/SE.2020.2417

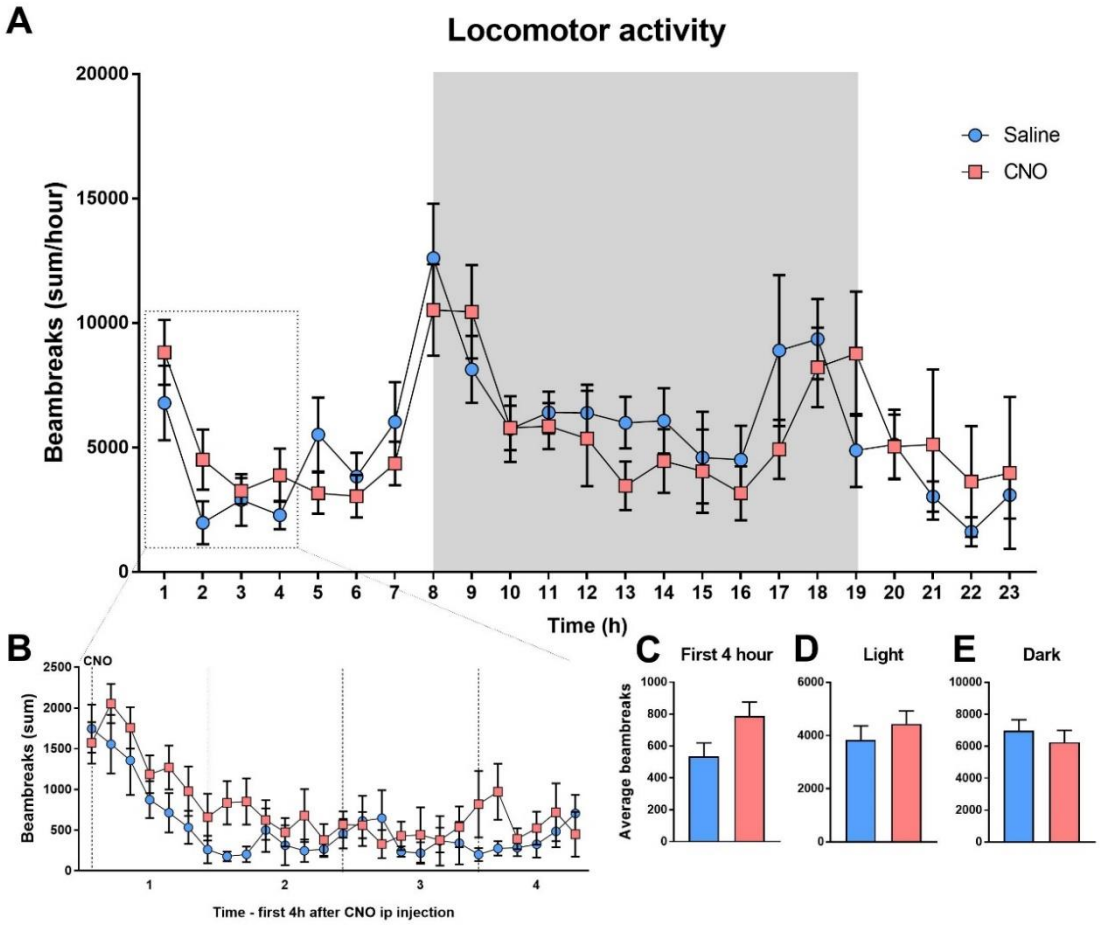

Figure 16. ***Effect of activation of CRH^{PVN} neurons on locomotor behavior***

Locomotor activity of CRH-IRES-Cre mice injected by pAAV-hSyn-DIO-hM3D(Gq)-mCherry vector into the PVN after CNO/saline treatment (A). The first four hour timeline of locomotor activity after CNO or saline (B). Average locomotor activity in the first four hour (C), in the light phase (D) and in the dark phase (E) after i.p. injections. Data were analyzed by repeated measures two-way ANOVA (n =7). Time and treatment being the repeated measures. Mean ± SEM values [not published].

4.5.2. Cumulative food intake

The average of cumulative food intake was significantly higher in the first four hours after CNO injection [t = 3.53; DF = 6; p = 0.0124] (Fig. 17B-C). However, there was no difference in cumulative food intake in the entire light phase [t = 1.761; DF = 6; p = 0.1287] (Fig. 17A and D), however, it was significantly decreased in the dark phase [t = 3.165; DF = 6; p = 0.0194] (Fig. 17E).

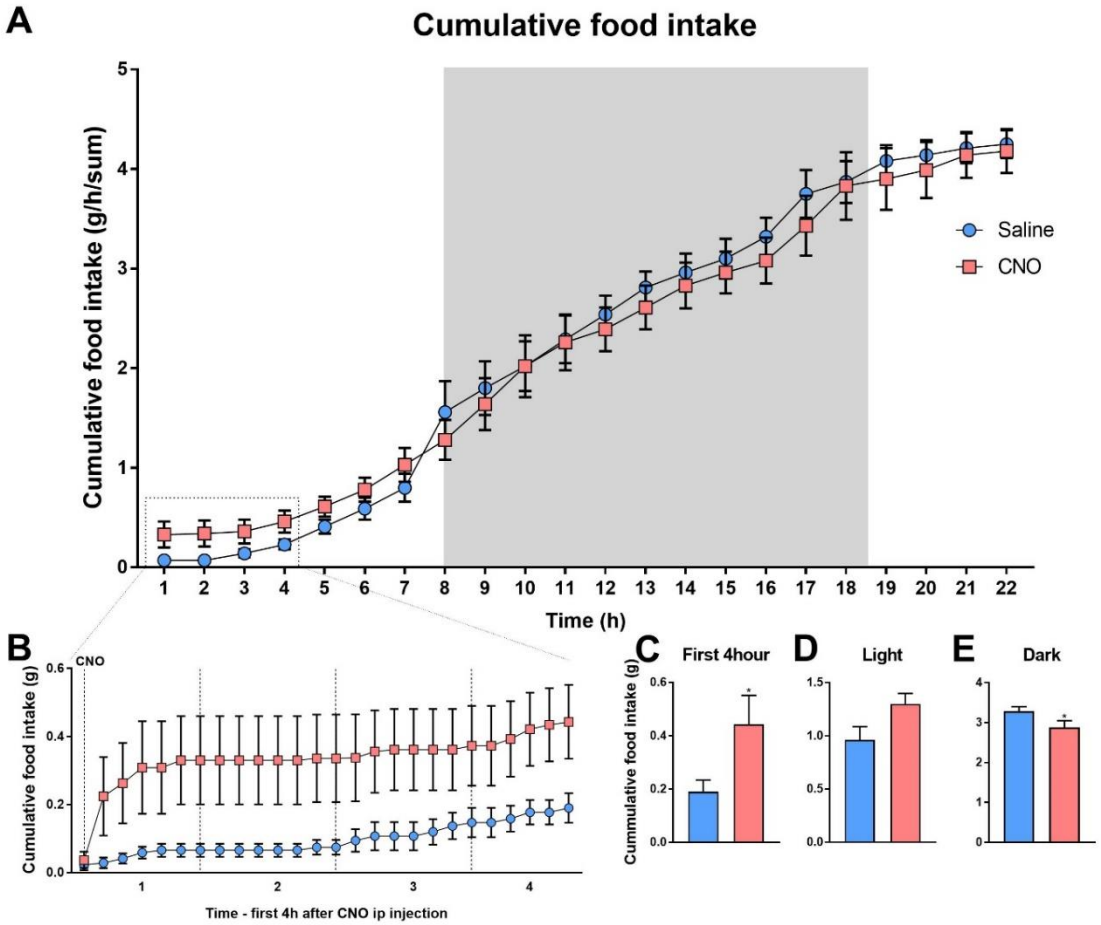

Figure 17. ***Effect of chemogenetic activation of CRH^{PVN} neurons on cumulative food intake.***

*Daily timeline of cumulative food intake after CNO treatment compared to the measurements after saline injection (A). The first four hour timeline of cumulative food intake after CNO/saline injections in DREADD expressing mice (B). Average cumulative food intake in the first four hour (C), in the light phase (D) and in the dark phase (E) after activation of CRH^{PVN} neurons. Data were analysed by paired t-test (n =7). Time being the repeated measures. Mean ± SEM values, *p<0.05 vs. control group [not published].*

4.5.3. Energy expenditure (EE)

After CNO injection, average of energy expenditure was significantly higher in the first four hour [F(1,6) = 15.61; p = 0.0075] (Fig. 18B-C). After the fourth hour, there was no difference in EE between saline and CNO treatment and the average of energy expenditure did not changed neither in the light (Fig. 18D) nor in the dark phase [light: F(1,6) = 4.758; p = 0.0719; dark: F(1,6) = 2.691; p = 0.1521] (Fig. 18E).

DOI:10.14753/SE.2020.2417

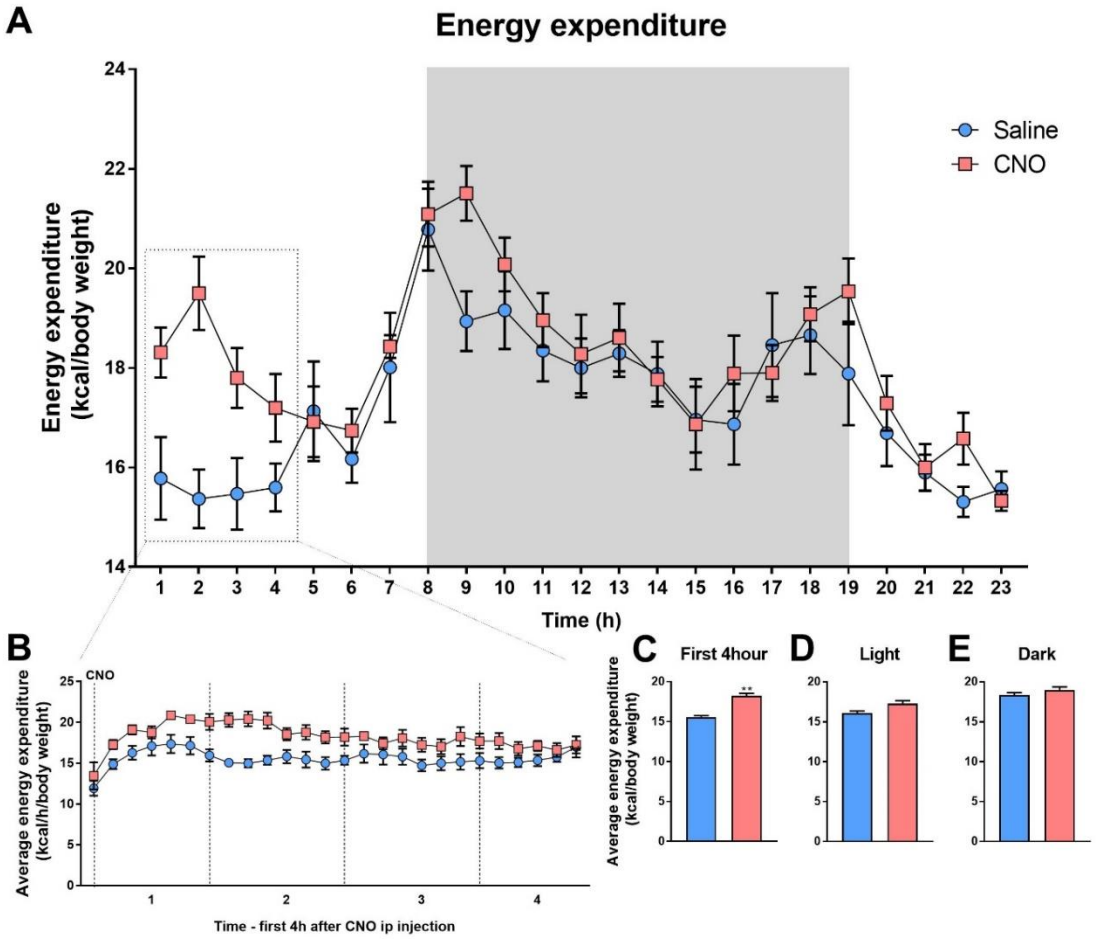

Figure 18. Effect of chemogenetic activation of CRH^{PVN} neurons on the energy expenditure.

*Daily timeline of energy expenditure after CNO treatment compared to the measurements after saline injection (A) in CRH-IRES-Cre mice injected with virus vectors encoding stimulatory DREADDs. The first four hour timeline of energy expenditure after activating CRH^{PVN} neurons by CNO (B). Average energy expenditure in the first four hour (C), in the light phase (D) and in the dark phase (E). Data were analysed by repeated measures two-way ANOVA (n =7). Time and treatment being the repeated measures. Mean ± SEM values, **p<0.01 vs. control group [not published].*

4.5.4. Respiratory exchange ratio (RER)

There was no difference in the respiratory exchange ratio during 23 hours of metabolic measurements after CNO injection compared to RER values after saline injection [first 4 hour: $F(1,6) = 0.03247$; $p = 0.8629$; light: $F(1,6) = 0.1221$; $p = 0.7387$; dark: $F(1,6) = 2.848$; $p = 0.1424$] (Fig. 19A-E).

DOI:10.14753/SE.2020.2417

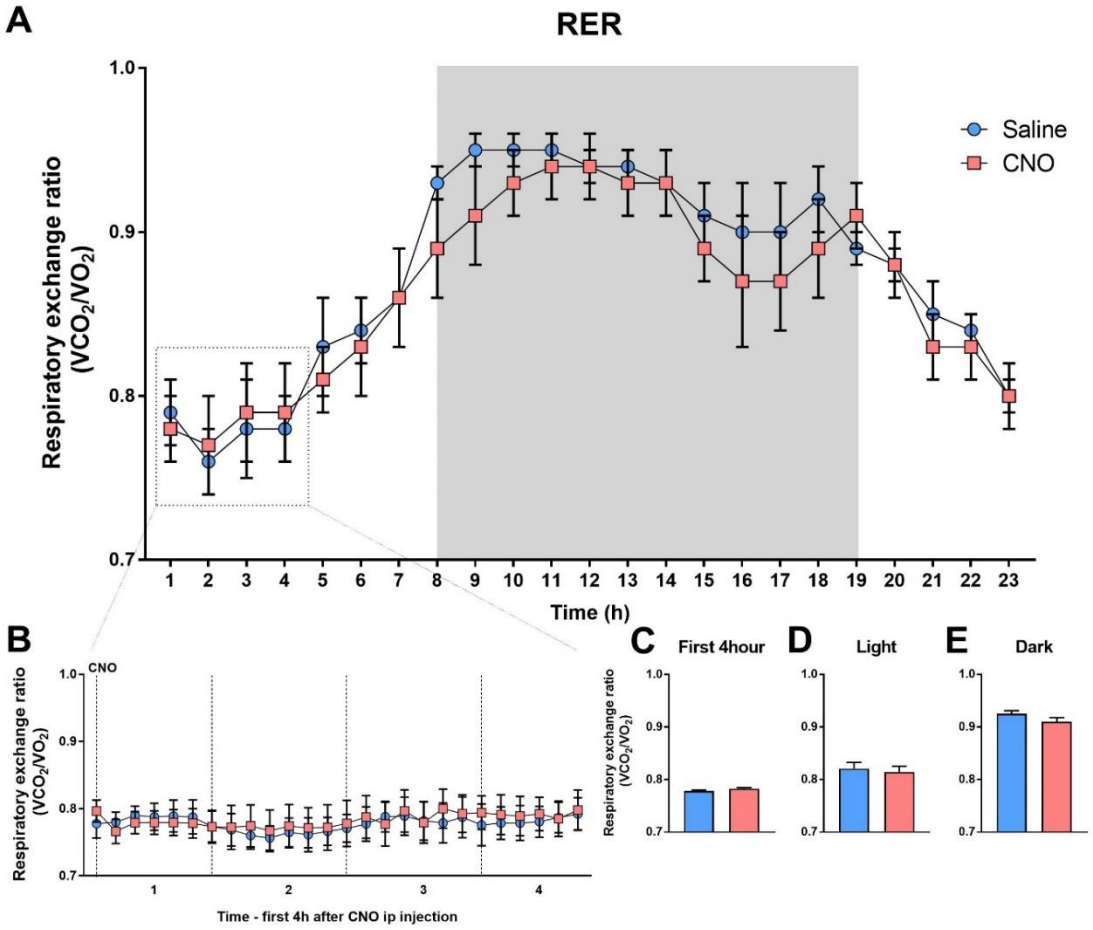

<u>Figure 19.</u> Effect of chemogenetic activation of CRH^{PVN} neurons on respiratory exchange ratio.

Daily timeline of respiratory exchange ratio after CNO treatment compared to the measurements after saline injection (A). The first four hour timeline of RER after CNO/saline injections in DREADD expressing mice (B). Average respiratory exchange ratio in the first four hour (C), in the light phase (D) and in the dark phase (E). Data were analyzed by repeated measures two-way ANOVA (n =7). Time and treatment being the repeated measures. Mean ± SEM values [not published].

4.5.5. Body composition

Body composition changes of DREADD expressing mice, was measured by MRI on the first day of acclimatization and at the end of metabolic measurements. As shown on Fig. 20, body weight and fat mass were significantly reduced [body weight: t = 2.541; DF = 6; p = 0.0440; fat mass: t = 2.954; DF = 5; p = 0.0317] and lean mass did not change [t = 0.5653; DF = 6; p = 0.5923] at the end of measurements.

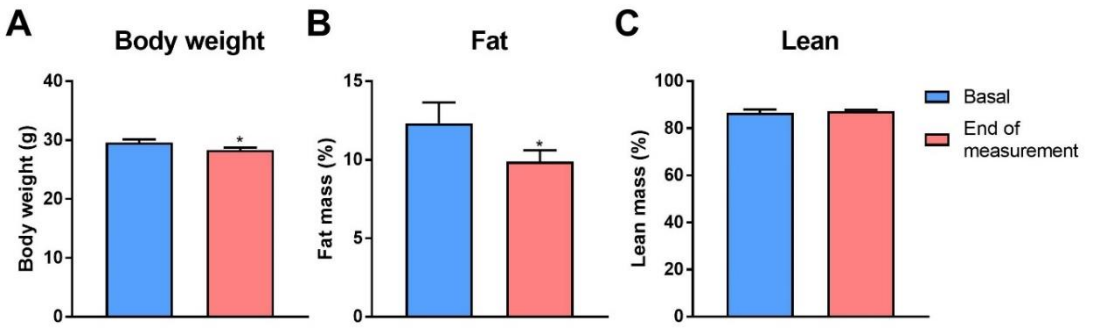

Figure 20. ***DREADD induced stress effect on body composition.***

*Basal body weight at the first day of acclimatization (blue) and body weight at the end of measurements (red) (A). Fat mass at the first day of acclimatization (blue) and fat mass at the end of measurements (red) (B). Basal lean mass at the first day of acclimatization (blue) and lean mass at the end of measurements (red) (C). Fat and lean mass represented in the percentage of body weight. Data were analysed by paired t-test (n =8). Time being the repeated measures. Mean ± SEM values, *p<0.05 vs. control group [not published].*

4.6. Control experiments

To examine whether CNO injection or virus injection are able to influence the metabolic system, control virus injected mice (DREADD gene was not included in plasmid (see chapter 4.2.) were kept in metabolic cages for 24h and their metabolic changes were measured after CNO injection. These results were compared to intact control mice and to DREADD injected mice after saline treatment. Locomotor activity of both virus injected mice (control and DREADD containing virus) was decreased in the dark phase compared to the intact control mice, however, this reduced locomotor activity was significant only after CNO injection [DREADD virus + saline vs. intact control: q = 2.735; DF = 65; p = 0.1373; control virus + CNO vs. intact control: q = 5.811; DF = 65; p = 0.0003] (Fig 21A). The average food intake, EE and RER did not changed neither in light nor in dark state after CNO treatment [Food intake - DREADD virus + saline vs. intact control: q = 0.9666; DF = 65; p = 0.7739; control virus + CNO vs. intact control: q = 0.7158; DF = 65; p = 0.8686; EE - DREADD virus + saline vs. intact control: q = 2.261; DF = 65; p = 0.2534; control virus + CNO vs. intact control: q = 0.6945; DF = 65; p = 0.8758; RER - DREADD virus + saline vs. intact control: q = 0.6873; DF = 65; p = 0.8782; control virus + CNO vs. intact control: q = 0.04946; DF = 65; p = 0.9993] (Fig 21B-D), however, energy expenditure was increased significantly in the first four hours

after i.p. injection compared to intact control mice [DREADD virus + saline vs. intact control: q = 5.266; DF = 9; p = 0.0119; control virus + CNO vs. intact control: q = 4.064; DF = 9; p = 0.044] (Fig. 21C).

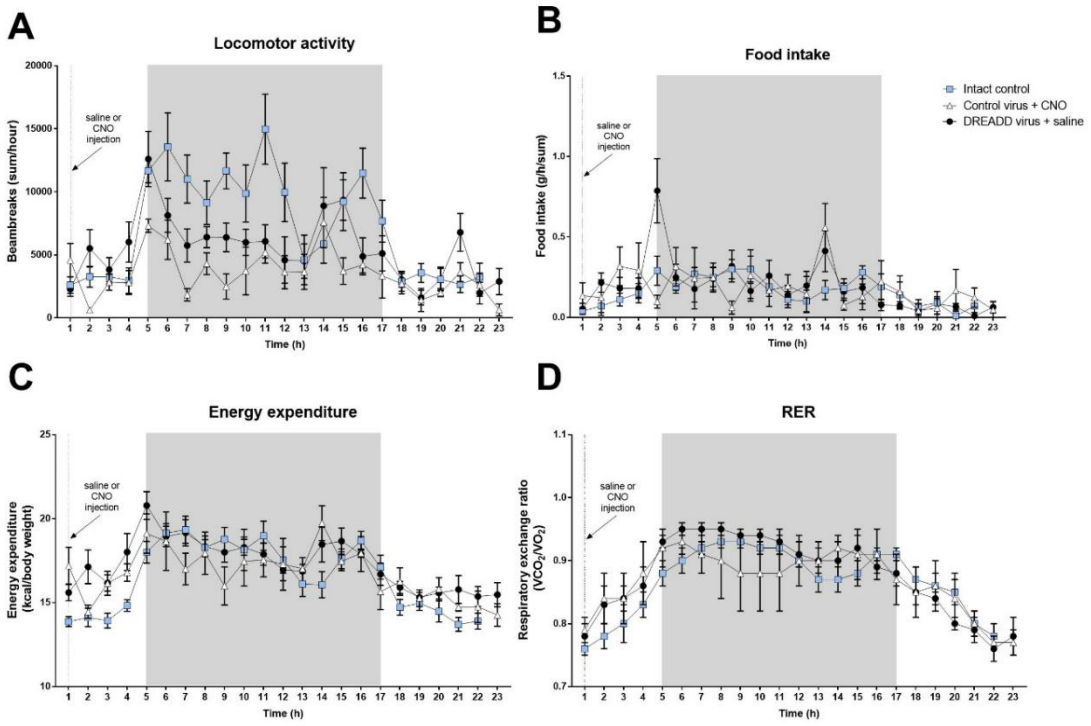

<u>Figure 21.</u> Effectiveness of virus injection and CNO injection on metabolic system. *Daily timeline of locomotor activity (A), food intake (B), energy expenditure (C) and respiratory exchange ratio (D). Blue – intact control (n=8), white – control virus + CNO i.p. injection (n=4) and black – DREADD virus + saline i.p. injection (n=7). Data were analysed by one-way ANOVA followed by Tukey's multiple comparisons test. Mean ± SEM values (not published).*

4.7. Effects of chronic stress

Mice exposed to chronic stress did not gain significant body weight by the end of stress protocol, when compared to non-stress controls as shown on Fig.18. [control – compared to initial bodyweight: t = 4.359; DF = 16; p = 0.001; CVS - compared to initial body weight: t = 1.588; DF = 16; p = 0.2464] (Fig. 22A). To check the behavioral effect of the CVS, mice were exposed to open field one day after the end of CVS procedure. Chronically stressed mice spent significantly less time in centrum (t = 2.332; DF = 8; p = 0.048) (Fig. 22D) and the latency of the first entry into corners were shorter (t = 3.651;

DF = 8; p = 0.0065) (Fig. 22E) compared to non-stressed controls. These mice were then sacrificed and different stress markers measured. CVS resulted in adrenal enlargement [t = 2.492; DF = 8; p = 0.0374] (Fig. 22B) and increased plasma corticosterone level [t = 2.532; DF = 8; p = 0.0351] (Fig. 22C).

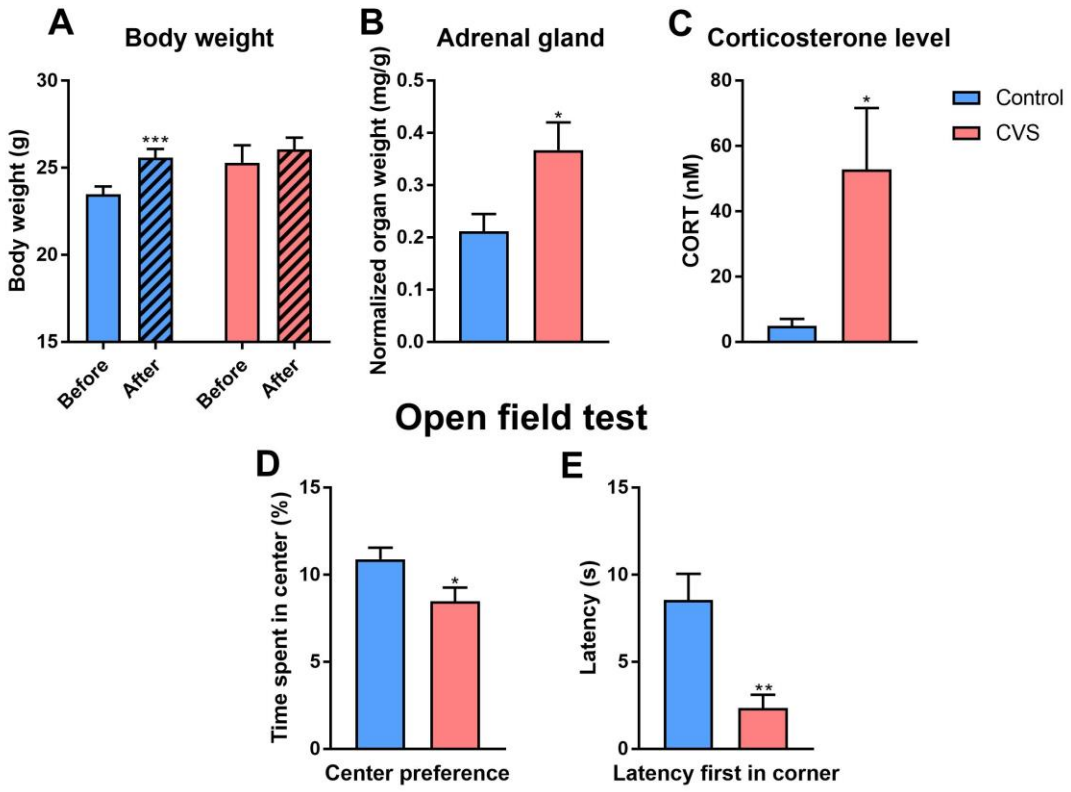

Figure 22. Effects of chronic stress on body weight, adrenals, plasma hormone level and behaviour.

*Body weights of control (blue) and chronically stressed mice before and after CVS protocol (A). Normalized adrenal gland weight (B). Plasma corticosterone level (C). Center preference (D) and the first latency to corner (E) during open field test. Data were analyzed by unpaired t-test (n=5/group). Mean ± SEM values, *p<0.05, **p<0.01, ***p<0.001 vs. control group. In case of body weight gain, repeated two-way ANOVA followed by Sidak's multiple comparison test were done (n =9). Time being the repeated measures. Mean ± SEM values, *p<0.05, **p<0.01, ***p<0.001 vs. initial body weight [not published].*

DOI:10.14753/SE.2020.2417

4.8. Effect of chronic variable stress on metabolism

After the CVS procedure, metabolic changes of the experimental mice were measured for 72 h. The first 24h (right after the CVS protocol) of the measurements were considered as stress effect and the last 24h was regarded as recovery of CVS exposed mice.

4.8.1. Locomotor activity

The average of locomotor activity chronically stressed mice was significantly higher in the light phase [q = 3.91; DF = 31; p = 0.0009], In the dark phase, locomotor activity was not changed significantly during the three days of measurements after CVS compared to the control mice [control vs. stress effect q = 2.144 DF = 33; p = 0.0716; control vs. recovery q = 1.867; DF = 33; p = 0.1254] (Fig. 23A-B).

DOI:10.14753/SE.2020.2417

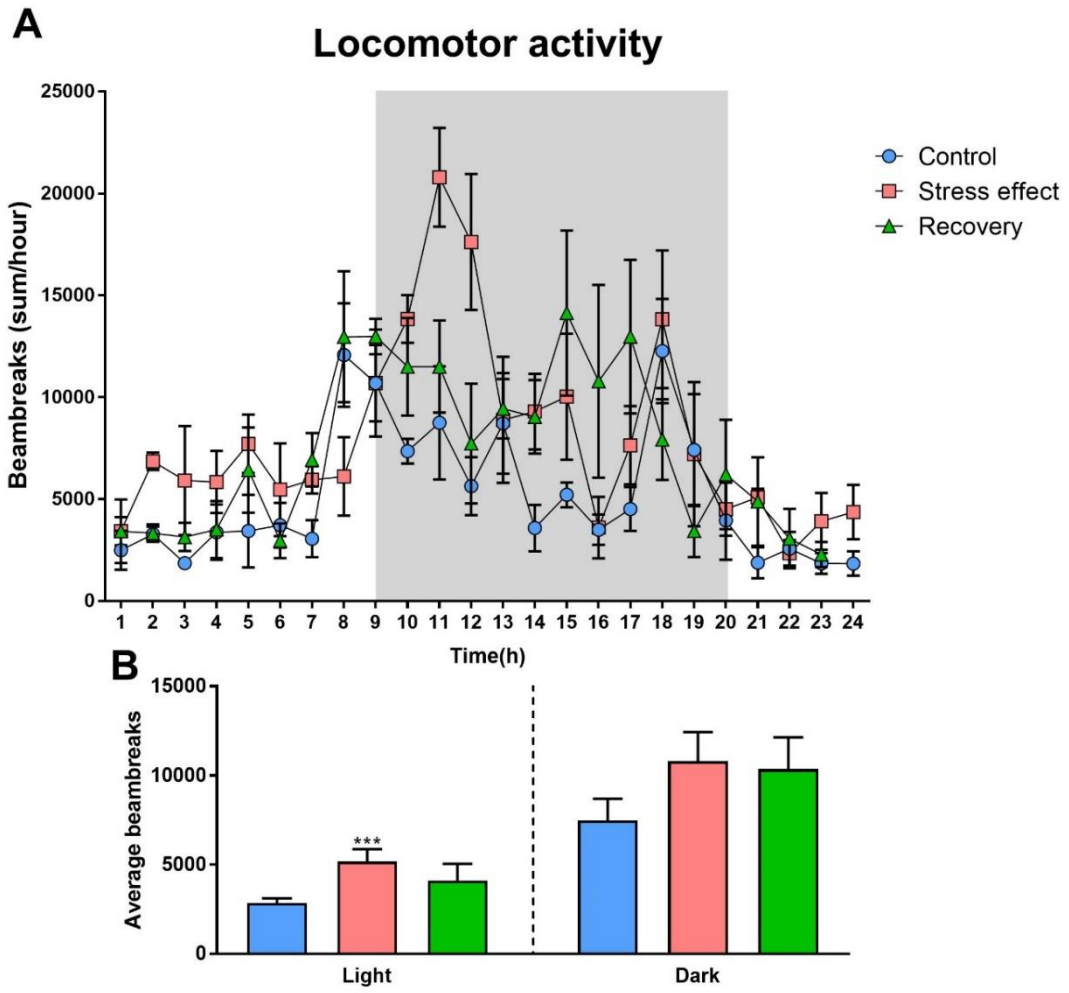

Figure 23. ***Chronic stress effect on locomotor activity.***

*Daily timeline of locomotor activity in control mice (blue) and mice exposed to chronic variable stress, CVS (red). (A). Average locomotor activity after chronic stress (red) during recovery (green) and in controls (blue) in the light and dark periods (B). Data were analysed by one-way ANOVA followed by Dunnett's multiple comparison test. Significance was calculated by repeated two-way ANOVA between stress effect and recovery (n =4). Time being the repeated measures. Mean ± SEM values, ***p<0.001 vs. control [not published].*

4.8.2. Cumulative food intake

Food consumption of the stressed mice was higher after CVS procedure but it was elevated significantly only during the active phase [light: q = 1.175; DF = 9; p = 0.4274; dark: q = 2.818; DF = 9; p = 0.0361]. The cumulative food intake reminds elevated during recovery compared to the control mice, however, it was not significant [light: q = 0.184; DF = 9; p = 0.9756; dark: q = 1.48; DF = 9; p = 0.2853] (Fig. 24A-B).

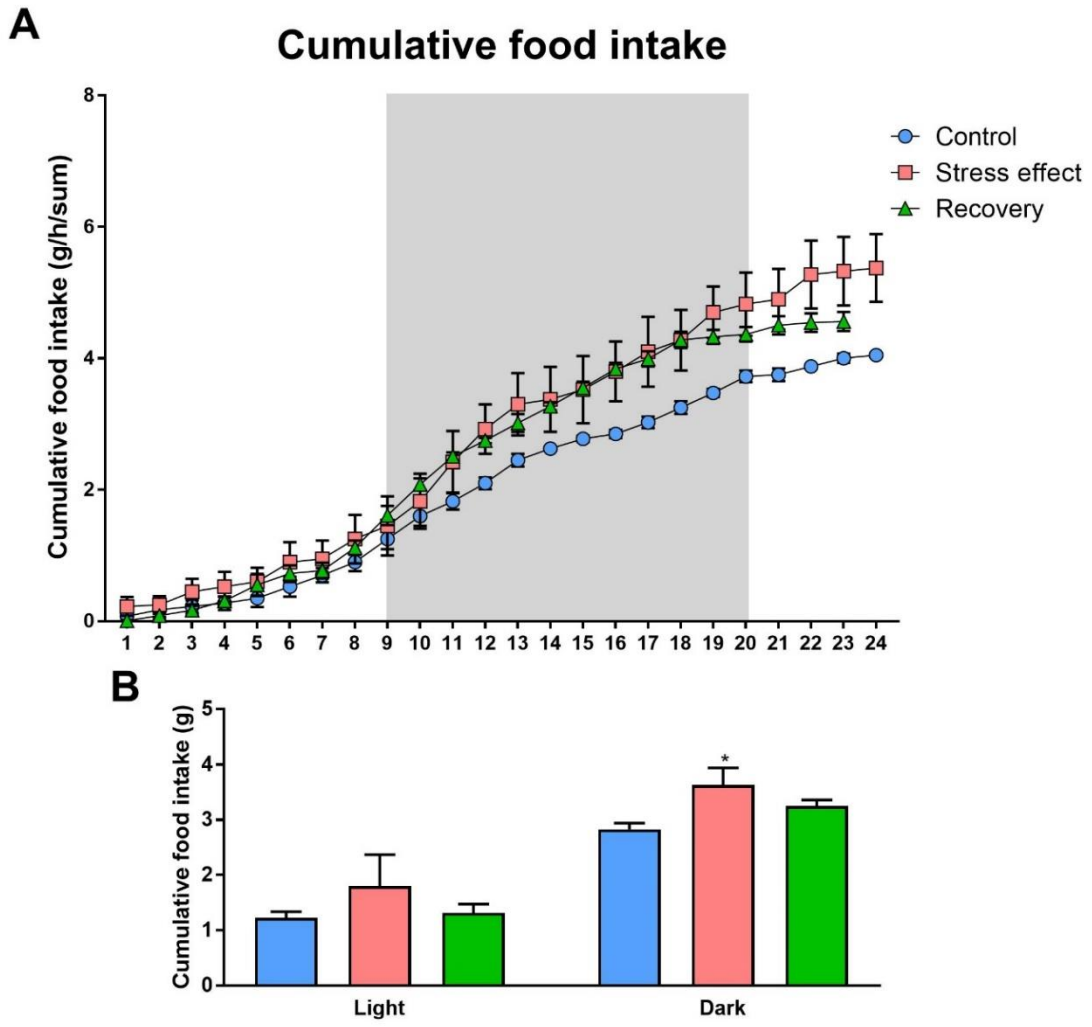

Figure 24. ***Chronic stress effect on cumulative food intake.***

*Daily timeline of cumulative food intake after chronic stress (red), during recovery (green) and control mice (blue) (A). Average cumulative food intake after chronic stress (red), during recovery (green) and in control mice (blue) in the light and dark phase (B). Data were analyzed by one-way ANOVA followed by Dunnett's multiple comparison test. Significance was calculated by paired t-test between stress effect and recovery (n =4). Time being the repeated measures. Mean ± SEM values, *p<0.05 vs. control group [not published].*

4.8.3. Energy expenditure

Energy expenditure of chronically stressed mice was continuously higher during the three days of metabolic measurements compared to control mice [control vs. stress effect - light: q = 20.6; DF = 33; p = <0.0001; dark: q = 10.3; DF = 33; p = <0.0001; control vs. recovery - light: q = 13.45; DF = 33; p = <0.0001; dark: q = 8.009; DF = 33; p = <0.0001]. However, statistical analyses revealed that during recovery, the average energy expenditure was decreased significantly in the active phase compared to the energy expenditure of stress effect [F(11, 36) = 2.325; p = 0.028] (Fig. 25A-B).

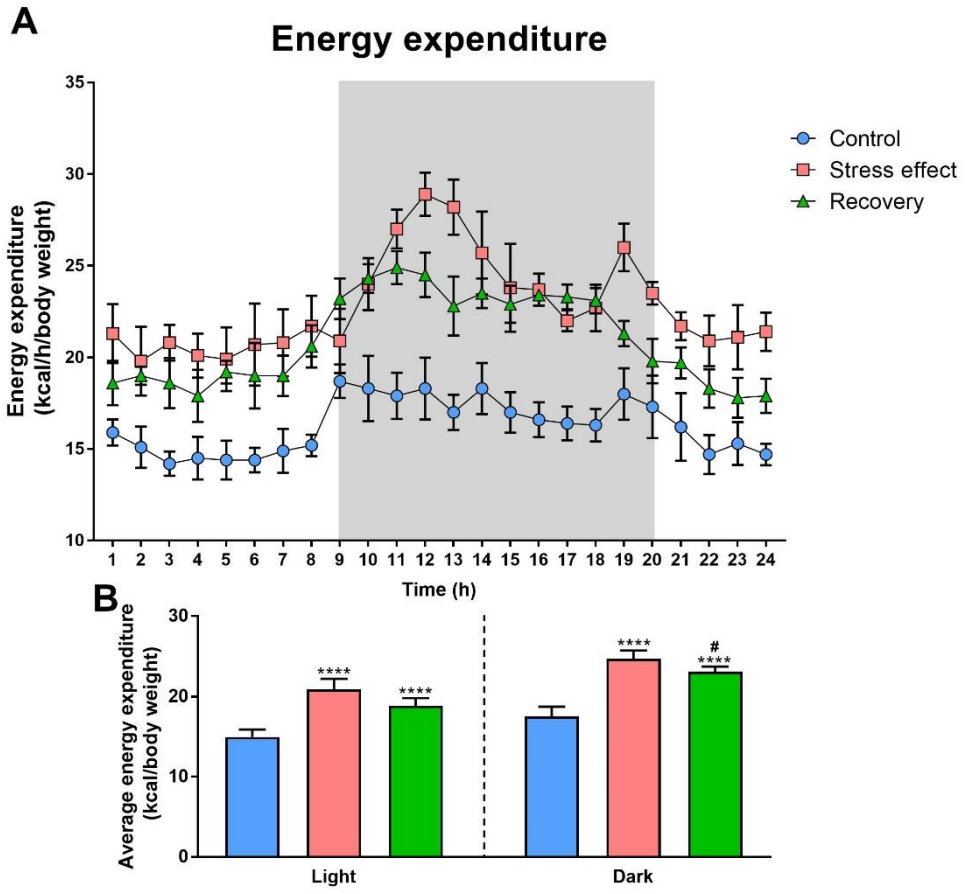

Figure 25. ***Effect of chronic stress on energy expenditure.***

*Daily timeline of energy expenditure after chronic stress (red), during recovery (green) and control mice (blue) (A). Average energy expenditure after chronic stress (red), during recovery (green) and in control mice (blue) in the light and dark phase (B). Data were analyzed by one-way ANOVA followed by Dunnett's multiple comparison test. Significance was calculated by repeated two-way ANOVA between stress effect and recovery (n =4). Time being the repeated measures. Mean ± SEM values, ****p<0.0001 vs. control, #<0.05 vs. stress effect [not published].*

4.8.4. Respiratory exchange ratio (RER)

During metabolic measurements, respiratory exchange ratio was continuously higher in the stressed mice after CVS procedure [light: q = 2.872; DF = 33; p = 0.0134; dark: q = 3.19; DF = 33; p = 0.006], however, the average RER of the stressed mice was dropped after two days to the control level but only under the light phase [light: q = 0.4596; DF = 33; p = 0.859; dark: q = 3.899; DF = 33; p = 0.0009] (Fig. 26A-B).

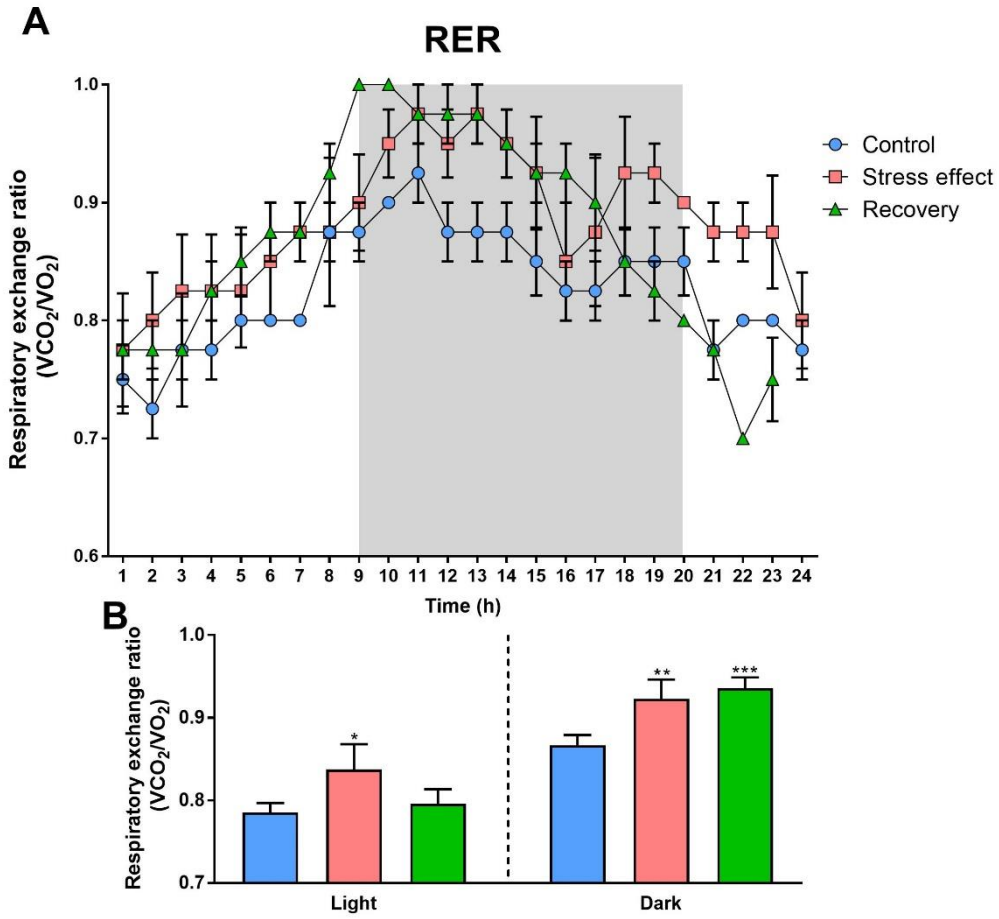

Figure 26. Effect of chronic stress on respiratory exchange ratio (RER).

*Daily timeline of respiratory exchange ratio after chronic stress (red), during recovery (green) and in control mice (blue) (A). Average respiratory exchange ratio after chronic stress (red), during recovery (green) and control mice (blue) in the light and dark state (B). Data were analysed by one-way ANOVA followed by Dunnett's multiple comparison test. Significance was calculated by repeated two-way ANOVA between stress effect and recovery (n =4). Time being the repeated measures. Mean ± SEM values, *p<0.05, **p<0.01, ***p<0.001 vs. control [not published].*

4.8.5. Body composition

Body composition was determined at the beginning (end of CVS) and the end of metabolic measurements. As shown on Figure 27., there was no difference in body weight between stressed and control mice at the beginning of measurements. However, fat mass was significantly lower and lean mass was higher in chronically stressed animals compared to the controls. During recovery, in chronically stressed mice, fat and lean mass were restored to the control level and body weight significantly increased.

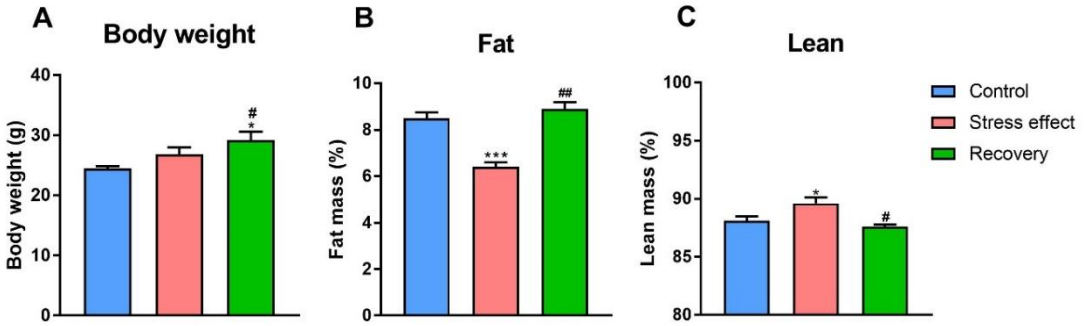

***Figure 27.* Chronic stress effect on body composition.**

*Body weight (A). Fat mass as % of body weight (B). Lean mass as % of body weight (C). Blue is the average of control mice, red is the average of stressed mice at the beginning and green is the average of CVS exposed mice at the end of measurement. Fat and lean mass represented in the percentage of body weight. Data were analysed by one-way ANOVA (n =4) and paired t-test was used to calculate significant differences between stress effect and recovery. Mean ± SEM values, *p<0.05, ***p<0.001 vs. control group, $^{\#}$<0.05, $^{\#\#\#}$<0.001 vs. group of stress effect [not published].*

4.9. Effect of chronic stress on gut microbiome and its restoration after rifaximin treatment

Next, we investigated the effect of chronic stress on gut microbiome. As shown on Fig. 28A exposure to “two hits” chronic stress paradigm resulted in significant reduction of DNA in the colon content indicating reduction of total colonic bacteria. Colon microbiome diversity was analyzed at phylum level and the results showed an increased abundance in the phylum of *Bacteriodetes* [$F(1,17) = 5.844$; $p = 0.0272$] and *Proteobacteria* [$t = 2.665$; $DF = 17$; $p = 0.0324$ compared to control]. Changes in *Firmicutes, Actinobacteria, Verrucomicrobia* and *Cyanobacteria* were not significant (Fig. 28B-C). Amount of *Clostridium* sp. was determined at genus level. Chronic stress resulted in increased abundance of *Clostridium* in response to stress (Fig. 28D) [$t = 2.707$; $DF = 17$; $p = 0.0297$ compared to control].

Rifaximin is a non-absorbable gut-acting antibiotic, which selectively eliminates pathogenic bacteria from the gastrointestinal tract and relieves diarrhea associated with *Clostridium difficile* infections.

Next, we have been interested in, if rifaximin treatment is able to restore stress-induced changes in gut microbiome. Antibiotic treatment reduced total DNA concentration in the colon content in non-stressed control animals while restored the abundance of *Proteobacteria* and decreased *Clostridium sp* ($t = 3.233$; $DF = 17$; $p = 0.0098$ compared to vehicle) in the chronically stressed mice (Fig. 28A-B-D).

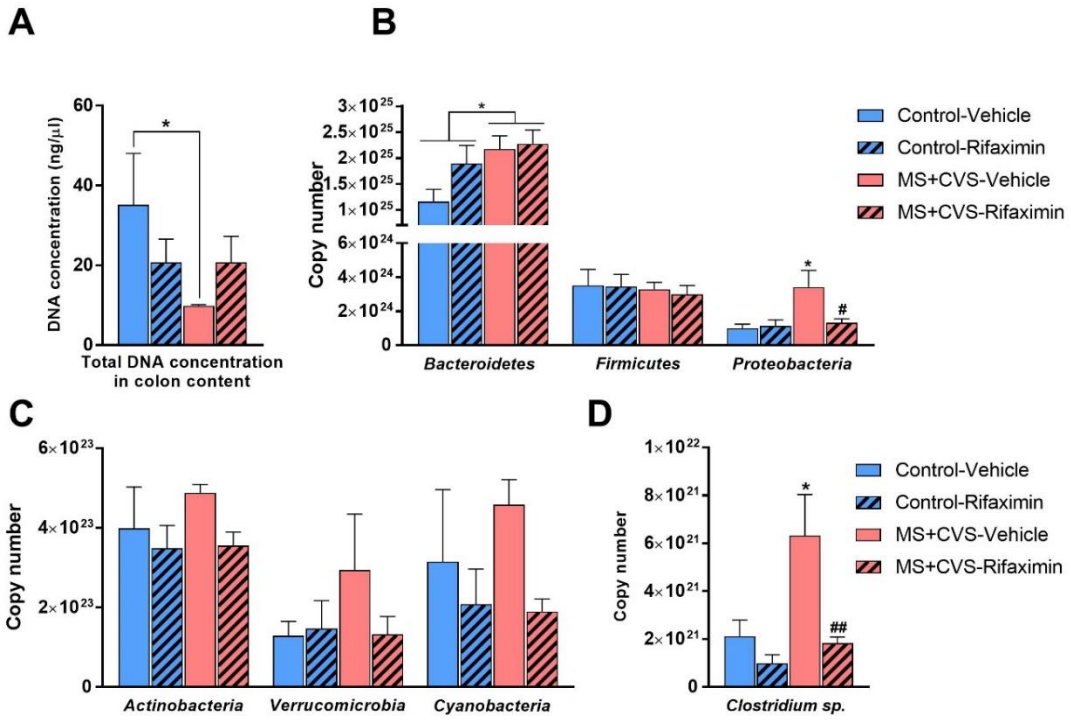

Figure 28. **Differences in the microbiome composition after chronic stress and rifaximin treatment.**

*Total DNA concentration of colon content (A), copy numbers of bacterial phyla in the colon content (B, C). Copy number of Clostridium sp. in different experimental groups (D). Data were analyzed by two-way ANOVA, followed by Sidak's multiple comparison test (n = 5–7 per group). Mean ± SEM values, *p < 0.05 vs. control group, #p < 0.05, ##p < 0.01, vs. MS + CVS-vehicle [102].*

4.10. Effect of rifaximin treatment on chronic stress-induced changes in organ weights, hormones and metabolic markers

Next, effects of rifaximin treatment was examined on different stress markers after MS+CVS procedure. During chronic variable stress, weight gain between experimental groups was not significantly different [F(1,18) = 0.2027; p = 0.8884)] (Fig. 29A). Normalized adrenal weight was higher in all MS + CVS exposed mice than in controls [F(1, 19)=4.512; p=0.047] (Fig. 29B). Two-way ANOVA did not reveal drug (rifaximin) effect. Thymus weights were not different among the groups [F(1, 19) = 1.759; p = 0.2005]. During CVS procedure, basal (morning), pre-stress corticosterone levels were significantly higher in CVS exposed mice than in controls [F (1, 18) = 7.181; p = 0.0153].

Two-way ANOVA indicated no drug effect [F(1, 18) = 0.1965; p = 0.6629] (Fig. 29C). Analysis of plasma corticosterone concentrations after acute EPM exposure revealed no significant differences among the treatment groups [F(1, 19) = 0.226; p = 0.6399] (Fig. 23D). Plasma glucose levels following acute stress were elevated in chronically stressed mice compared to controls [F(1, 13) = 22.44; p = 0.0004] (Fig. 29E). In addition, post hoc test revealed elevated plasma TG level in stressed mice [t = 2.627; DF = 18; p = 0.0339 compared to vehicle control], while there was no difference between the two, antibiotic treated groups (Fig. 29F).

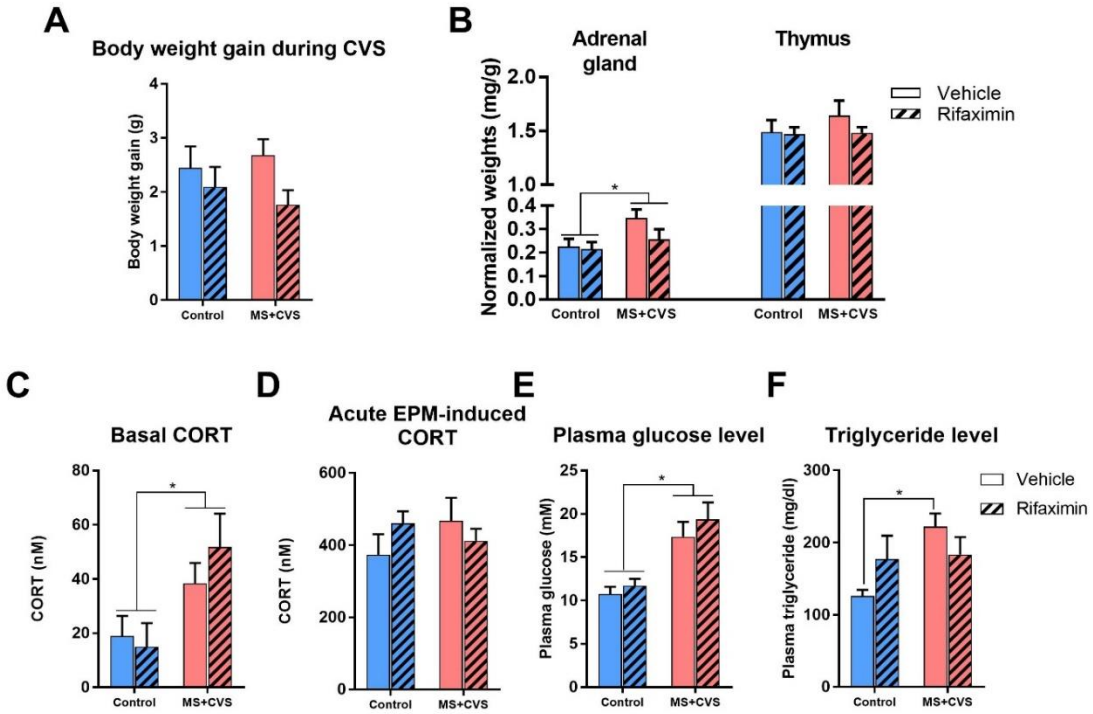

***Figure 29*. Effect of chronic stress and rifaximin treatment on different stress markers.**

*Body weight gain during CVS (A). Normalized adrenal gland and thymus weights (B). Basal corticosterone level during CVS (C). Effect of single acute stress (EPM exposure) on corticosterone level after chronic stress (D), plasma glucose level (E), plasma triglyceride level (F). Data were analyzed by two-way ANOVA, followed by Sidak's multiple comparison test (n = 5–7 per group). Mean ± SEM values, *p < 0.05 vs. control group [102].*

DOI:10.14753/SE.2020.2417

4.11. Effect of rifaximin on chronic stress-induced changes on behavior

4.11.1. Ethogram

To examine the effects of chronic stress and rifaximin on mouse behavior, we observed and quantified four distinct elements: walking, surveying, rearing and grooming during 5 min in novel environment (Fig. 30A). Compared to no-stress controls, all mice which have been exposed previously to MS + CVS displayed exaggerated locomotor-related behavior. The frequencies of all four selected behavioral elements were increased significantly in stressed mice [survey: $F(1, 41) = 66.76$; $p < 0.0001$; walk: $F(1, 41) = 58.67$; $p < 0.0001$; rear: $F(1, 41) = 49.28$; $p < 0.0001$; groom: $F(1, 41) = 33.35$; $p < 0.0001$] (Fig. 30B). Similarly, total duration of walking, rearing and grooming were increased significantly in stressed mice, however surveying decreased [surveying: $F(1, 41) = 104.1$; $p < 0.0001$; walking: $F(1, 41) = 39.18$; $p < 0.0001$; rearing: $F(1, 41) = 37.69$; $p < 0.0001$; grooming: $F(1, 41) = 17.38$; $p < 0.0002$] (Fig. 30C). Rifaximin treatment had no effect on the behavioral pattern of control and MS + CVS mice.

DOI:10.14753/SE.2020.2417

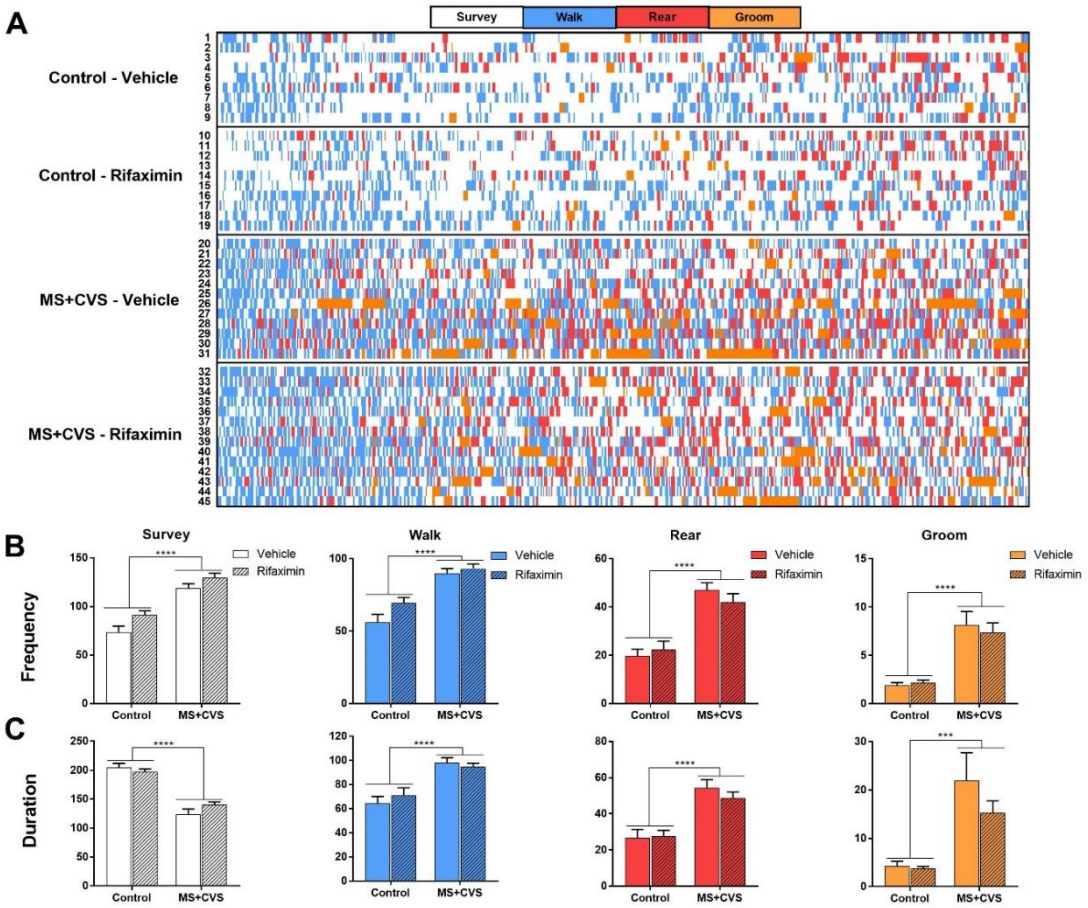

Figure 30. ***Behavioral activity of control and chronically stressed mice with or without rifaximin treatment in a novel environment (open field arena)***

*Each row represents one mouse (A). Frequency (B) and duration (C) of selected behavioral elements. Data were analyzed by two-way ANOVA (n = 9–14 per group). Mean ± SEM values, **p < 0.01, ***p < 0.001, ****p < 0.0001 vs. control group [102].*

4.11.2. Open field, EPM, sucrose consumption test

Increased locomotion was detected during the open field test in MS + CVS mice. Velocity [$F(1, 41) = 24.24$; $p < 0.0001$] and distance moved [$F(1, 41)=24.29$; $p < 0.0001$] was higher in chronically stressed mice (Fig. 31A–B). In addition, stressed mice spent less time in the center [$F(1, 41) = 10.38$; $p = 0.0025$] and their first latency to border was shorter than those of controls [$F(1, 41) = 12.65$; $p < 0.0010$] (Fig. 31C–D). To reveal anxiety-like behavior after MS + CVS, elevated plus maze test was performed. As shown in Fig. 31F preference for the open arms of stressed mice was significantly lower compared to control animals [$F (1, 28) = 13.95$; $p = 0.0009$]. Neophobia was assessed by sucrose consumption tests before and after the chronic stress procedure (Fig. 31G). MS + CVS resulted in a significant decrease of sucrose consumption (novelty) in stressed mice [$t = 4.148$; $DF = 19$; $p = 0.0022$] and the same reduced sucrose consumption was seen in CVS + antibiotic treated mice [$t = 3.251$; $DF = 19$; $p = 0.0167$], however, there was no difference in control groups. In each behavior tests (novel environment, open field, elevated plus maze and sucrose consumption based neophobia) rifaximin treatment had no effect.

DOI:10.14753/SE.2020.2417

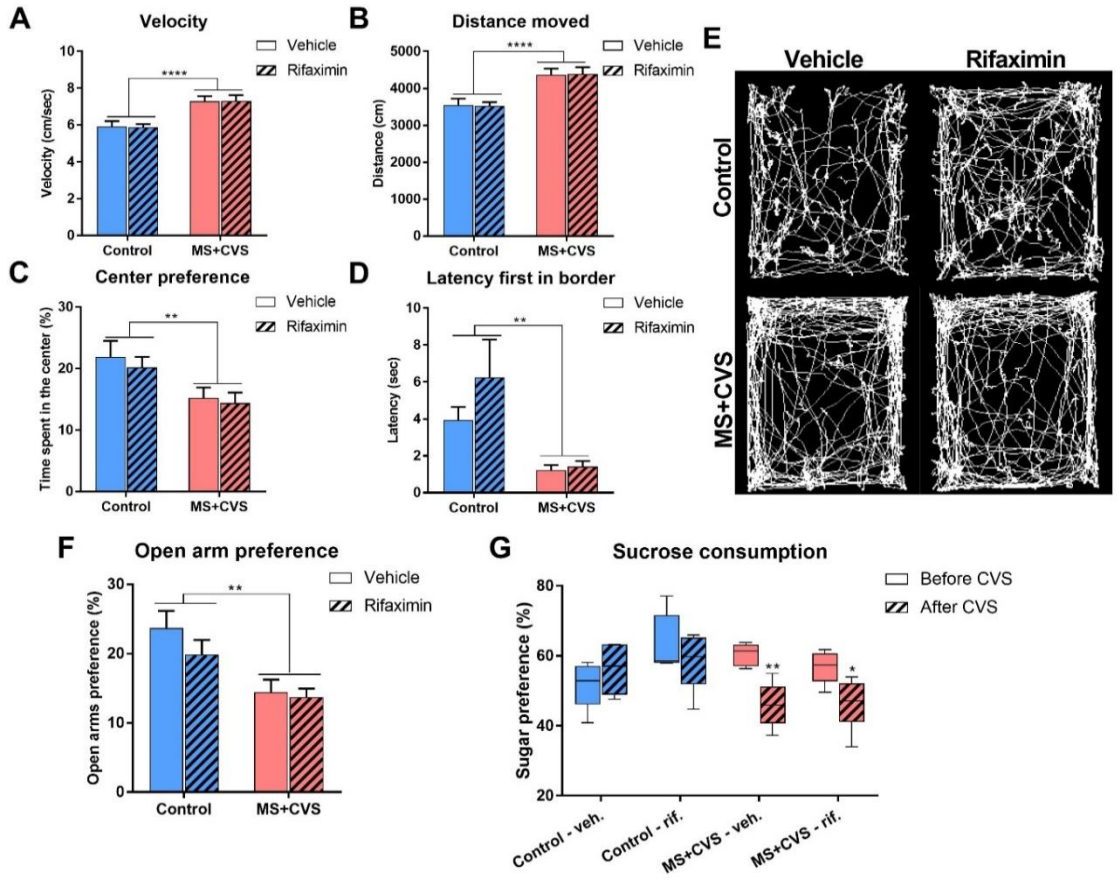

Figure 31. ***Anxiety-like behavior and neophobia after MS + CVS.***

*Open field results: Velocity during open field test (A), distance moved (B) center preference (C) first latency in border (D) and exploration maps of the experimental mice (E). Open arm preference in elevated plus maze test (F). Data were analyzed by two-way ANOVA (n = 9–14 per group). Mean ± SEM values, **p < 0.01, ****p < 0.0001 vs. control group. Sugar consumption of experimental mice before and after CVS procedure (G). Data were analyzed by repeated measures two-way ANOVA followed by Sidak's multiple comparison test (n = 5–7 per group). Mean ± SEM values, *p < 0.05, **p < 0.01 vs. control group [102].*

4.12. Effect of MS+CVS and rifaximin treatment on the gut and gut-related immunity

4.12.1. Colon mucosa, tight junction protein expression and gut permeability

MS + CVS significantly reduced the thickness of colonic mucosa compared to control [t=3,082; DF=19; p=0.0122]. Mucosa thickness was not different in rifaximin-treated groups (Fig. 32A-B). Colonic mRNA expression (Fig. 32C) of tight junction proteins, occludin [F(1, 19) = 11.27; p = 0.0033] and tight junction proteins TJP1 [F(1, 19) = 6.26; p = 0.0216] and TJP2 [F(1, 19) = 6.613; p = 0.0187] but not TJP3 was increased in both rifaximin treated groups, but remained unchanged in response to stress. In case of MUC2 mRNA there was no significant difference between the groups [F(1, 19) = 4.012; p = 0.597]. Expression of Reg3b, a C-type lectin with antimicrobial activity, was significantly elevated in chronically stressed mice. Rifaximin treatment restored Reg3b mRNA level to that of the controls [t = 3.811; DF = 19; p = 0.0024 compared to control, t = 4.398; DF = 19; p = 0.0006 compared to vehicle, interaction: F(1, 19) = 10.21; p = 0.0048].

Next, we tested gut permeability *in vivo*, using FITC-labelled 4 kDa dextran. Increased gut permeability has been revealed in chronically stressed mice, while rifaximin treatment restored the normal, non-stressed values [t = 2.72; DF = 18; p = 0.0301 compared to control, t = 3.449; DF = 18; p = 0.0066 compared to vehicle, interaction: F(1, 18) = 6.109; p = 0.0251] (Fig. 32D).

DOI:10.14753/SE.2020.2417

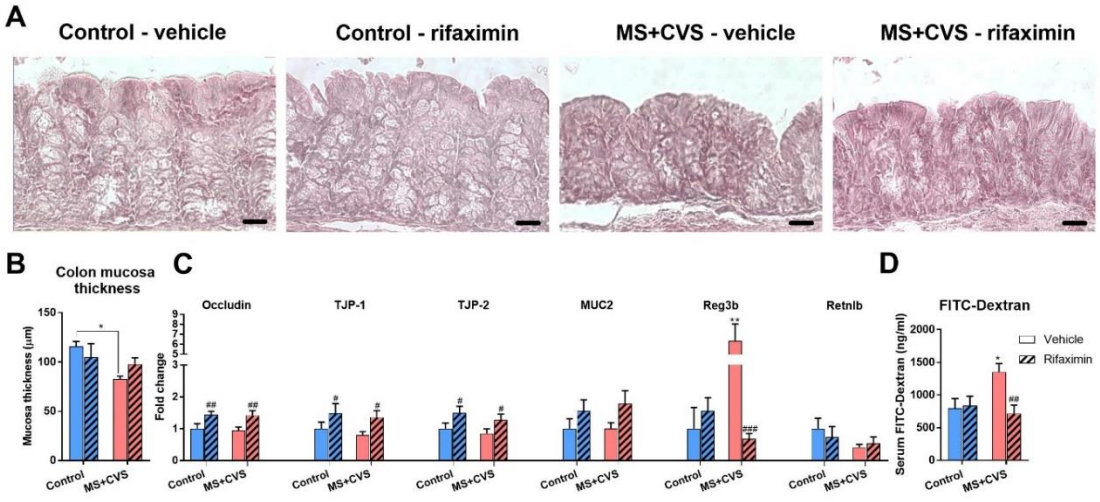

Figure 32. ***Effects of stress and rifaximin on colon mucosa.***

*Representative images of hematoxylin-eosin stained colon sections (A) (scale bar: 20 µm) and bar graphs showing mean values ± SEM of mucosa thickness (B), mRNA levels of different permeability markers and antimicrobial defence-related genes from colon tissue (C), changes in gut permeability as measured by serum concentration of orally administered FITC-dextran (mean values ± SEM) (D). Data were analyzed by two-way ANOVA, followed by Sidak's multiple comparison test (n = 5–7 per group). Mean ± SEM values, *p < 0.05, **p < 0.01, vs. non-stressed control group, $^{\#}p < 0.05$, $^{\#\#}p < 0.01$, $^{\#\#\#}p < 0.001$, vs. corresponding vehicle-treated group [102].*

4.12.2. Gut permeability, macrophage infiltration, local- and systemic bacterial load

Next, we checked whether increased gut permeability results in local piling of macrophages in the gut mucosa. In control, vehicle-treated mice immunoreactivity corresponding to macrophage marker F4/80 was primarily confined to the submucosa. Essentially the same distribution was revealed in non-stressed, rifaximin-treated mice (Fig. 33A). However, in MS-CVS mice, an increase of F4/80 positive profiles and macrophage infiltration to the lamina propria was detected. Rifaximin treatment of MS-CVS animals restored the distribution of F4/80 positive macrophages to that seen in control animals (Fig. 33A). Quantitative histological analysis of F4/80 positive (+) areas revealed significant rifaximin effect in the submucosa [$F(1, 19) = 6.316$; $p = 0.0211$]. In the lamina propria of MS-CVS animals, the area covered by F4/80+ profiles were significantly increased in stressed mice, which was reduced to that of the controls in response to rifaximin treatment [$t = 14.69$; $DF = 19$; $p < 0.0001$ compared to control, $t = 14.78$; $DF = 19$; $p < 0.0001$ compared to vehicle, interaction: $F(1, 19) = 105.4$; $p < 0.0001$], (Fig. 33B). Gut lymphatics are drained in mesenteric lymph nodes, which gate intestinal bacteria and pathogen-associated molecular patterns, PAMPs. To assess bacterial translocation in chronically stressed mice, we PCR amplified bacterial DNA from mesenteric lymph nodes using universal 16S ribosomal primers. Compared to non-stressed controls, chronic stress resulted in 50% elevation of bacterial load in the MLN [$t = 2.781$; $DF = 18$; $p = 0.0245$]. Rifaximin administration interfered with stress-induced increase of bacterial load (Fig. 33C). To reveal if chronic stress induces systemic endotoxemia, plasma LPS levels were measured. Higher LPS level was detected in plasma of stressed mice than in the controls [$t = 2.61$; $DF = 18$; $p = 0.0351$] but the increase of plasma LPS was not detected in antibiotic treated mice (Fig. 33D).

DOI:10.14753/SE.2020.2417

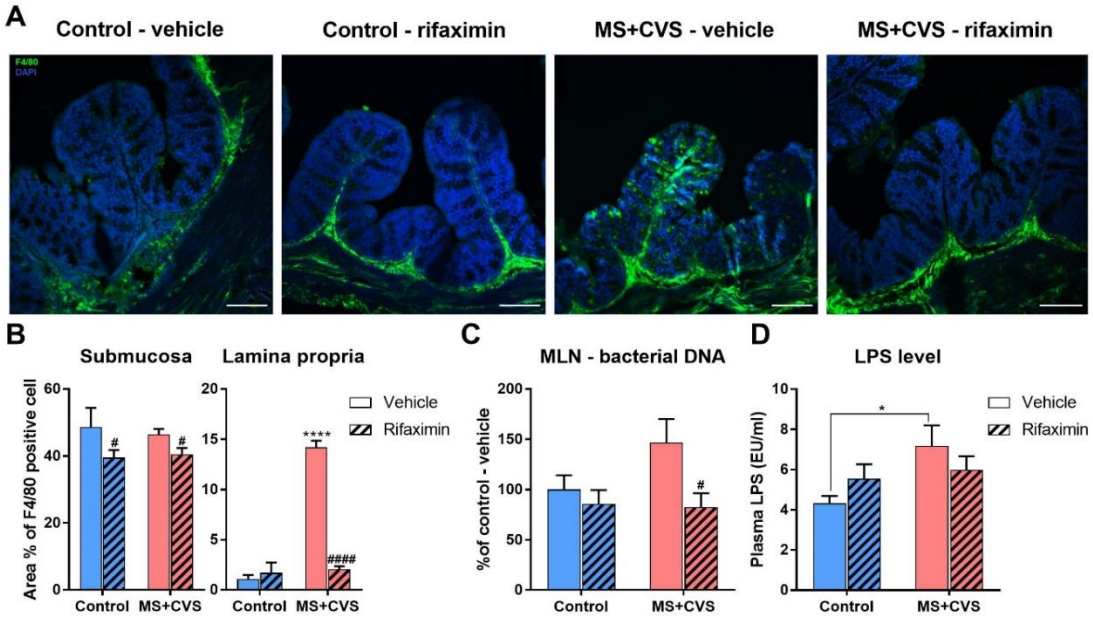

Figure 33. ***Macrophage infiltration to lamina propria, local- and systemic bacterial load.***

*Representative images of F4/80 immunostained colon sections showing distinct macrophage distribution (green-F4/80) in stressed and rifaximin-treated animals (on blue-DAPI background staining). (Scale bar: 100 μm) (A). Quantitative analysis of F4/80 immunostaining in the submucosa and lamina propria (B). Bacterial load in the mesenteric lymph node expressed as % of control-vehicle group (C). Plasma LPS concentration in control, MS + CVS groups, with or without rifaximin treatment (D). Data were analyzed by two-way ANOVA, followed by Sidak's multiple comparison test (n = 5–7 per group). Mean ± SEM values, *p < 0.05, **p < 0.01, vs. control group, $^{\#}p < 0.05$, $^{\#\#}p < 0.01$, $^{\#\#\#}p < 0.001$, vs. corresponding vehicle group [102].*

4.13. Hypothesis: correlation between Parkinson's disease prevalence, consumption of certain antibiotics and gut microbial dysbiosis

Systemic antibiotics significantly affect the microbiome resulting chronic dysbiosis in the gut, which may contribute to pathogenesis of neurological diseases. For instance, Parkinson's disease (PD) is often associated with gastrointestinal symptoms. Gut dysbiosis in PD favors curli-producing *Enterobacteria*. Curli is a bacterial α-synuclein (αSyn) which is deposited first in the enteric nervous system and amyloid deposits are propagated in a prion like manner to the central nervous system. In addition, antibiotics result in a low-grade systemic inflammation, which also contributes to damage of neurons in enteric- and central nervous system. We tested the hypothesis whether consumption of different groups of antibiotics, belonging to four major groups (penicillin /J01C/, cephalosporin /J01D/, quinolones /J01M/, macrolides /J01F/) is associated with the change of Parkinson's disease (PD) prevalence in different European countries [100]. Significant positive correlation ($r=0.537$, $p=0.002$) was found between the consumption of narrow spectrum + penicillinase (β-lactamase) resistant penicillin (J01CE+J01CF) and the increased prevalence of PD (Fig. 34). The geographical distribution of the correlation is also worth of mentioning (Fig.34). While the correlation was strong in the Scandinavian countries (Denmark, Sweden and Norway), it is also interesting to note, that PD prevalence decreased in Holland, France, Italy, Israel, countries with low-to-average J01CE+J01CF exposure.

DOI:10.14753/SE.2020.2417

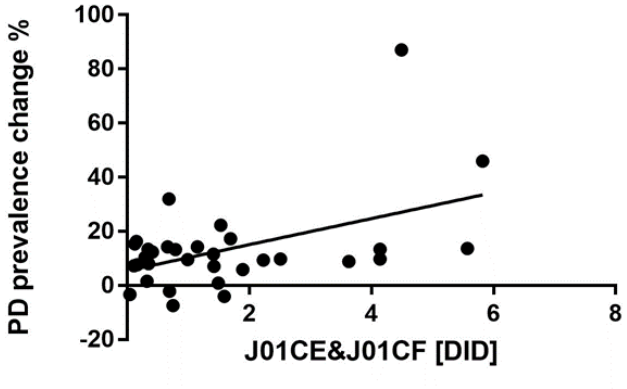

Figure 34. ***Correlation between consumption of certain penicillins and prevalence of Parkinson's disease.***

Consumption of narrow spectrum β-lactamase sensitive (J01CE) and β-lactamase resistant penicillins is expressed in DID (DID=Defined Daily Dose (DDD)/1000 Inhabitants/Day) [103].

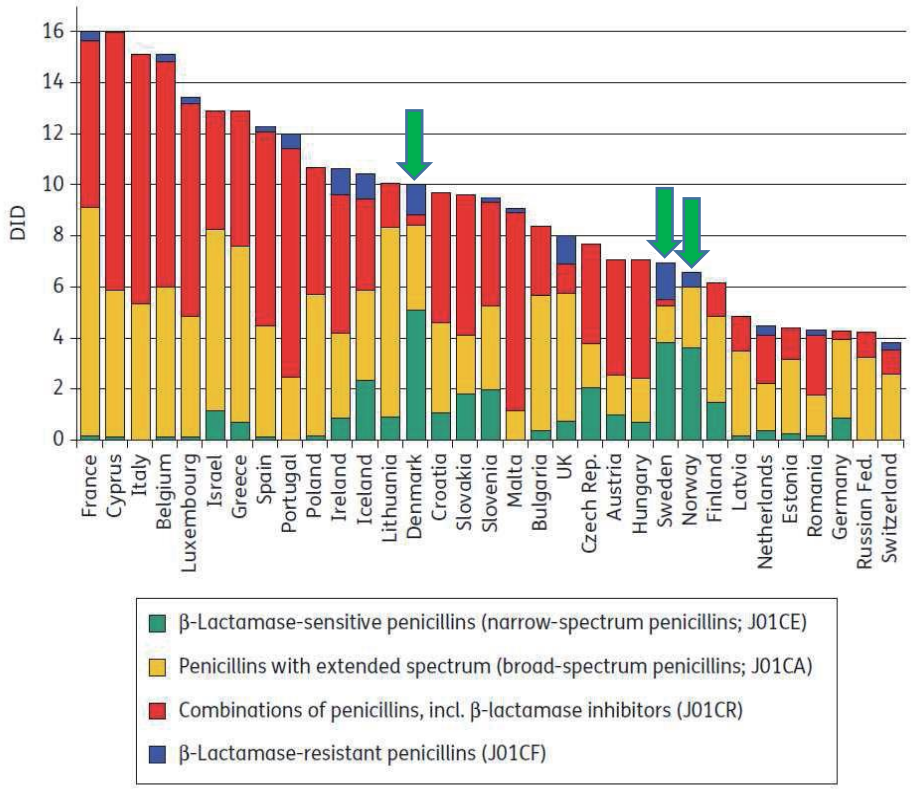

Figure 35. ***Chart indicating penicillin consumption in different European Union (EU) countries (ESAC project).***

Penicillin consumption is expressed in DID. DID is the Defined Daily Dose (DDD)/1000 Inhabitants/Day. Countries marked with green arrows consume the highest amount of narrow spectrum penicillin (green) and β-lactamase resistant penicillin (blue) within their respective column (total consumption) [103].

DOI:10.14753/SE.2020.2417

5. Discussion

5.1. The effect of acute stress and effect of the activation of CRH^{PVN} on metabolic system

The hypothalamic paraventricular nucleus harbors neurons that integrate neurondocrine, autonomic and behavioral responses to stress. These, functionally distinct cell types are spatially distributed in the rat hypothalamus, however are intermingled within the pareventricular region in case of mice and human [104].

It is well established that hypophyseotropic neurons of the PVN initiate the neuroendocrine stress cascade, while autonomic parvocellular neurons of the PVN that project to the brain stem and spinal cord are preganglionic cells of the sympathetic nervous system. Activation of the sympatho-medullary and sympatho-adrenal systems all involved in recruitment of bodily resources to "fight or flight" responses. While the neuronal circuits regulating HPA axis activity are well described, much less is known about the means with which stress-induced metabolic and behavioral responses are organized.

Fight or flight- either stress-coping strategies require energy. Only a few studies addressed directly metabolic changes accompanying acute or chronic stress. Here we have shown that acute restraint stress results in a significant elevation of energy expenditure in the first four hours post-stress and in the light (passive) phase of the circadian rhythm 12h later. The first 4h time window for special detailed metabolic analysis has been selected because most of the acute stress-induced hormonal changes and neuronal activation occur in this time frame. Our results are in agreement with previous findings on stress-induced elevation of energy expenditure in mice exposed to tail suspension stress [105]. By contrast, Spiers et al. did not detect significant changes in energy expenditure of male mice restrained for 2 hours [106]. These authors however, analyzed the whole 96h post-stress data together.

Hormonal stress mediators (adrenaline, noradrenaline and glucocorticoids) have profound effect on energy metabolism. Adrenaline increases blood glucose concentration via stimulation of hepatic glucose production and inhibition of glucose disposal in insulin-dependent tissues [107]. Adrenaline boosts lipolysis in the white adipose tissue and activates uncoupling protein UCP-1-mediated thermogenesis in the brown adipose tissue through beta adrenergic receptors [108].

Stress-induced level of corticosteroids results in hyperglycaemia via increased gluconeogenesis in the liver, and impaired glucose uptake efficiency [109]. Excess glucocorticoids decreases of fat depots and elevates circulating fatty acid through increased hydrolysis of circulating triglycerides by activation of lipoprotein lipase. Furthermore, glucocorticoids also increase *de novo* lipid production in hepatocytes through increased expression of fatty acid synthase [110].

Based on the complex effects of major stress-mediators on the energy metabolism, it is very likely that the energy consumed during acute stress response originates predominantly from fatty acid oxidation. However, this is not supported by the respiratory exchange ratio data obtained in our study. Although RER values of acutely restrained mice are below of that of the non-stressed controls throughout the whole circadian cycle post-stress, the difference from the control measurement is not significant.

The acute stress-induced energy expenditure correlates with the increased activity of mice especially in the first couple of hours after releasing mice from the restrainers. Using an automated video and vibration behavioral analysis system („Behavioral Spectrometer"), Brodkin et al. detected dramatic changes in behavior of stressed mice. There were large increases in grooming of all body parts (i.e., paw, face, head, cheek, leg, back, and genitals) accompanied by a moderate increase in scratching. By contrast, restraint produced dramatic decreases in locomotion (walk and run) and a mild decrease in the orienting behaviors of sniff and survey [111]. Unfortunately, TSE Phenomaster, used in our studies, detects the sum of XYZ activities and can't differentiate between distinct behavior elements. Nevertheless, it has been previously revealed that restraint and other psychogenic stressors increase grooming behavior shortly after stress [112] and therefore it is likely that early increases in activity seen in our acutely restrained mice might be due to grooming or rearing [113]. By contrast, activity following acute restraint stress, was significantly decreased in the dark phase of circadian rhythm. This, delayed and sustained reduction of locomotor activity has been reported in previous studies [106, 111, 114].

Reduced activity following stress may serve to replenish depleted energy stores. This is supported by increased food intake seen in the fourth hour post stress, two hours after the peak of energy expenditure. Stress-eating is a well-known behavior and conserved across species. Both humans and laboratory rodents have been shown to increase their food intake following stress or negative emotions [115, 116]. Furthermore, stressed organisms prefer comfort (high fat, high sugar) food [117]. Stress-induced

glucocorticoids are key factors for responding to reduced energy stores. They increase food intake and alter food choice [118].

Corticotropin-releasing hormone, CRH plays an important role in food choice and activity. Expression of this neuropeptide rapidly increases after stress not only in the hypothalamic paraventricular nucleus but in other brain regions involved in stress regulation [108]. CRH and other members of it's family of neuropeptides (urocortin 1,2,3) have significant anorexigenic and thermogenic activities [119]. Furthermore, centrally administered CRH increases physical locomotor activity. Eavens et al., demonstrated that CRH increases locomotor activity independently of pituitary hormone secretion, since CRH induced locomotor activity was seen in hypophysectomised following intracerebroventricular (icv) administration of in dose dependent manner rats [120]. Coincident data was revealed by Lowry et al. reporting that CRF antagonist α-helical CRF9–41 (ahCRF) reduced stress induced locomotor activity in dose dependent manner [121].

To identify if CRH neurons in the hypothalamic paraventricular nucleus are involved in stress-related metabolic and activity responses, we have used a chemogenetic approach. Using CRH-IRES-Cre mice (on the same C57BL6 background as in metabolic experiments), we have challenged CRH^{PVN} neurons and recorded metabolic parameters and physical activity. Previous studies from our laboratory confirmed that selective activation of CRH^{PVN} neurons results in plasma CORT elevation similar to that seen in response to acute stress. Hormonal assessment also indicated that the effect of neuronal activation following chemogenetic activation lasts longer (up to 4-5h) than an acute stress, however the peak CORT levels are comparable. Chemogenetic activation of CRH^{PVN} neurons recapitulates some, but not all metabolic markers seen after acute restraint. Energy expenditure is increased during the first 4 hours after CNO injection, similar to that seen in restrained mice, however the second peak in the next day light phase was not detected. Food intake was the other marker that showed similarities between acutely stressed animals and following chemogenetic activation of CRH^{PVN} cells. In both cases, cumulative food intake was increased. There were differences, however, in the timing. Following acute restraint stress, food intake gradually increased post-stress and became significant by the fourth hour, while it was promptly elevated after CNO injection and remained on a plato in chemogenetically chellenged mice. Neither restraint, nor chemogenetic activation of CRH^{PVN} neurons affected respiratory exchange ratios.

We could not detect over changes in locomotor activity following CNO administration to CRH-IRES-Cre mice with pAAV-hSyn-DIO-hM3D(Gq)-mCherry injection into the PVN. These results underscore the importance of relevant control experiments and highlight the drawback of CNO as an activator of DREADD receptors. When CRH_IRES-Cre mice were injected with control virus construct into the PVN, we detected decreased locomotor activity following CNO injection. Recent pharmacokinetic analysis demonstrated CNO reverse-metabolization to its parent compound clozapine in mice and rats, yielding plasma concentrations that may be sufficient to occupy inter alia dopamine $D_{2/3}$ and serotonin $5HT_{2A}$ receptors in the brain. Clozapine is an antipsychotic drug, which is widely used for schizophrenia treatment. The drug is an effective agonist at $GABA_B$ receptor and the $GABA_B$ receptor deficient mice exhibit altered locomotor behaviour [122, 123]. For these reasons, the authors of the pharmacological study of CNO propose the use of appropriate control groups and appropriate DREADD activating drug with which we can avoid its side effects [124].

It is very likely, that the CNO counteracts with the effects of CRH^{PVN} on locomotion. Indeed, optogenetic silencing of CRH^{PVN} neurons resulted in reduced physical activity, grooming and rearing following foot shock stress indicating a stimulatory role of CRH^{PVN} neurons in regulation of physical activity [125].

It should also be noted, that we could not detect over changes of EE and RER values after CNO injected control animals, although clozapine has metabolic side effects [126].

5.2. Metabolic changes after chronic stress and during recovery

Acute stress response is a short term adaptation process to environmental stimuli. This short term adaptation could even be beneficial and increase resilience. However, continuous stress load may result in both physical and emotional health problems over time. During chronic stress, the permanently increased glucocorticoid level keeps the blood glucose level high, as we have confirmed in the two-hits protocol, and these effects are associated with elevated insulin level leading to insulin resistance and diabetes mellitus [127]. Fat mobilizing effects of glucocorticoids and catecholamines are also dominant in chronic stress, that result elevated TG level and thus trigger the risk of hypertriglyceridemia, NAFLD or atherosclerosis [64].

In our experiment, increased food intake was detected in chronically stressed mice, during the dark (active) phase of the circadian rhythm. CVS leads to dysregulated HPA

axis and it consequently influences energy intake and homeostasis. Chronic stress can impact on multiple appetite-related hormones and neuropeptids [128]. Release of hypothalamic CRF suppresses food intake [129, 130], in contrast, glucocorticoids stimulate appetite [131] and induce preference for consumption of palatable food [132]. However, the permanent elevated glucocorticoids suppress CRH release from PVN and vasopressin becomes the main regulator of ACTH secretion during chronic stress [133].

Previous study indicated altered locomotor activity in mice, which were exposed to social defeat stress for 10 days [134]. Locomotion was decreased during chronic stress and it remained reduced for two days after stress. By contrast, increased locomotor activity was detected in our study after CVS, however it was induced significantly only during the resting phase. Similar to our study, Hiroshi Ito et al revealed hyper-locomotion activity after 7 days of chronic restraint stress. These changes associated with increased synaptic plasticity in the anterior cingulate cortex (ACC) by induced excitability because of the disruption of the inhibitory effect of $GABA_A$ receptor signaling pathway [135]. Another study compared the effect of chronic restraint and variable stress on locomotor behavior. Only chronic restraint stress altered locomotion, whereas chronic variable stress has no effect [136]. To conclude, these results confirm the assumption that chronic stress induced locomotor behavior changes probably highly influenced by the period and the severity of chronic stress. In addition, there is might be one concrete explanation to this result, which underlines the increased locomotion during resting state. Previous studies indicated, glucocorticoid administration increases wakefulness and induces reduction of REM sleep [137, 138].

The permanent presence of stressful stimuli during chronic stress is accompanied with continuous homeostatic adaptation, which demands energy. These processes constantly activate the sympathetic nerve system and HPA axis, thus, catabolic pathways are activated predominantly through the effects of glucocorticoids and catecholamines [139]. In addition, UCP1 expression is stimulated by the sympathetic nervous system in brown adipose tissue and thus, stress induces hyperthermia [140]. All these changes consequently lead to increased energy expenditure. Therefore, not surprisingly, elevated energy expenditure of the stressed mice was detected after CVS.

Respiratory exchange ratio was also higher in the stressed mice, which suggest that carbohydrate utilization was rather preferred to support energy expenditure. Besides the carbohydrate utilization, interestingly, higher lean and lower fat mass were measured by MRI. Lean is equivalent with the muscle tissue mass, that was higher probably because

of the increased locomotor activity. A possible explanation of the lower fat mass is might be the glucocorticoid effect on GLUT4 membrane protein. In a previous study, alleviated level of GLUT4 expression was observed in fat cells but it was induced in skeletal muscle after administration of dexamethasone or with the concomitant injection of sucrose [141]. Accordingly of this result, GLUT4 could decrease glucose transport into adipocyte and this effect accompanied with reduced adipose tissue [142]. In contrast, glucose transport would be increased into the enlarged skeletal muscle tissue and thus the preference for utilization of carbohydrates would increase.

Next, we have been interested how the metabolic homeostasis recovers after chronic stress. Although a short recovery period was selected, in a previous study indicated that 2 weeks of visible burrow system (VBS) model of chronic stress increased corticosterone level, which returned to the control level after one week. Furthermore, the reduced body weight of subordinate and dominant rats increased continuously during recovery but only the body weight of dominant mice restored to the control level, whereas the body weight of the subordinate mice reminds significantly lower even three weeks after VBS compared to the control group. These changes were associated with increased food intake, fat and lean mass gain during the three weeks of recovery [143]. Previous studies indicated other restorable effects in hippocampus. Three weeks of chronic stress induced impaired spatial working, reference memory and retracted CA3 dendrites were reversible after 3 weeks of recovery [144]. Lin M. et al indicated restoration of behavioral impairment and the alteration in the glutamate receptor expression to the normal level after 35 days of recovery [145]. Within the hippocampus, another important hub of stress regulation, Gray J. D. and colleagues identified 700 genes differentially expressed in chronically stressed animals compared to non-stressed controls. 21 days of resting period hippocampal gene expression was compared again and found an additional 700 genes to be differently expressed, however only 36 genes overlapped between the stressed and rested animals [146]. Another study revealed that recovery time of the immune system is highly dependent from the severity of the stressor. In this study, rats were exposed to daily restraint stress for 2, 4 and 8 weeks followed by 6 weeks of recovery and the results showed that the longer exposure time of the stress the higher of the immune system damage, whereas shorter exposure time shortened the recovery time [147]. In spite of these results, glucocorticoid levels seems to be independent from the severity of the stress during recovery. Ottenweller J. E. et al demonstrated that 10, 7, 4 and 3 days footshock stress did not produced higher corticosterone level in rats compared to each other and the

exposure time has no effect on the glucocorticoid level reduction during three days of recovery [148]. In addition, X. Mengyang and colleagues indicated the reversibility of the microbial changes after three weeks of recovery, in spite of the restored microbiome, the difference of the microbial metabolites was more persistent, it was still detectable three weeks after the end of stress [149]. In our study, the most striking results were the body composition changes. Beside increased body weight, restored fat and lean mass level were measured after three days of recovery. In the other metabolic parameters, only a decreasing tendency was measured, except for the energy expenditure changes during the active phase, where significant reduction was observed after three days of recovery. The conclusion of these data, most of the chronic stress induced changes are reversible, however the reversibility time depends on different parameters like exposure time, recovery time and severity of stressor, etc.

5.3. Chronic stress effect on colon microbiome and gut

There is a well-documented mutual interaction between the gut microbiome and host stress response [150, 151]. Chronic stress is an important environmental factor, which triggers gut dysbiosis and in turn, altered microbiome has an impact on neuroendocrine-autonomic and behavioral aspects of the stress response. Growing evidence indicates a link between stress and microbial dysbiosis [150, 152, 153]. Previous studies from different laboratories revealed distinct stress-induced changes of the gut microbiome composition depending on the stressor (water avoidance [154, 155] repeated restraint [156], social defeat/disruption [157-159] and origin of bacterial sampling (fecal [160], luminal [161] mucosal [162]. General conclusion of these studies is that chronic psychological stress results in outgrowth of *Bacteroidetes* and decrease the abundance of *Firmicutes*. Here we confirm and extend these observations to show that MS-CVS “two hits” paradigm is also capable to increase *Bacteroidetes* and *Proteobacteria* in chronically stressed mice, which is accompanied here with an overall decrease of total bacterial DNA concentration in the colon content.

A number of studies have identified early life adversity as an important factor affecting gut microbiome [163]. Studies in rats, mice and Rhesus monkeys revealed decrease of microbial diversity following maternal separation [164] or limited nesting [165]. Here, we have used the “two hits” model of chronic adversity by combination of early life stress,

maternal separation and chronic variable stress paradigm, both of which might have an impact on gut microbiome.

Among the bacterial species studied here, the copy number of *Clostridia* increased significantly as a result of MS-CVS stress paradigm. This finding is in agreement with those of [157, 166]. Although some *Clostridia* are pathogenic and are responsible for diarrhea in the elderly, we did not observe serious diarrhea or watery feces in our stressed mice.

"Leaky gut" is generally held as a hallmark of chronic stress-related pathologies [167, 168]. In the present MS-CVS model we did not detect stress-induced changes in colonic expression of tight junction proteins (Occludin, TJP1-3) and muc2. However, we did find significant decrease of mucosa thickness, signs of epithelial damage. Furthermore, increased transcellular transport was detected in the gut of chronically stressed mice by FITC-dextran method, indicating impaired barrier function [169]. The leaky barrier should allow various feed/microbiome related antigens to initiate local immune responses. Such an innate immune activation has been revealed by infiltration of F4/80 positive macrophages into the lamina propria of MS-CVS exposed mice, which was prevented by rifaximin treatment during chronic variable stress. Gut lymphatics are drained in mesenteric lymph nodes (MLN), where a significant bacterial load has been revealed in our chronically stressed mice. This finding is compatible with the report by Velin et al. [170] where 30 times increased E coli passage was detected in chronically stressed rats, ex vivo. In addition to this local bacterial translocation to MLN, significant elevation of LPS was detected in the plasma of MS-CVS mice, indicating systemic endotoxemia.

Another noteworthy finding of this study is the stress-induced colonic upregulation of Reg3b. Reg3b is a C-type lectin, which belongs to antimicrobial peptide (AMP) family and involved in gut barrier functions [171]. Further studies are required to clarify if increased expression of Reg3b mRNA may represent an adaptive compensatory host mechanism to impaired barrier and increased bacterial burden

Chronic stress exposure is a risk factor for psychiatric disorders, such as anxiety and depression, subsets of which are accompanied or driven by activated immune system [172, 173]. Parallel to stress-induced microbiome changes, chronic stress increases gut permeability and results in a leaky gut, through which bacterial cell wall components might reach the systemic circulation, trigger toll like receptors and result in low grade

systemic inflammation. LPS and related proinflammatory cytokines activate the HPA axis [174] and promote deterioration of stress-induced anxiety [175].

In search for the causal role of microbiome in the development of stress-related psychopathologies, Langgartner et al. showed that stress-induced psychobiological changes can be transmitted by fecal transplantation from stressed to non-stressed mice [158]. In contrary, our present results suggest that settlement of stress-induced changes in the gut does not alleviate MS-CVS-induced locomotor hyperactivity, anxiety-like symptoms in open field and elevated plus maze tests and anhedonia. One explanation for the resistance of stress-induced behavior to improvement of gut and immune functions would be the timing of rifaximin treatment. It is likely that behavior needs more time than gut to recover from CVS. Another possibility would be that early life adversity i.e. maternal separation results in permanent changes in the gut flora [163] and behavior, which do not change after antibiotic treatment in the adulthood. Indeed, it has been shown that early life events result in epigenetic modulation of stress/anxiety-related genes such as hypomethylation of the Crh promoter in the PVN of maternally deprived adult rats [176] and reduction in histone H3 acetylation at human/rat glucocorticoid receptor (GR, NR3C1) promoter in the hippocampus [177].

5.4. Antibiotic effect on gut microbiome

Among the factors, influencing the gut microbiome, antibiotic exposure has profound and sometimes persisting impact on the bacterial composition, diversity and function of the intestinal flora [178]. In addition to the use antibiotics for medical reasons, the human body is unintentionally exposed to antibiotics present in feeds and in the environment. Animal husbandry use subtherapeutic dose of different antibiotics to increase the growth rate and feed efficiency, as well as for disease prevention in overcrowded locations including aquacultures [179-181]. Antibiotics decrease the microbial diversity of the gut flora, modulate *Bacteroidetes*/*Firmicutes* ratio and result in overgrowth of opportunistic pathogens [182, 183]. For instance, a 7-day treatment with commonly used antibiotic groups: fluoroquinolones and β-lactams, significantly decreased microbial diversity by 25% and reduced the core phylogenetic microbiota from 29 to 12 taxa [184, 185]. Another recent study on healthy subjects, found an immediate bloom of *Enterobacteria* and other pathobionts along with significant depletion of *Bifidobacteria* and butyrate-producing species in response to a meropenem, gentamicin and vancomycin cocktail. Although the microbiome of the subjects recovered to near-baseline composition within 1.5 months,

some common species, which were present in all subjects before the treatment, remained undetectable after 4 months [186].

There is a general agreement in the literature that, apart from genetic background, PD is caused by some external effect and the primary change leading to the disease is the modified gut flora, dysbiosis. Even the suspected toxic agents, like pesticides, operate through the altered microbiome in the process of developing PD. Considering the fact that antibiotics are powerful agents influencing the microbiome, it is likely that some penicillins, as "external factors" initiate gut dysbiosis, which contribute to the development of PD. Our study compared global antibiotic consumption to the change of PD prevalence in different European countries in the past 25 years might provide some clues elucidating the issue [100]. To support our hypothesis, a recent work evaluated the impact of antibiotic exposure on the risk of PD in a register-based case- control study in Finland. This study also found significant association between exposure to certain types of oral antibiotics and increased risk of PD, with a delay that is consistent with the proposed duration of a prodromal period [187]. Our findings show connection between high consumption of narrow spectrum penicillin and the highest prevalence change of PD. Two major mechanisms may underlie the connection between exposure of certain antibiotics and increased prevalence of PD: First, antibiotics induce gut dysbiosis, a microbial imbalance, in which certain curly- producing bacteria gain abundance in the microbiome. Curly, as a functional α-synuclein (αSyn), excreted to the extracellular space and exaggerates additional amyloid deposition. The αSyn pathology has the ability to spread from the gastrointestinal tract to the brain and results in loss of vulnerable dopamine synthesizing neurons in the substantia nigra. Second, these antibiotics may promote inflammation, via translocation of live gut bacteria and inhibition of anti-inflammatory, short chain fatty acid (SCFA) (butyrate)-producing bacteria. Systemic inflammation in general-, and local neuroinflammation (microglia activation), in special-, contribute to PD pathogenesis.

Rifaximin, which is a non-absorbable antibiotic, specifically targets Clostridia and other Gram negative and positive bacteria. Therefore, we hypothesized that rifaximin treatment of mice exposed to MS-CVS will restore microbiome related gut-brain axis and behavioral changes to normal. Indeed, stress-induced *Clostridia* were significantly attenuated by antibiotic treatment. In addition, rifaximin administration prevented stress-induced increases of *Proteobacteria*, but not *Bacteroidetes*. These data confirm previous findings that rifaximin do not significantly affect the overall composition of the human

fecal microbiome [188] and only mild changes are observed in mice [189]. More recently, rifaximin was recommended for treatment of post-infectious irritable bowel disease (IBS) and related abdominal discomfort [190, 191]. In search for the mechanism of rifaximin action, increased expression of gut tight junction proteins emerged [189]. We have confirmed increased mRNA levels of tight junction proteins occludin, tjp1 and tjp2, but not tjp3, in colon samples of stressed and non-stressed, rifaximin treated mice. Increased expression of tight junction proteins along with slightly increased muc2 indicates improved gut barrier function after rifaximin administration.

Rifaximin administration during CVS prevented the increase of LPS plasma levels, suggesting that rifaximin effects go beyond anti-pathogenic activity. The endotoxemia reducing effects of rifaximin has already been shown in chronic liver disease [192]; however, the mechanisms of action and molecular targets remain unknown.

Finally, rifaximin reduced pathogenic bacteria and improved gut barrier, however, did not enforce the abundance of beneficial “psychobiotic” bacteria. It has been shown that administration of certain *Lactobacilli* and *Bifidobacteria* have anxiolytic/antidepressive effects [193-195].

Recent studies implicate that antibiotic usage in human and farm animals results in dysbiosis, provoke systemic inflammation, which might be responsible for long-term metabolic- (obesity), behavioral- and mental changes. However, we did not detect any significant behavioral changes in unstressed mice treated with antibiotic for 3 weeks. Future work should focus on the interaction between systemic antibiotics and stress in regulation of microbiota-gut-brain axis.

In conclusion, combination of early life adversity with adult chronic variable stress (CVS) paradigm in mice results in gut dysbiosis and impaired gut barrier function along with increased locomotor activity, anxiety-like behavior and neophobia. Rifaximin treatment during CVS decreases stress-induced pathogenic bacteria, restores gut barrier functions, reduces local and systemic bacterial load, however, does not improve stress-induced behavioral changes.

DOI:10.14753/SE.2020.2417

6. Conclusion

The main conclusion of my dissertation are:

1. Acute psychogenic stress has profound effect on the metabolic parameters, energy expenditure and food intake as well as on locomotor activity.

2. The hypothalamic paraventruclar nucleus is a part of a neuronal circuit, which mediates acute stress effects on metabolism and activity.

3. Chronic stress results in lasting changes of body composition and metabolism, with increased food intake, energy expenditure and respiratory exchange ratio. These chronic stress-induced alterations recover differently after cessation of the challenge.

4. Chronic stress results in gut dysbiosis, increased gut permeability and recruitment of activated macrophages in the colonic mucosa.

5. Rifaximin -a gut specific antibiotic- restores stress-induced changes in gut microbiome, gut permeability and bacterial load, however these positive changes in the gut are not accompanied by restoration of normal behavior.

6. Gut dysbiosis following systemic antibiotic treatment might be a risk factor in the development certain neurodegenerative disorders, such as Parkinson’s disease.

DOI:10.14753/SE.2020.2417

7. Summary

Stress is a non-specific adaptation reaction from the body to different environmental changes. The response triggers various complex mechanisms in which the metabolic system is also involved. The activation of the HPA axis demand high energy requirement. Thus, chronic stress, which is a permanent long lasting process, can provoke various metabolic related maladaptive diseases. In contrast, simple acute stress is rapid response, which can be even beneficial. In addition, it is well established, chronic stress induces "leaky gut" syndrome and dysbiosis in the gut microbiome and thus, it further aggravates the chronic stress induced maladaptive process like neuronal or behavioral impairments.

In this current dissertation, we examined the metabolic changes after the activation of HPA axis by acute stress or potentiation of CRH neurons in PVN. We also observed the effect of chronic stress and recovery on metabolic system. In addition, we investigated antibiotic effect during chronic stress on behavior and colon physiogy; and its correlation with Parkinson's disease (PD).

Acute stress has a short-term effect on locomotion and food intake. Whereas, energy expenditure was affected for a long-term. These changes were accompanied with dropped body weight and fat mass. The activation of CRH^{PVN} neurons similarly influenced metabolic system as acute stress, however, there were also differences. Long-term effect of HPA activation was not seen and the food intake behavior was different in the first four hours. Chronic stress evoked robust changes in metabolic system and slight alteration was seen after three days of recovery. Two hits paradigm stress induced dysbiosis in gut microbiome. In addition, we found extenuation of colonic mucosa, increased bacterial translocation to mesenteric lymph node, elevation of plasma LPS levels and infiltration of F4/80 positive macrophages into the colon lamina propria. Chronically stressed mice displayed anxiety-like behavior and neophobia. Rifaximin treatment decreased *Clostridium* concentration, gut permeability and LPS plasma concentration and increased colonic expression of tight junction proteins (TJP1,TJP2) and occludin. However, these beneficial effects of rifaximin in chronically stressed mice was not accompanied by positive changes in behavior. Finally, significant correlation was calculated between antibiotic consumption and PD prevalence.

These findings emphasized the role of metabolic system after stress and help to understand the development of different stress induced metabolic related diseases and the relation between gut microbiome and different neuronal impairments.

DOI:10.14753/SE.2020.2417

8. Összefoglalás

A stressz egy adaptációs válasz folyamat, különböző környezeti változások hatására. A válaszreakció során különböző mechanizmusok indukálódnak, amelyek rengeteg energiát igényelnek, ezért a metabolikus rendszernek kiemelt szerepe van a stressz során. A stressz időbeli lefolyása alapján megkülönböztetünk akut és krónikus stresszt. Számos tanulmány bizonyította már, hogy a folyamatos stressz jelenléte diszbiózist eredményez a bél mikrobiomban és gerjeszti a bél átjárhatóságát, amely tovább súlyosbítja különböző maladaptív folyamatok hatását.

Disszertációmban a stressz indukálta metabolikus változásokat vizsgáltuk akut stressz után illetve, a CRH neuronoknak milyen szerepe van ezekben a változásokban. Továbbá tanulmányoztuk a metabolikus változásokat krónikus stresszt követően és a felépülés alatt is. Valamint vizsgáltuk a krónikus stressz során az antibiotikus hatást a viselkedésre, a vastagbél fiziológiájára és az antibiotikum fogyasztás korrelációját a Parkinson-kór prevalenciájával (PD).

Az akut stressz a lokomotoros aktivitást a táplálékfelvételt és az energia felhasználást indukálja. A CRH^{PVN} neuronok aktiválásával hasonló metabolikus változásokat indukáltunk, mint az akut stressz során. Azonban különbségeket is meg lehetett figyelni. Az emelkedett energiafelhasználás hosszú távon nem volt megfigyelhető és a táplálékfelvétel eltérő volt az első négy órában. A krónikus stressznek jelentős hatása volt a metabolikus rendszerre és a három napos felépülés után enyhe csökkenést lehetett csak megfigyelni. A két csapás stressz paradigma diszbiozist idézett elő a vastagbél mikrobiomájában. Ezenk,ívül a vastagbél nyálkahártyája elvékonyodott, megnövekedett a bakteriálistranszlokáció a mesenteriális nyirokcsomókban, a plazma LPS szintje szignifikánsan magasabb volt, megnövekedett az F4 / 80 pozitív makrofágok száma a lamina propria-ban és a krónikus stressz szorongásos viselkedést és neophobiát váltott ki. Egy nem felszívódó antibiotikum kezelés (rifaximin) hatására helyre tudtuk állítani a mikrobiom diszbiózist és a krónikus stressz indukálta változásokat a vastagbélben. Azonban a viselkedésbeli változásokra nem volt hatással.

Ezek az eredmények a metabolikus rendszer stresszben betöltött szerepét emelik ki, és segítenek megérteni a metabolizmussal kapcsolatos stressz indukálta betegségek kialakulását, valamint a bél mikrobiom és a különböző neurológiai kórképek közötti kapcsolatot.

9. References

1. Cannon W.B. (1929) ORGANIZATION FOR PHYSIOLOGICAL HOMEOSTASIS. Physiological Reviews. **9**(3): 399-431.
2. Cannon W. (1929) Organization for physiological homeostasis. Physiol Rew. **9**: 399-431.
3. Selye H. (1936) A syndrome produced by diverse nocious agents. Nature. **138**: 32.
4. Selye H. (1950) Stress and the general adaptation syndrome. British medical journal. **1**(4667): 1383-1392.
5. Selye H. (1946) The general adaptation syndrome and the diseases of adaptation. J Clin Endocrinol Metab. **6**: 117-230.
6. McEwen B.S. (2007) Physiology and neurobiology of stress and adaptation: central role of the brain. Physiol Rev. **87**(3): 873-904.
7. Wong D.L., T.C. Tai, D.C. Wong-Faull, R. Claycomb, E.G. Meloni, K.M. Myers, W.A. Carlezon, Jr., and R. Kvetnansky. (2012) Epinephrine: a short- and long-term regulator of stress and development of illness : a potential new role for epinephrine in stress. Cell Mol Neurobiol. **32**(5): 737-748.
8. Tsigos C., I. Kyrou, E. Kassi, and G.P. Chrousos. Endotext. K.R. Feingold, et al., South Dartmouth (MA), 2000.
9. Pacak K. and M. Palkovits. (2001) Stressor specificity of central neuroendocrine responses: implications for stress-related disorders. Endocr Rev. **22**(4): 502-548.
10. Herman J.P., H. Figueiredo, N.K. Mueller, Y. Ulrich-Lai, M.M. Ostrander, D.C. Choi, and W.E. Cullinan. (2003) Central mechanisms of stress integration: hierarchical circuitry controlling hypothalamo-pituitary-adrenocortical responsiveness. Front Neuroendocrinol. **24**(3): 151-180.
11. Mifsud K.R. and J.M.H.M. Reul. (2016) Acute stress enhances heterodimerization and binding of corticosteroid receptors at glucocorticoid target genes in the hippocampus. Proceedings of the National Academy of Sciences of the United States of America. **113**(40): 11336-11341.
12. Gjerstad J.K., S.L. Lightman, and F. Spiga. (2018) Role of glucocorticoid negative feedback in the regulation of HPA axis pulsatility. Stress. **21**(5): 403-416.
13. Reichlin S. (1967) Function of the hypothalamus. Am J Med. **43**(4): 477-485.

14. Saper C.B. (2006) Staying awake for dinner: hypothalamic integration of sleep, feeding, and circadian rhythms. Prog Brain Res. **153**: 243-252.
15. Baskin D.G., B.J. Wilcox, D.P. Figlewicz, and D.M. Dorsa. (1988) Insulin and insulin-like growth factors in the CNS. Trends Neurosci. **11**(3): 107-111.
16. Baskin D.G., J.F. Breininger, and M.W. Schwartz. (1999) Leptin receptor mRNA identifies a subpopulation of neuropeptide Y neurons activated by fasting in rat hypothalamus. Diabetes. **48**(4): 828-833.
17. Zigman J.M., J.E. Jones, C.E. Lee, C.B. Saper, and J.K. Elmquist. (2006) Expression of ghrelin receptor mRNA in the rat and the mouse brain. J Comp Neurol. **494**(3): 528-548.
18. Ahima R.S. and J.S. Flier. (2000) Leptin. Annu Rev Physiol. **62**: 413-437.
19. Considine R.V., M.K. Sinha, M.L. Heiman, A. Kriauciunas, T.W. Stephens, M.R. Nyce, J.P. Ohannesian, C.C. Marco, L.J. McKee, T.L. Bauer, and et al. (1996) Serum immunoreactive-leptin concentrations in normal-weight and obese humans. N Engl J Med. **334**(5): 292-295.
20. Hulsey M.G., H. Lu, T. Wang, R.J. Martin, and C.A. Baile. (1998) Intracerebroventricular (i.c.v.) administration of mouse leptin in rats: behavioral specificity and effects on meal patterns. Physiol Behav. **65**(3): 445-455.
21. Elias C.F., J.F. Kelly, C.E. Lee, R.S. Ahima, D.J. Drucker, C.B. Saper, and J.K. Elmquist. (2000) Chemical characterization of leptin-activated neurons in the rat brain. J Comp Neurol. **423**(2): 261-281.
22. Gautron L., M. Lazarus, M.M. Scott, C.B. Saper, and J.K. Elmquist. (2010) Identifying the efferent projections of leptin-responsive neurons in the dorsomedial hypothalamus using a novel conditional tracing approach. J Comp Neurol. **518**(11): 2090-2108.
23. Myers M.G., Jr., H. Munzberg, G.M. Leinninger, and R.L. Leshan. (2009) The geometry of leptin action in the brain: more complicated than a simple ARC. Cell Metab. **9**(2): 117-123.
24. Fulton S., B. Woodside, and P. Shizgal. (2000) Modulation of brain reward circuitry by leptin. Science. **287**(5450): 125-128.
25. Szczypka M.S., M.A. Rainey, D.S. Kim, W.A. Alaynick, B.T. Marck, A.M. Matsumoto, and R.D. Palmiter. (1999) Feeding behavior in dopamine-deficient mice. Proc Natl Acad Sci U S A. **96**(21): 12138-12143.

26. Fulton S., P. Pissios, R.P. Manchon, L. Stiles, L. Frank, E.N. Pothos, E. Maratos-Flier, and J.S. Flier. (2006) Leptin regulation of the mesoaccumbens dopamine pathway. Neuron. **51**(6): 811-822.
27. Huo L., L. Maeng, C. Bjorbaek, and H.J. Grill. (2007) Leptin and the control of food intake: neurons in the nucleus of the solitary tract are activated by both gastric distension and leptin. Endocrinology. **148**(5): 2189-2197.
28. Roder P.V., B. Wu, Y. Liu, and W. Han. (2016) Pancreatic regulation of glucose homeostasis. Exp Mol Med. **48**: e219.
29. Baura G.D., D.M. Foster, D. Porte, Jr., S.E. Kahn, R.N. Bergman, C. Cobelli, and M.W. Schwartz. (1993) Saturable transport of insulin from plasma into the central nervous system of dogs in vivo. A mechanism for regulated insulin delivery to the brain. J Clin Invest. **92**(4): 1824-1830.
30. Benoit S.C., E.L. Air, L.M. Coolen, R. Strauss, A. Jackman, D.J. Clegg, R.J. Seeley, and S.C. Woods. (2002) The catabolic action of insulin in the brain is mediated by melanocortins. J Neurosci. **22**(20): 9048-9052.
31. Figlewicz D.P. and S.C. Benoit. (2009) Insulin, leptin, and food reward: update 2008. Am J Physiol Regul Integr Comp Physiol. **296**(1): R9-R19.
32. McNay E.C., C.T. Ong, R.J. McCrimmon, J. Cresswell, J.S. Bogan, and R.S. Sherwin. (2010) Hippocampal memory processes are modulated by insulin and high-fat-induced insulin resistance. Neurobiol Learn Mem. **93**(4): 546-553.
33. Figlewicz D.P., A.J. Sipols, R.J. Seeley, M. Chavez, S.C. Woods, and D. Porte, Jr. (1995) Intraventricular insulin enhances the meal-suppressive efficacy of intraventricular cholecystokinin octapeptide in the baboon. Behav Neurosci. **109**(3): 567-569.
34. Bagdade J.D., E.L. Bierman, and D. Porte, Jr. (1967) The significance of basal insulin levels in the evaluation of the insulin response to glucose in diabetic and nondiabetic subjects. J Clin Invest. **46**(10): 1549-1557.
35. Werther G.A., A. Hogg, B.J. Oldfield, M.J. McKinley, R. Figdor, A.M. Allen, and F.A. Mendelsohn. (1987) Localization and characterization of insulin receptors in rat brain and pituitary gland using in vitro autoradiography and computerized densitometry. Endocrinology. **121**(4): 1562-1570.
36. Williams K.W., L.O. Margatho, C.E. Lee, M. Choi, S. Lee, M.M. Scott, C.F. Elias, and J.K. Elmquist. (2010) Segregation of acute leptin and insulin effects in

distinct populations of arcuate proopiomelanocortin neurons. J Neurosci. **30**(7): 2472-2479.

37. Castaneda T.R., J. Tong, R. Datta, M. Culler, and M.H. Tschop. (2010) Ghrelin in the regulation of body weight and metabolism. Front Neuroendocrinol. **31**(1): 44-60.
38. Brubaker P.L. and Y. Anini. (2003) Direct and indirect mechanisms regulating secretion of glucagon-like peptide-1 and glucagon-like peptide-2. Can J Physiol Pharmacol. **81**(11): 1005-1012.
39. Ueno H., H. Yamaguchi, M. Mizuta, and M. Nakazato. (2008) The role of PYY in feeding regulation. Regul Pept. **145**(1-3): 12-16.
40. Turton M.D., D. O'Shea, I. Gunn, S.A. Beak, C.M. Edwards, K. Meeran, S.J. Choi, G.M. Taylor, M.M. Heath, P.D. Lambert, J.P. Wilding, D.M. Smith, M.A. Ghatei, J. Herbert, and S.R. Bloom. (1996) A role for glucagon-like peptide-1 in the central regulation of feeding. Nature. **379**(6560): 69-72.
41. Cummings D.E. and J. Overduin. (2007) Gastrointestinal regulation of food intake. J Clin Invest. **117**(1): 13-23.
42. Meister B. (2007) Neurotransmitters in key neurons of the hypothalamus that regulate feeding behavior and body weight. Physiol Behav. **92**(1-2): 263-271.
43. Stanley B.G., S.E. Kyrkouli, S. Lampert, and S.F. Leibowitz. (1986) Neuropeptide Y chronically injected into the hypothalamus: a powerful neurochemical inducer of hyperphagia and obesity. Peptides. **7**(6): 1189-1192.
44. Billington C.J., J.E. Briggs, M. Grace, and A.S. Levine. (1991) Effects of intracerebroventricular injection of neuropeptide Y on energy metabolism. Am J Physiol. **260**(2 Pt 2): R321-327.
45. Erickson J.C., K.E. Clegg, and R.D. Palmiter. (1996) Sensitivity to leptin and susceptibility to seizures of mice lacking neuropeptide Y. Nature. **381**(6581): 415-421.
46. Guyon A., G. Conductier, C. Rovere, A. Enfissi, and J.L. Nahon. (2009) Melanin-concentrating hormone producing neurons: Activities and modulations. Peptides. **30**(11): 2031-2039.
47. Tsujino N. and T. Sakurai. (2009) Orexin/hypocretin: a neuropeptide at the interface of sleep, energy homeostasis, and reward system. Pharmacol Rev. **61**(2): 162-176.

48. Dietrich M.O. and T.L. Horvath. (2009) Feeding signals and brain circuitry. Eur J Neurosci. **30**(9): 1688-1696.
49. Millington G.W. (2007) The role of proopiomelanocortin (POMC) neurones in feeding behaviour. Nutr Metab (Lond). **4**: 18.
50. Magni P., E. Dozio, M. Ruscica, F. Celotti, M.A. Masini, P. Prato, M. Broccoli, A. Mambro, M. More, and F. Strollo. (2009) Feeding behavior in mammals including humans. Ann N Y Acad Sci. **1163**: 221-232.
51. Rogge G., D. Jones, G.W. Hubert, Y. Lin, and M.J. Kuhar. (2008) CART peptides: regulators of body weight, reward and other functions. Nat Rev Neurosci. **9**(10): 747-758.
52. Millington G.W.M. (2007) The role of proopiomelanocortin (POMC) neurones in feeding behaviour. Nutrition & Metabolism. **4**.
53. Lechan R.M. and C. Fekete. (2006) The TRH neuron: a hypothalamic integrator of energy metabolism. Prog Brain Res. **153**: 209-235.
54. Wittmann G., T. Fuzesi, P.S. Singru, Z. Liposits, R.M. Lechan, and C. Fekete. (2009) Efferent projections of thyrotropin-releasing hormone-synthesizing neurons residing in the anterior parvocellular subdivision of the hypothalamic paraventricular nucleus. J Comp Neurol. **515**(3): 313-330.
55. King B.M. (2006) The rise, fall, and resurrection of the ventromedial hypothalamus in the regulation of feeding behavior and body weight. Physiol Behav. **87**(2): 221-244.
56. Wang C., E. Bomberg, C. Billington, A. Levine, and C.M. Kotz. (2007) Brain-derived neurotrophic factor in the hypothalamic paraventricular nucleus reduces energy intake. Am J Physiol Regul Integr Comp Physiol. **293**(3): R1003-1012.
57. Lizarbe B. and S. Cerdan. (2013) Neuroglial metabolic compartmentation during hypothalamic activation. Journal of Neurochemistry. **125**: 88-88.
58. Moriya T., R. Aida, T. Kudo, M. Akiyama, M. Doi, N. Hayasaka, N. Nakahata, R. Mistlberger, H. Okamura, and S. Shibata. (2009) The dorsomedial hypothalamic nucleus is not necessary for food-anticipatory circadian rhythms of behavior, temperature or clock gene expression in mice. European Journal of Neuroscience. **29**(7): 1447-1460.
59. Gooley J.J., A. Schomer, and C.B. Saper. (2006) The dorsomedial hypothalamic nucleus is critical for the expression of food- entrainable circadian rhythms. Nature Neuroscience. **9**(3): 398-407.

60. Vardanyan R. H.V. (Chapter 11 - Adrenergic (Sympathomimetic) Drugs) in *Synthesis of Best-Seller Drugs*, H.V. Vardanyan R., Editor. Academic press. p. 189-199.
61. de Kloet E.R., M. Joels, and F. Holsboer. (2005) Stress and the brain: from adaptation to disease. Nat Rev Neurosci. **6**(6): 463-475.
62. Barthel A. and D. Schmoll. (2003) Novel concepts in insulin regulation of hepatic gluconeogenesis. Am J Physiol Endocrinol Metab. **285**(4): E685-692.
63. van Donkelaar E.L., K.R. Vaessen, J.L. Pawluski, A.S. Sierksma, A. Blokland, R. Canete, and H.W. Steinbusch. (2014) Long-term corticosterone exposure decreases insulin sensitivity and induces depressive-like behaviour in the C57BL/6NCrl mouse. PLoS One. **9**(10): e106960.
64. Han Y., M. Lin, X. Wang, K. Guo, S. Wang, M. Sun, J. Wang, X. Han, T. Fu, Y. Hu, and J. Fu. (2015) Basis of aggravated hepatic lipid metabolism by chronic stress in high-fat diet-fed rat. Endocrine. **48**(2): 483-492.
65. Heinrichs S.C., F. Menzaghi, E.M. Pich, R.L. Hauger, and G.F. Koob. (1993) Corticotropin-Releasing Factor in the Paraventricular Nucleus Modulates Feeding Induced by Neuropeptide-Y. Brain Research. **611**(1): 18-24.
66. Palkovits M. (2003) Hypothalamic regulation of food intake. Ideggyogy Sz. **56**(9-10): 288-302.
67. Greenwood-Van Meerveld B., A.C. Johnson, and D. Grundy. (2017) Gastrointestinal Physiology and Function. Handb Exp Pharmacol. **239**: 1-16.
68. Konturek P.C., T. Brzozowski, and S.J. Konturek. (2011) Stress and the gut: pathophysiology, clinical consequences, diagnostic approach and treatment options. J Physiol Pharmacol. **62**(6): 591-599.
69. Sherwin E., K.V. Sandhu, T.G. Dinan, and J.F. Cryan. (2016) May the Force Be With You: The Light and Dark Sides of the Microbiota-Gut-Brain Axis in Neuropsychiatry. Cns Drugs. **30**(11): 1019-1041.
70. Rajilic-Stojanovic M. and W.M. de Vos. (2014) The first 1000 cultured species of the human gastrointestinal microbiota. FEMS Microbiol Rev. **38**(5): 996-1047.
71. Lloyd-Price J., G. Abu-Ali, and C. Huttenhower. (2016) The healthy human microbiome. Genome Med. **8**(1): 51.
72. Prakash S., L. Rodes, M. Coussa-Charley, and C. Tomaro-Duchesneau. (2011) Gut microbiota: next frontier in understanding human health and development of biotherapeutics. Biologics. **5**: 71-86.

73. Cresci G.A. and E. Bawden. (2015) Gut Microbiome. Nutrition in Clinical Practice. **30**(6): 734-746.

74. Borre Y.E., G.W. O'Keeffe, G. Clarke, C. Stanton, T.G. Dinan, and J.F. Cryan. (2014) Microbiota and neurodevelopmental windows: implications for brain disorders. Trends Mol Med. **20**(9): 509-518.

75. Wang Y. and L.H. Kasper. (2014) The role of microbiome in central nervous system disorders. Brain Behav Immun. **38**: 1-12.

76. Forsythe P., N. Sudo, T. Dinan, V.H. Taylor, and J. Bienenstock. (2010) Mood and gut feelings. Brain Behav Immun. **24**(1): 9-16.

77. De Vadder F., P. Kovatcheva-Datchary, D. Goncalves, J. Vinera, C. Zitoun, A. Duchampt, F. Backhed, and G. Mithieux. (2014) Microbiota-generated metabolites promote metabolic benefits via gut-brain neural circuits. Cell. **156**(1-2): 84-96.

78. Breton J., N. Tennoune, N. Lucas, M. Francois, R. Legrand, J. Jacquemot, A. Goichon, C. Guerin, J. Peltier, M. Pestel-Caron, P. Chan, D. Vaudry, J.C. do Rego, F. Lienard, L. Penicaud, X. Fioramonti, I.S. Ebenezer, T. Hokfelt, P. Dechelotte, and S.O. Fetissov. (2016) Gut Commensal E. coli Proteins Activate Host Satiety Pathways following Nutrient-Induced Bacterial Growth. Cell Metab. **23**(2): 324-334.

79. Ridaura V.K., J.J. Faith, F.E. Rey, J. Cheng, A.E. Duncan, A.L. Kau, N.W. Griffin, V. Lombard, B. Henrissat, J.R. Bain, M.J. Muehlbauer, O. Ilkayeva, C.F. Semenkovich, K. Funai, D.K. Hayashi, B.J. Lyle, M.C. Martini, L.K. Ursell, J.C. Clemente, W. Van Treuren, W.A. Walters, R. Knight, C.B. Newgard, A.C. Heath, and J.I. Gordon. (2013) Gut microbiota from twins discordant for obesity modulate metabolism in mice. Science. **341**(6150): 1241214.

80. Wen L., R.E. Ley, P.Y. Volchkov, P.B. Stranges, L. Avanesyan, A.C. Stonebraker, C. Hu, F.S. Wong, G.L. Szot, J.A. Bluestone, J.I. Gordon, and A.V. Chervonsky. (2008) Innate immunity and intestinal microbiota in the development of Type 1 diabetes. Nature. **455**(7216): 1109-1113.

81. Collins S.M., M. Surette, and P. Bercik. (2012) The interplay between the intestinal microbiota and the brain. Nature Reviews Microbiology. **10**(11): 735-742.

82. Vich Vila A., F. Imhann, V. Collij, S.A. Jankipersadsing, T. Gurry, Z. Mujagic, A. Kurilshikov, M.J. Bonder, X. Jiang, E.F. Tigchelaar, J. Dekens, V. Peters, M.D.

Voskuil, M.C. Visschedijk, H.M. van Dullemen, D. Keszthelyi, M.A. Swertz, L. Franke, R. Alberts, E.A.M. Festen, G. Dijkstra, A.A.M. Masclee, M.H. Hofker, R.J. Xavier, E.J. Alm, J. Fu, C. Wijmenga, D. Jonkers, A. Zhernakova, and R.K. Weersma. (2018) Gut microbiota composition and functional changes in inflammatory bowel disease and irritable bowel syndrome. Sci Transl Med. **10**(472).

83. O'Mahony S.M., G. Clarke, Y.E. Borre, T.G. Dinan, and J.F. Cryan. (2015) Serotonin, tryptophan metabolism and the brain-gut-microbiome axis. Behav Brain Res. **277**: 32-48.
84. Aguilar-Toala J.E., R. Garcia-Varela, H.S. Garcia, V. Mata-Haro, A.F. Gonzalez-Cordova, B. Vallejo-Cordoba, and A. Hernandez-Mendoza. (2018) Postbiotics: An evolving term within the functional foods field. Trends in Food Science & Technology. **75**: 105-114.
85. Borody T.J. and A. Khoruts. (2012) Fecal microbiota transplantation and emerging applications. Nature Reviews Gastroenterology & Hepatology. **9**(2): 88-96.
86. van Nood E., A. Vrieze, M. Nieuwdorp, S. Fuentes, E.G. Zoetendal, W.M. de Vos, C.E. Visser, E.J. Kuijper, J.F.W.M. Bartelsman, J.G.P. Tijssen, P. Speelman, M.G.W. Dijkgraaf, and J.J. Keller. (2013) Duodenal Infusion of Donor Feces for Recurrent Clostridium difficile. New England Journal of Medicine. **368**(5): 407-415.
87. Fuchsl A.M., I.D. Neumann, and S.O. Reber. (2014) Stress resilience: a low-anxiety genotype protects male mice from the consequences of chronic psychosocial stress. Endocrinology. **155**(1): 117-126.
88. Prescott L.M., J.M. Willey, L. Sherwood, and C.J. Woolverton, Prescott's microbiology. McGraw-Hill Education. 2014.
89. Duncko R., M. Schwendt, and D. Jezova. (2003) Altered glutamate receptor and corticoliberin gene expression in brain regions related to hedonic behavior in rats. Pharmacol Biochem Behav. **76**(1): 9-16.
90. Zelena D., Z. Mergl, A. Foldes, K.J. Kovacs, Z. Toth, and G.B. Makara. (2003) Role of hypothalamic inputs in maintaining pituitary-adrenal responsiveness in repeated restraint. Am J Physiol Endocrinol Metab. **285**(5): E1110-1117.
91. Andersen C.L., J.L. Jensen, and T.F. Orntoft. (2004) Normalization of real-time quantitative reverse transcription-PCR data: a model-based variance estimation

approach to identify genes suited for normalization, applied to bladder and colon cancer data sets. Cancer Res. **64**(15): 5245-5250.

92. Bacchetti De Gregoris T., N. Aldred, A.S. Clare, and J.G. Burgess. (2011) Improvement of phylum- and class-specific primers for real-time PCR quantification of bacterial taxa. J Microbiol Methods. **86**(3): 351-356.
93. Guo X., X. Xia, R. Tang, J. Zhou, H. Zhao, and K. Wang. (2008) Development of a real-time PCR method for Firmicutes and Bacteroidetes in faeces and its application to quantify intestinal population of obese and lean pigs. Lett Appl Microbiol. **47**(5): 367-373.
94. Mirhosseini S.Z., A. Seidavi, M. Shivazad, M. Chamani, A.A. Sadeghi, and R. Pourseify. (2010) Detection of Clostridium sp and its Relation to Different Ages and Gastrointestinal Segments as Measured by Molecular Analysis of 16S rRNA Genes. Brazilian Archives of Biology and Technology. **53**(1): 69-76.
95. Oh K.H., D.H. Jeong, S.H. Shin, and Y.C. Cho. (2012) Simultaneous Quantification of Cyanobacteria and Microcystis spp. Using Real-Time PCR. Journal of Microbiology and Biotechnology. **22**(2): 248-255.
96. Larmonier C.B., D. Laubitz, F.M. Hill, K.W. Shehab, L. Lipinski, M.T. Midura-Kiela, R.M.T. McFadden, R. Ramalingam, K.A. Hassan, M. Golebiewski, D.G. Besselsen, F.K. Ghishan, and P.R. Kiela. (2013) Reduced colonic microbial diversity is associated with colitis in NHE3-deficient mice. American Journal of Physiology-Gastrointestinal and Liver Physiology. **305**(10): G667-G677.
97. Dewar M.L., J.P. Arnould, L. Krause, P. Dann, and S.C. Smith. (2014) Interspecific variations in the faecal microbiota of Procellariiform seabirds. FEMS Microbiol Ecol. **89**(1): 47-55.
98. Ranjan K., F.S. Paula, R.C. Mueller, C. Jesus Eda, K. Cenciani, B.J. Bohannan, K. Nusslein, and J.L. Rodrigues. (2015) Forest-to-pasture conversion increases the diversity of the phylum Verrucomicrobia in Amazon rainforest soils. Front Microbiol. **6**: 779.
99. Nadkarni M.A., F.E. Martin, N.A. Jacques, and N. Hunter. (2002) Determination of bacterial load by real-time PCR using a broad-range (universal) probe and primers set. Microbiology-Sgm. **148**: 257-266.
100. Collaborators G.B.D.P.s.D. (2018) Global, regional, and national burden of Parkinson's disease, 1990-2016: a systematic analysis for the Global Burden of Disease Study 2016. Lancet Neurol. **17**(11): 939-953.

101. Winkler Z., D. Kuti, S. Ferenczi, K. Gulyas, A. Polyak, and K.J. Kovacs. (2017) Impaired microglia fractalkine signaling affects stress reaction and coping style in mice. Behav Brain Res. **334**: 119-128.

102. Kuti D., Z. Winkler, K. Horvath, B. Juhasz, M. Paholcsek, A. Stagel, G. Gulyas, L. Czegledi, S. Ferenczi, and K.J. Kovacs. (2020) Gastrointestinal (non-systemic) antibiotic rifaximin differentially affects chronic stress-induced changes in colon microbiome and gut permeability without effect on behavior. Brain Behav Immun. **84**: 218-228.

103. Ternak G., D. Kuti, and K.J. Kovacs. (2020) Dysbiosis in Parkinson's disease might be triggered by certain antibiotics. Medical Hypotheses. **137**.

104. Kadar A., E. Sanchez, G. Wittmann, P.S. Singru, T. Fuzesi, A. Marsili, P.R. Larsen, Z. Liposits, R.M. Lechan, and C. Fekete. (2010) Distribution of hypophysiotropic thyrotropin-releasing hormone (TRH)-synthesizing neurons in the hypothalamic paraventricular nucleus of the mouse. J Comp Neurol. **518**(19): 3948-3961.

105. Lew P.S., D. Wong, T. Yamaguchi, A. Leckstrom, J. Schwartz, J.G. Dodd, and T.M. Mizuno. (2009) Tail suspension increases energy expenditure independently of the melanocortin system in mice. Can J Physiol Pharmacol. **87**(10): 839-849.

106. Spiers J.G., H.C. Chen, F.J. Steyn, N.A. Lavidis, T.M. Woodruff, and J.D. Lee. (2017) Noninvasive assessment of altered activity following restraint in mice using an automated physiological monitoring system. Stress. **20**(1): 59-67.

107. Sherwin R.S. and L. Sacca. (1984) Effect of epinephrine on glucose metabolism in humans: contribution of the liver. Am J Physiol. **247**(2 Pt 1): E157-165.

108. Sharara-Chami R.I., M. Joachim, M. Mulcahey, S. Ebert, and J.A. Majzoub. (2010) Effect of epinephrine deficiency on cold tolerance and on brown adipose tissue. Mol Cell Endocrinol. **328**(1-2): 34-39.

109. McMahon M., J. Gerich, and R. Rizza. (1988) Effects of glucocorticoids on carbohydrate metabolism. Diabetes Metab Rev. **4**(1): 17-30.

110. Peckett A.J., D.C. Wright, and M.C. Riddell. (2011) The effects of glucocorticoids on adipose tissue lipid metabolism. Metabolism. **60**(11): 1500-1510.

111. Brodkin J., D. Frank, R. Grippo, M. Hausfater, M. Gulinello, N. Achterholt, and C. Gutzen. (2014) Validation and implementation of a novel high-throughput behavioral phenotyping instrument for mice. Journal of neuroscience methods. **224**: 48-57.

112. Dunn A.J. and A.H. Swiergiel. (1999) Behavioral responses to stress are intact in CRF-deficient mice. Brain Research. **845**(1): 14-20.

113. Kalueff A.V., A.M. Stewart, C. Song, K.C. Berridge, A.M. Graybiel, and J.C. Fentress. (2016) Neurobiology of rodent self-grooming and its value for translational neuroscience. Nature reviews. Neuroscience. **17**(1): 45-59.

114. Pertsov S.S., I.V. Alekseeva, E.V. Koplik, N.E. Sharanova, N.V. Kirbaeva, and M.M. Gapparov. (2014) Dynamics of locomotor activity and heat production in rats after acute stress. Bull Exp Biol Med. **157**(1): 10-14.

115. Greeno C.G. and R.R. Wing. (1994) Stress-induced eating. Psychol Bull. **115**(3): 444-464.

116. Tomiyama A.J., I. Schamarek, R.H. Lustig, C. Kirschbaum, E. Puterman, P.J. Havel, and E.S. Epel. (2012) Leptin concentrations in response to acute stress predict subsequent intake of comfort foods. Physiology & behavior. **107**(1): 34-39.

117. Dallman M.F., N.C. Pecoraro, and S.E. la Fleur. (2005) Chronic stress and comfort foods: self-medication and abdominal obesity. Brain Behav Immun. **19**(4): 275-280.

118. Dallman M.F., S.E. la Fleur, N.C. Pecoraro, F. Gomez, H. Houshyar, and S.F. Akana. (2004) Minireview: Glucocorticoids—Food Intake, Abdominal Obesity, and Wealthy Nations in 2004. Endocrinology. **145**(6): 2633-2638.

119. Richard D., Q. Huang, and E. Timofeeva. (2000) The corticotropin-releasing hormone system in the regulation of energy balance in obesity. Int J Obes Relat Metab Disord. **24 Suppl 2**: S36-39.

120. Eaves M., K. Thatcherbritton, J. Rivier, W. Vale, and G.F. Koob. (1985) Effects of Corticotropin Releasing-Factor on Locomotor-Activity in Hypophysectomized Rats. Peptides. **6**(5): 923-926.

121. Lowry C.A. and F.L. Moore. (1991) Corticotropin-releasing factor (CRF) antagonist suppresses stress-induced locomotor activity in an amphibian. Horm Behav. **25**(1): 84-96.

122. Wu Y., M. Blichowski, Z.J. Daskalakis, Z. Wu, C.C. Liu, M.A. Cortez, and O.C. Snead, 3rd. (2011) Evidence that clozapine directly interacts on the GABAB receptor. Neuroreport. **22**(13): 637-641.

123. Vacher C.M., M. Gassmann, S. Desrayaud, E. Challet, A. Bradaia, D. Hoyer, P. Waldmeier, K. Kaupmann, P. Pevet, and B. Bettler. (2006) Hyperdopaminergia

and altered locomotor activity in GABAB1-deficient mice. J Neurochem. **97**(4): 979-991.

124. Manvich D.F., K.A. Webster, S.L. Foster, M.S. Farrell, J.C. Ritchie, J.H. Porter, and D. Weinshenker. (2018) The DREADD agonist clozapine N-oxide (CNO) is reverse-metabolized to clozapine and produces clozapine-like interoceptive stimulus effects in rats and mice. Sci Rep. **8**(1): 3840.
125. Füzesi T., N. Daviu, J.I. Wamsteeker Cusulin, R.P. Bonin, and J.S. Bains. (2016) Hypothalamic CRH neurons orchestrate complex behaviours after stress. Nature communications. **7**: 11937-11937.
126. Yuan H.-Y., H.-X. Liang, G.-R. Liang, G.-X. Zhang, and H.-D. Li. (2008) Effects of clozapine administration on body weight, glucose tolerance, blood glucose concentrations, plasma lipids, and insulin in male C57BL/6 mice: A parallel controlled study. Current therapeutic research, clinical and experimental. **69**(2): 142-149.
127. Joseph J.J. and S.H. Golden. (2017) Cortisol dysregulation: the bidirectional link between stress, depression, and type 2 diabetes mellitus. Annals of the New York Academy of Sciences. **1391**(1): 20-34.
128. Adam T.C. and E.S. Epel. (2007) Stress, eating and the reward system. Physiol Behav. **91**(4): 449-458.
129. Benoit S.C., T.E. Thiele, S.C. Heinrichs, P.A. Rushing, K.A. Blake, and R.J. Steeley. (2000) Comparison of central administration of corticotropin-releasing hormone and urocortin on food intake, conditioned taste aversion, and c-Fos expression. Peptides. **21**(3): 345-351.
130. Heinrichs S.C., F. Menzaghi, E.M. Pich, R.L. Hauger, and G.F. Koob. (1993) Corticotropin-releasing factor in the paraventricular nucleus modulates feeding induced by neuropeptide Y. Brain Res. **611**(1): 18-24.
131. Shimizu H., H. Arima, M. Watanabe, M. Goto, R. Banno, I. Sato, N. Ozaki, H. Nagasaki, and Y. Oiso. (2008) Glucocorticoids increase neuropeptide Y and agouti-related peptide gene expression via adenosine monophosphate-activated protein kinase signaling in the arcuate nucleus of rats. Endocrinology. **149**(9): 4544-4553.
132. Warne J.P. (2009) Shaping the stress response: interplay of palatable food choices, glucocorticoids, insulin and abdominal obesity. Mol Cell Endocrinol. **300**(1-2): 137-146.

133. Aubry J.M., V. Bartanusz, D. Jezova, D. Belin, and J.Z. Kiss. (1999) Single stress induces long-lasting elevations in vasopressin mRNA levels in CRF hypophysiotrophic neurones, but repeated stress is required to modify AVP immunoreactivity. J Neuroendocrinol. **11**(5): 377-384.

134. Ota S.M., D. Suchecki, and P. Meerlo. (2018) Chronic social defeat stress suppresses locomotor activity but does not affect the free-running circadian period of the activity rhythm in mice. Neurobiol Sleep Circadian Rhythms. **5**: 1-7.

135. Ito H., M. Nagano, H. Suzuki, and T. Murakoshi. (2010) Chronic stress enhances synaptic plasticity due to disinhibition in the anterior cingulate cortex and induces hyper-locomotion in mice. Neuropharmacology. **58**(4-5): 746-757.

136. Marin M.T., F.C. Cruz, and C.S. Planeta. (2007) Chronic restraint or variable stresses differently affect the behavior, corticosterone secretion and body weight in rats. Physiol Behav. **90**(1): 29-35.

137. Bradbury M.J., W.C. Dement, and D.M. Edgar. (1998) Effects of adrenalectomy and subsequent corticosterone replacement on rat sleep state and EEG power spectra. Am J Physiol. **275**(2): R555-565.

138. Vazquez-Palacios G. and J. Velazquez-Moctezuma. (2000) Effect of electric foot shocks, immobilization, and corticosterone administration on the sleep-wake pattern in the rat. Physiol Behav. **71**(1-2): 23-28.

139. McEwen B.S. Stress: Concepts, Cognition, Emotion, and Behavior. G. Fink, Academic Press, San Diego, 2016: 39-55.

140. Cassard-Doulcier A.M., C. Gelly, N. Fox, J. Schrementi, S. Raimbault, S. Klaus, C. Forest, F. Bouillaud, and D. Ricquier. (1993) Tissue-specific and beta-adrenergic regulation of the mitochondrial uncoupling protein gene: control by cis-acting elements in the 5'-flanking region. Mol Endocrinol. **7**(4): 497-506.

141. Coderre L., G.A. Vallega, P.F. Pilch, and S.R. Chipkin. (1996) In vivo effects of dexamethasone and sucrose on glucose transport (GLUT-4) protein tissue distribution. Am J Physiol. **271**(4 Pt 1): E643-648.

142. Katz E.B., A.E. Stenbit, K. Hatton, R. DePinho, and M.J. Charron. (1995) Cardiac and adipose tissue abnormalities but not diabetes in mice deficient in GLUT4. Nature. **377**(6545): 151-155.

143. Melhorn S.J., E.G. Krause, K.A. Scott, M.R. Mooney, J.D. Johnson, S.C. Woods, and R.R. Sakai. (2010) Meal patterns and hypothalamic NPY expression during

chronic social stress and recovery. Am J Physiol Regul Integr Comp Physiol. **299**(3): R813-822.

144. Hoffman A.N., A. Krigbaum, J.B. Ortiz, A. Mika, K.M. Hutchinson, H.A. Bimonte-Nelson, and C.D. Conrad. (2011) Recovery after chronic stress within spatial reference and working memory domains: correspondence with hippocampal morphology. Eur J Neurosci. **34**(6): 1023-1030.
145. Lin M., G. Hou, Y. Zhao, and T.F. Yuan. (2018) Recovery of Chronic Stress-Triggered Changes of Hippocampal Glutamatergic Transmission. Neural Plast. **2018**: 9360203.
146. Gray J.D., T.G. Rubin, R.G. Hunter, and B.S. McEwen. (2014) Hippocampal gene expression changes underlying stress sensitization and recovery. Mol Psychiatry. **19**(11): 1171-1178.
147. Sarjan H.N. and H.N. Yajurvedi. (2018) Chronic stress induced duration dependent alterations in immune system and their reversibility in rats. Immunol Lett. **197**: 31-43.
148. Ottenweller J.E., R.J. Servatius, W.N. Tapp, S.D. Drastal, M.T. Bergen, and B.H. Natelson. (1992) A chronic stress state in rats: effects of repeated stress on basal corticosterone and behavior. Physiol Behav. **51**(4): 689-698.
149. Xu M., C. Wang, K.N. Krolick, H. Shi, and J. Zhu. (2020) Difference in post-stress recovery of the gut microbiome and its altered metabolism after chronic adolescent stress in rats. Sci Rep. **10**(1): 3950.
150. Cryan J.F. and T.G. Dinan. (2012) Mind-altering microorganisms: the impact of the gut microbiota on brain and behaviour. Nat Rev Neurosci. **13**(10): 701-712.
151. Foster J.A., L. Rinaman, and J.F. Cryan. (2017) Stress & the gut-brain axis: Regulation by the microbiome. Neurobiol Stress. **7**: 124-136.
152. De Palma G., S.M. Collins, P. Bercik, and E.F. Verdu. (2014) The microbiota-gut-brain axis in gastrointestinal disorders: stressed bugs, stressed brain or both? J Physiol. **592**(14): 2989-2997.
153. Watanabe Y., S. Arase, N. Nagaoka, M. Kawai, and S. Matsumoto. (2016) Chronic Psychological Stress Disrupted the Composition of the Murine Colonic Microbiota and Accelerated a Murine Model of Inflammatory Bowel Disease. PLoS One. **11**(3): e0150559.
154. Xu D., J. Gao, M. Gillilland, 3rd, X. Wu, I. Song, J.Y. Kao, and C. Owyang. (2014) Rifaximin alters intestinal bacteria and prevents stress-induced gut

inflammation and visceral hyperalgesia in rats. Gastroenterology. **146**(2): 484-496.e484.

155. Yoshikawa K., C. Kurihara, H. Furuhashi, T. Takajo, K. Maruta, Y. Yasutake, H. Sato, K. Narimatsu, Y. Okada, M. Higashiyama, C. Watanabe, S. Komoto, K. Tomita, S. Nagao, S. Miura, H. Tajiri, and R. Hokari. (2017) Psychological stress exacerbates NSAID-induced small bowel injury by inducing changes in intestinal microbiota and permeability via glucocorticoid receptor signaling. J Gastroenterol. **52**(1): 61-71.
156. Maltz R.M., J. Keirsey, S.C. Kim, A.R. Mackos, R.Z. Gharaibeh, C.C. Moore, J. Xu, V. Bakthavatchalu, A. Somogyi, and M.T. Bailey. (2018) Prolonged restraint stressor exposure in outbred CD-1 mice impacts microbiota, colonic inflammation, and short chain fatty acids. PLoS One. **13**(5): e0196961.
157. Bailey M.T., S.E. Dowd, J.D. Galley, A.R. Hufnagle, R.G. Allen, and M. Lyte. (2011) Exposure to a social stressor alters the structure of the intestinal microbiota: implications for stressor-induced immunomodulation. Brain Behav Immun. **25**(3): 397-407.
158. Langgartner D., C.A. Vaihinger, M. Haffner-Luntzer, J.F. Kunze, A.J. Weiss, S. Foertsch, S. Bergdolt, A. Ignatius, and S.O. Reber. (2018) The Role of the Intestinal Microbiome in Chronic Psychosocial Stress-Induced Pathologies in Male Mice. Front Behav Neurosci. **12**: 252.
159. Werbner M., Y. Barsheshet, N. Werbner, M. Zigdon, I. Averbuch, O. Ziv, B. Brant, E. Elliot, S. Gelberg, M. Titelbaum, O. Koren, and O. Avni. (2019) Social-Stress-Responsive Microbiota Induces Stimulation of Self-Reactive Effector T Helper Cells. mSystems. **4**(4).
160. Gautam A., R. Kumar, N. Chakraborty, S. Muhie, A. Hoke, R. Hammamieh, and M. Jett. (2018) Altered fecal microbiota composition in all male aggressor-exposed rodent model simulating features of post-traumatic stress disorder. J Neurosci Res. **96**(7): 1311-1323.
161. Szyszkowicz J.K., A. Wong, H. Anisman, Z. Merali, and M.C. Audet. (2017) Implications of the gut microbiota in vulnerability to the social avoidance effects of chronic social defeat in male mice. Brain Behav Immun. **66**: 45-55.
162. Galley J.D., Z. Yu, P. Kumar, S.E. Dowd, M. Lyte, and M.T. Bailey. (2014) The structures of the colonic mucosa-associated and luminal microbial communities

are distinct and differentially affected by a prolonged murine stressor. Gut Microbes. **5**(6): 748-760.

163. Rincel M., P. Aubert, J. Chevalier, P.A. Grohard, L. Basso, C. Monchaux de Oliveira, J.C. Helbling, E. Levy, G. Chevalier, M. Leboyer, G. Eberl, S. Laye, L. Capuron, N. Vergnolle, M. Neunlist, H. Boudin, P. Lepage, and M. Darnaudery. (2019) Multi-hit early life adversity affects gut microbiota, brain and behavior in a sex-dependent manner. Brain Behav Immun. **80**: 179-192.
164. Bailey M.T. and C.L. Coe. (1999) Maternal separation disrupts the integrity of the intestinal microflora in infant rhesus monkeys. Dev Psychobiol. **35**(2): 146-155.
165. Moussaoui N., M. Larauche, M. Biraud, J. Molet, M. Million, E. Mayer, and Y. Tache. (2016) Limited Nesting Stress Alters Maternal Behavior and In Vivo Intestinal Permeability in Male Wistar Pup Rats. PLoS One. **11**(5): e0155037.
166. Pearson-Leary J., C. Zhao, K. Bittinger, D. Eacret, S. Luz, A.S. Vigderman, G. Dayanim, and S. Bhatnagar. (2019) The gut microbiome regulates the increases in depressive-type behaviors and in inflammatory processes in the ventral hippocampus of stress vulnerable rats. Mol Psychiatry.
167. Camilleri M. (2019) Leaky gut: mechanisms, measurement and clinical implications in humans. Gut. **68**(8): 1516-1526.
168. Maes M., F. Coucke, and J.C. Leunis. (2007) Normalization of the increased translocation of endotoxin from gram negative enterobacteria (leaky gut) is accompanied by a remission of chronic fatigue syndrome. Neuro Endocrinol Lett. **28**(6): 739-744.
169. Fukui H. (2016) Endotoxin and other microbial translocation markers in the blood: a clue to understand leaky gut syndrome. Cell. Mol. Med. **2**(3:24): 1-14.
170. Velin A.K., A.C. Ericson, Y. Braaf, C. Wallon, and J.D. Soderholm. (2004) Increased antigen and bacterial uptake in follicle associated epithelium induced by chronic psychological stress in rats. Gut. **53**(4): 494-500.
171. Shin J.H. and R.J. Seeley. (2019) Reg3 Proteins as Gut Hormones? Endocrinology. **160**(6): 1506-1514.
172. Slattery D.A., N. Uschold, M. Magoni, J. Bar, M. Popoli, I.D. Neumann, and S.O. Reber. (2012) Behavioural consequences of two chronic psychosocial stress paradigms: anxiety without depression. Psychoneuroendocrinology. **37**(5): 702-714.

173. Renault J. and A. Aubert. (2006) Immunity and emotions: lipopolysaccharide increases defensive behaviours and potentiates despair in mice. Brain Behav Immun. **20**(6): 517-526.

174. Turnbull A.V., S. Lee, and C. Rivier. (1998) Mechanisms of hypothalamic-pituitary-adrenal axis stimulation by immune signals in the adult rat. Ann N Y Acad Sci. **840**: 434-443.

175. Anisman H., L. Kokkinidis, and Z. Merali. (2002) Further evidence for the depressive effects of cytokines: Anhedonia and neurochemical changes. Brain, Behavior, and Immunity. **16**(5): 544-556.

176. Chen J., A.N. Evans, Y. Liu, M. Honda, J.M. Saavedra, and G. Aguilera. (2012) Maternal deprivation in rats is associated with corticotrophin-releasing hormone (CRH) promoter hypomethylation and enhances CRH transcriptional responses to stress in adulthood. Journal of neuroendocrinology. **24**(7): 1055-1064.

177. Suderman M., P.O. McGowan, A. Sasaki, T.C. Huang, M.T. Hallett, M.J. Meaney, G. Turecki, and M. Szyf. (2012) Conserved epigenetic sensitivity to early life experience in the rat and human hippocampus. Proc Natl Acad Sci U S A. **109 Suppl 2**: 17266-17272.

178. Francino M.P. (2015) Antibiotics and the Human Gut Microbiome: Dysbioses and Accumulation of Resistances. Front Microbiol. **6**: 1543.

179. Singh P., A. Karimi, K. Devendra, P.W. Waldroup, K.K. Cho, and Y.M. Kwon. (2013) Influence of penicillin on microbial diversity of the cecal microbiota in broiler chickens. Poult Sci. **92**(1): 272-276.

180. Yu M., C. Mu, C. Zhang, Y. Yang, Y. Su, and W. Zhu. (2018) Marked Response in Microbial Community and Metabolism in the Ileum and Cecum of Suckling Piglets After Early Antibiotics Exposure. Front Microbiol. **9**: 1166.

181. Dobrzanska D.A., M.T.F. Lamaudiere, J. Rollason, L. Acton, M. Duncan, S. Compton, J. Simms, G.D. Weedall, and I.Y. Morozov. (2020) Preventive antibiotic treatment of calves: emergence of dysbiosis causing propagation of obese state-associated and mobile multidrug resistance-carrying bacteria. Microb Biotechnol. **13**(3): 669-682.

182. Dudek-Wicher R.K., A. Junka, and M. Bartoszewicz. (2018) The influence of antibiotics and dietary components on gut microbiota. Prz Gastroenterol. **13**(2): 85-92.

183. Zarrinpar A., A. Chaix, Z.Z. Xu, M.W. Chang, C.A. Marotz, A. Saghatelian, R. Knight, and S. Panda. (2018) Antibiotic-induced microbiome depletion alters metabolic homeostasis by affecting gut signaling and colonic metabolism. Nat Commun. **9**(1): 2872.

184. Panda S., I. El khader, F. Casellas, J. Lopez Vivancos, M. Garcia Cors, A. Santiago, S. Cuenca, F. Guarner, and C. Manichanh. (2014) Short-term effect of antibiotics on human gut microbiota. PLoS One. **9**(4): e95476.

185. Jernberg C., S. Lofmark, C. Edlund, and J.K. Jansson. (2010) Long-term impacts of antibiotic exposure on the human intestinal microbiota. Microbiology. **156**(Pt 11): 3216-3223.

186. Palleja A., K.H. Mikkelsen, S.K. Forslund, A. Kashani, K.H. Allin, T. Nielsen, T.H. Hansen, S. Liang, Q. Feng, C. Zhang, P.T. Pyl, L.P. Coelho, H. Yang, J. Wang, A. Typas, M.F. Nielsen, H.B. Nielsen, P. Bork, J. Wang, T. Vilsboll, T. Hansen, F.K. Knop, M. Arumugam, and O. Pedersen. (2018) Recovery of gut microbiota of healthy adults following antibiotic exposure. Nat Microbiol. **3**(11): 1255-1265.

187. Mertsalmi T.H., E. Pekkonen, and F. Scheperjans. (2020) Antibiotic exposure and risk of Parkinson's disease in Finland: A nationwide case-control study. Mov Disord. **35**(3): 431-442.

188. Soldi S., S. Vasileiadis, F. Uggeri, M. Campanale, L. Morelli, M.V. Fogli, F. Calanni, M. Grimaldi, and A. Gasbarrini. (2015) Modulation of the gut microbiota composition by rifaximin in non-constipated irritable bowel syndrome patients: a molecular approach. Clin Exp Gastroenterol. **8**: 309-325.

189. Jin Y., X. Ren, G. Li, Y. Li, L. Zhang, H. Wang, W. Qian, and X. Hou. (2018) Beneficial effects of Rifaximin in post-infectious irritable bowel syndrome mouse model beyond gut microbiota. J Gastroenterol Hepatol. **33**(2): 443-452.

190. Acosta A., M. Camilleri, A. Shin, S. Linker Nord, J. O'Neill, A.V. Gray, A.J. Lueke, L.J. Donato, D.D. Burton, L.A. Szarka, A.R. Zinsmeister, P.L. Golden, and A. Fodor. (2016) Effects of Rifaximin on Transit, Permeability, Fecal Microbiome, and Organic Acid Excretion in Irritable Bowel Syndrome. Clin Transl Gastroenterol. **7**: e173.

191. Ponziani F.R., F. Scaldaferri, V. Petito, F. Paroni Sterbini, S. Pecere, L.R. Lopetuso, A. Palladini, V. Gerardi, L. Masucci, M. Pompili, G. Cammarota, M.

Sanguinetti, and A. Gasbarrini. (2016) The Role of Antibiotics in Gut Microbiota Modulation: The Eubiotic Effects of Rifaximin. Dig Dis. **34**(3): 269-278.

192. Bajaj J.S., D.M. Heuman, A.J. Sanyal, P.B. Hylemon, R.K. Sterling, R.T. Stravitz, M. Fuchs, J.M. Ridlon, K. Daita, P. Monteith, N.A. Noble, M.B. White, A. Fisher, M. Sikaroodi, H. Rangwala, and P.M. Gillevet. (2013) Modulation of the metabiome by rifaximin in patients with cirrhosis and minimal hepatic encephalopathy. PLoS One. **8**(4): e60042.
193. Borre Y.E., R.D. Moloney, G. Clarke, T.G. Dinan, and J.F. Cryan. (2014) The impact of microbiota on brain and behavior: mechanisms & therapeutic potential. Adv Exp Med Biol. **817**: 373-403.
194. Bravo J.A., P. Forsythe, M.V. Chew, E. Escaravage, H.M. Savignac, T.G. Dinan, J. Bienenstock, and J.F. Cryan. (2011) Ingestion of Lactobacillus strain regulates emotional behavior and central GABA receptor expression in a mouse via the vagus nerve. Proc Natl Acad Sci U S A. **108**(38): 16050-16055.
195. Dinan T.G., C. Stanton, and J.F. Cryan. (2013) Psychobiotics: a novel class of psychotropic. Biol Psychiatry. **74**(10): 720-726.

10. Publication of the author

Publications that form the basis of the Ph.D. dissertation:

Kuti D; Winkler Z; Horvath K; Juhasz B; Paholcsek M; Stagel A; Gulyas G; Czegledi L; Ferenczi S; Kovacs K.J.
Gastrointestinal (Non-systemic) Antibiotic Rifaximin Differentially Affects Chronic Stress-induced Changes in Colon Microbiome and Gut Permeability without Effect on Behavior. ***BRAIN BEHAVIOR AND IMMUNITY*** 84 pp. 218-228., 11 p. (2020)
IF: 6,17

Ternak G; **Kuti D**; Kovacs KJ.
Dysbiosis in Parkinson's Disease might be Triggered by Certain Antibiotics.
MEDICAL HYPOTHESES 137 Paper: 109564, 5 p. (2020)
IF: 1,322

Winkler Z; Kuti D; Ferenczi S; Gulyas K; Polyak A; Kovacs KJ
Impaired microglia fractalkine signaling affects stress reaction and coping style in mice.
BEHAVIOURAL BRAIN RESEARCH 334 pp. 119-128., 10 p. (2017)
IF: 3,173

Other Publications:

Vas V; Hahner T; Kudlik G; Ernszt D; Kvell K; Kuti D; Kovacs KJ; Tovari J; Trexler M; Mero BL
Analysis of Tks4 Knockout Mice Suggests a Role for Tks4 in Adipose Tissue Homeostasis in the Context of Beigeing.
CELLS 8 : 8 Paper: 831 , 20 p. (2019)
IF: 5,656

Winkler Z; Kuti D; Polyak A; Juhasz B; Gulyas K; Lenart N; Denes A; Ferenczi S; Kovacs KJ Hypoglycemia-activated Hypothalamic Microglia Impairs Glucose Counterregulatory Responses.
SCIENTIFIC REPORTS 9:1 Paper: 6224, 14 p. (2019) 3.
IF: 4,011

Polyak A; Winkler Z; Kuti D; Ferenczi S; Kovacs KJ
Brown adipose tissue in obesity: Fractalkine-receptor dependent immune cell recruitment affects metabolic-related gene expression.
BIOCHIMICA ET BIOPHYSICA ACTA-MOLECULAR AND CELL BIOLOGY OF LIPIDS 1861:11 pp. 1614-1622., 9 p. (2016)
IF: 5,547

Kriszt R; Winkler Z; Polyak A; Kuti D; Molnar C; Hrabovszky E; Kallo I; Szoke Z; Ferenczi S; Kovacs KJ
Xenoestrogens Ethinyl Estradiol and Zearalenone Cause Precocious Puberty in Female Rats via Central Kisspeptin Signaling.
ENDOCRINOLOGY 156 : 11 pp. 3996-4007., 12 p. (2015)
IF: 4,159

DOI:10.14753/SE.2020.2417

11. Acknowledgement

First and foremost, I am very grateful to my supervisor Krisztina Kovács for applied me and hiring in her research group. I have learned a lot over the years under her hands. Therefore, I would like to thank to guiding and supporting me, and that she promoted my scientific progress.

I am thankful to my all the past and present colleagues of the Laboratory of Molecular Neuroendocrinology: Szilamér Ferenczi, Winkler Zsuzsanna, Polyák Ágnes, Krisztina Horváth, Dóra Kővári, and Juhász Balázs, for their help. I am very pleased for all co-workers to assist in my work and help to extend my technical background, particularly to Levente Czeglédi, Gabriella Gulyás, Csaba Fekete, Anett Stiftné Szilvásy-Szabó, Dóra Zelena, Virág Vass and Gábor Ternák. Last, but not least, I would like to express my thanks to my family and friends for their support and encouragement during my studies and the preparation of my PhD dissertation. Finally, thanks to God for helping me along the way.